Università degli Studi di Milano
Facoltà di Scienze Matematiche, Fisiche e Naturali
Dipartimento di Scienze della Terra "Ardito Desio"
Scuola di Dottorato **"**Terra, Ambiente e Biodiversità"
Dottorato di Ricerca in Scienze della Terra
Ciclo XXI – Raggruppamento disciplinare GEO/08

Innovative approaches to evaluate geochemical risk related to sulphide-bearing Abandoned Mine Lands

PhD Thesis

Diego Servida
Matr. N. R06296

Tutori
Prof. Luisa De Capitani
Dott. Giovanni Grieco

Anno Accademico
2007-2008

Coordinatore
Prof. Stefano Poli

A tutti quelli che lavorano
con passione e disponibilità

Index

Abstract

Abandoned Mine Lands (AML) are often perceived to have significant environmental impacts, particularly on superficial and ground waters, from water contaminated with acid and elevated metals flowing from eroding waste dumps and from underground workings. These conditions would require risk assessment and remediation in case of necessity.

However AML have heritage and historical value because of their age and the significance of their structures and the processes used. This value could be destroyed by remediation done following the environmental law in force.

Take into account the particular features of AML (terrains characterised by natural high metal and metalloid concentrations) and environmental law problems (the inability of agencies to cite or allocate clear ownership for the problems at the sites), rise the need to develop an approach that allows the right and complete geo-environmental characterisation of AML and that supports the management and/or the remediation of AML.

The main problems related to AML comprise:

- the identification and characterisation of mine dumps;
- the assessment of the geochemical hazard;
- the persistence in time of the chemical processes which occur at the site.

Mine dumps are the waste products of exploitation, composed mainly of rocks with metal concentration too low to be economic but rather high to be a source of environmental pollution.

A preliminary low-cost identification of mine dumps could be done by means of digital elaboration of topographic maps. This operation allows to identify and to evaluate the morphology and dimension of mine dumps having bibliographic data and CAD software (Servida et al., 2009).

Mine dumps characterisation could be completed and refined by Electrical Resistivity Ground Imaging (ERGI) investigations (Mele et al., 2007) that enable to reduce direct investigation number and, consequently, to reduce costs and acquisition time. Moreover ERGI investigations supply 3D information concerning a more extended area.

Geochemical hazard related to sulphide-bearing AML could not be evaluated taking into account only the metal and metalloid concentrations of terrains, since it is high by nature. It is suggested to evaluate geochemical hazard starting from the combination of high metal and metalloid concentrations and of the acid production or neutralising potential of terrains by AMIRA procedure (IWRI & EGI, 2002). Hazard evaluation was performed by geostatistical

analyses, resulting from 1) the interpolation of the terrain chemical features on the whole area, 2) the overlapping of previous results and 3) the adding of the topographic setting. This approach allows to identify the areas where the presence of metal and metalloids is really hazardous. It also supports the choice of areas that need any treatment.

Since AMD processes have a key-role in environmental damages from mining pollution, it is important to know their persistence in time. No studies about this topic have already done. In a preliminary step, the persistence of AMD processes could be calculated starting from common data as yearly rainfall, mining waters pH and acid production or neutralising potential of terrains. The following step is to consider the results of kinetic tests.

These approaches have been developed on three pilot sites with different geo-environmental setting:

- Rio Marina mining district (Elba Island, LI), characterised by hematite + pyrite ore association, exploited for iron from Etruscan age till 1981;
- Libiola mine (GE), characterised by chalcopyrite + pyrite ore association, exploited for copper from 1864 till 1962;

The application of the proposed methodologies and techniques allows a better geo-environmental characterisation of AML.

Moreover we think that the proposed approach for the assessment of geochemical risk related to AML could contribute to reduce the areas that need remediation. Consequently will be possible to reduce costs of remediation and impact of remediation on AML.

Chapter 1

Metal mining and the environment

1.1 Ore deposits

A "mineral deposit" is an anomalous concentration of metal minerals. (Guilbert & Park Jr., 1986). It becomes an "ore deposit" if 1) it contains elements or minerals that are useful and valuable, 2) occurring in a form, with a grade and tonnage that allow their exploitation, transport and processing and 3) could be exploited with the existing technologies (Guilbert & Park Jr., 1986; Evans, 1987; Craig et al., 1996; Robb, 2005).

Many geological, social, economic, technological and environmental factors are important in the evaluation of an ore deposit (Evans, 1987):

- Ore grade: is the concentration of a metal in an ore deposit. Considering the geochemistry and the range of concentration factors that characterise the different ore deposit types, metal can be divided into "geochemically abundant metals" and "geochemically scarce metals". The first ones occur in large quantities in the Earth's crust (such as Fe) and require only a relatively small degree of enrichment in order to make a viable deposit. By contrast, "geochemically scarce metals" (such as Cu) are much more sparsely distributed in the Earth's crust. The economics of mining dictate that these metals need to be concentrated by factors in the hundreds in order to form potentially viable deposits, degrees of enrichment that are one order of magnitude higher than those applicable to more abundant metals (Tab. 1). The lowest grade of ore which can be mined from an ore deposit is termed cut-off.
- By-products: is the occurrence of metal into an ore deposit, the sales of whom may help finance the mining of another.
- Commodity prices: the prices of metal are governed by supply and demand, and control the most part of mining activity.
- Mineralogical form of ore: it governs the ease with which existing technology can extract and refine certain metals.
- Grain size of ore: it governs the recovery percentage.
- Undesirable substances: deleterious substances may be present into or associated with the ore minerals.

	Average crustal abundance	Typical exploitable grade	Approximate concentration factor
Al	8.2 %	30 %	x4
Fe	5.6 %	50 %	x9
Cu	55 ppm	1%	x180
Zn	70 ppm	5%	x700
Au	4 ppb	5 ppm	x1250
Sn	2 ppm	0.5%	x2500

Tab. 1 - Average crustal abundances for selected metals and typical concentration factors that need to be achieved in order to produce a viable ore deposit (modified after Evans, 1987 and Robb, 2005)

- Size and shape of deposit: it governs the mining strategy and the volume of rocks to be worked.
- Cost of capital: bigger is the planned mining operation, bigger is the required initial capital.
- Location: the geographical factor governs the cost of transporting.
- Environmental consideration: conflicts over land use must be taken into account.
- Taxation: governments could oppose, support or encourage mineral development with taxation or incentives.
- Political factors: the stability of the government must be taken into account.

1.2 Mining districts

The working steps regarding the exploitation of an ore deposit comprise: exploration, extraction, mineral processing, metallurgic treatment and disposal of gangue material, waste rocks and tailings. In these steps are voluntarily not considered the economic operations.

1.2.1 Exploration

Mineral exploration (resource evaluation and reserve definition) is the process undertaken by companies, partnerships or corporations in the endeavour of finding ore deposit to mine through geological surveys, geophysical methods, remote sensing and geochemical methods.

1.2.2 Extraction

Extraction methods may vary considerably and it is the discipline of engineers trained in mining engineering to determine the safest, cost effective and efficient method of mining the ore body. Mining techniques can be divided into two basic excavation types: 1) surface mining and 2) subsurface mining.

Surface mining generally involves open pit mining. Open pit are developed as conical chasms with terraced benches that spiral downward to the bottom of the pit. These benches serve as a haulage roads and working platforms on the steep sloping sides of the pit. Extraction proceeds by drilling, blasting and loading material into trucks. This technique is an economically method of extraction involving large tonnages of ore and high rates of production. Surface mining is preferred to underground mining when the ore is at low depth because is less expensive and safer. However it often results in a greater environmental impact than underground mining (Craig et al., 1996).

Underground mining, involving a system of subsurface workings, is used to extract ore minerals that cannot be found near the surface. Most mines consist of one or more means of access via vertical shaft, horizontal adits or inclined roadways. These provide transportation of men, machinery, materials, extracted ore and wastes. They also form part of the system of ventilation and the control of underground water that are essential to mining operation. Shafts, adits and roadways lead to the region where ore is extracted that is referred to as a stop. Usually there are intersecting horizontal tunnels (drifts and crosscut) often on several levels joined by further vertical openings (raises or winzes). The greatest problems related to underground mining, in addition to air and water, are the increasing of the temperature with the depth and the potential rock-falls and cave-ins (Craig et al., 1996).

1.2.3 Mineral processing

The first treatment is useful to divide ore mineral from gangue material and to concentrate ore mineral for the following treatments. Dividing and concentrating processes are based on the physical properties of the minerals that occur into the ore and include magnetic separation, gravity separation, and flotation.

To streamline the separation the first stage of processing is a size reduction (comminution) of blocks up to a meter across down to particles only a few tenths or hundredths of millimetres in diameter. This is achieved by first crushing and then grinding/milling the ores (Craig et al., 1996).

Taking into account the researched mineral/element, the economic conditions and the available technologies the ore mineral could be divided in two portions: the first one with a grade of researched mineral over the cut-off value, called "concentrate", and the second one with a grade of researched mineral under cut-off value, called "waste rocks".

1.2.4 Metallurgic treatment

The concentred portion is then roasted and/or smelted for releasing the metal from the other elements to which it is chemically bonded in the mineral. Some metals are recovered with heap-leaching methodology: it consists in piling the concentrate and allowing that an appropriate solution percolates down through its (Craig et al., 1996). The discard of any metallurgic treatment is termed "tailing".

Ore bodies often contain more than one valuable metal. Tailings of a previous process may be used as a concentrate in another process to extract a secondary product from the original ore.

1.2.5 Disposal

Material discarded after manual selection and mineral processing (waste rock, cfr. § 1.2.3) and material discarded after metallurgic treatment (tailing, cfr. § 1.2.4) are disposed of. Sometimes waste rocks and tailings are put back into the openings created by the mining (back-filling). More often they are piled close to the exploitation area creating mine dumps. Only few times they could be used to fill lands, because they must not contain 1) acid-generating mineralogical phases (eg: pyrite), 2) high concentration of metallic mineralogical phases and 3) chemical substances used for separation of different elements (eg: amalgam for gold extraction) that could be hazardous for the environment.

1.2.6 Closure

Mining works could come to the end for different main reasons: the resource exhaustion or the change of another variable (social, economic, technological or environmental).

1.2.7 Rehabilitation and reclamation

After closure every mine lands should be submitted to rehabilitation or reclamation workings.

Land rehabilitation is the process of returning the land in a given area to some degree of its former state, after some process has resulted in its damage. While it is rarely possible to restore the land to its original condition, the rehabilitation process usually attempts to bring some degree of restoration.

Land reclamation is instead the process of creating useful landscapes that meet a variety of goals, typically creating productive ecosystems (or sometimes industrial or municipal land) from mined land.

1.3 Abandoned mines

Abandoned Mine Lands (AML) are commonly known as "Abandoned Mines" in North America, as "Derelict Mines" in Australia and sometimes are called "Orphan Mines" because there are no organizations clearly responsible for their rehabilitation or maintenance.

AML are often perceived to have significant environmental impacts, but, on the other hand, they have also heritage and historical value because of their age and the significance of their structures and the processes used.

However, the defining characteristic of AML is the inability of agencies to cite or allocate clear ownership for the problems at the sites or for the site and the land itself. Often ownership of the site has inadvertently reverted to the owner of the surrounding land on which the AML lies.

Some national, state and local government agencies have compiled inventories of the distribution of AML and of the environmental risks and liabilities associated with them as Canada and USA. (Centre for Mined Land Rehabilitation, 2008).

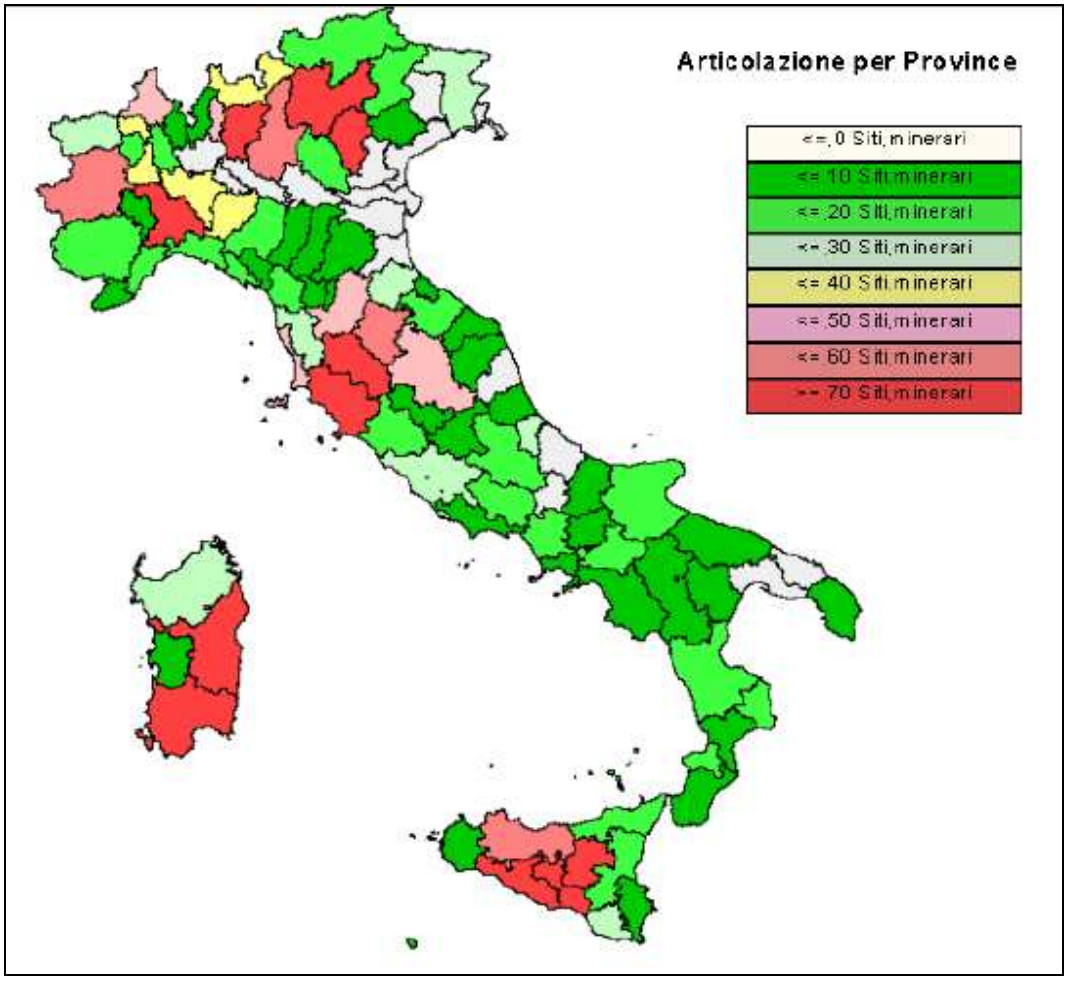

Fig. 1 - Classification of Italian provinces based on the number of AML identified

In Italy APAT (2006) has just compiled a first inventory of AML. The project began with the stated objectives of accurately locating and documenting abandoned mine sites, recording the factors relevant to public safety and environmental hazards that they pose, assessing their state of preservation and quantifying the "aggregate" risk at each site. The inventory is intended to provide a basis for planning for future rehabilitation at high risk sites. In the U.S.A. mines were considered as abandoned if they were non-operational since 1990. The database contains 2722 historic mine sites divided for provinces (**Fig. 1**).

As shown by **Fig. 1** the most part of Italian AML is concentrated in four main areas. From N to S these correspond with main mining districts that were active in the last century: Orobic Alps (exploited for Pb-Zn), Tuscany (exploited for Fe), Sardinia (exploited for Pb-Zn) and Sicily (exploited for S).

1.4 AML related risks

Main issues related to AML can be grouped into 3 classes:

- hydrogeochemical risks;
- geotechnical risks;
- landscape deterioration.

1.4.1 Hydro geochemical risks

Geochemical risk is usually the most dangerous risk at AML and it has in such kind of environment peculiar characters. It can be defined as the risk due to high toxic element anomalies in superficial media, that interact with biosphere and it is responsible for damage to ecosystem and human health (Dall'aglio, 2004). In AML it is mainly related to acid drainage processes and water pollution.

Acid drainage: the formation of acid drainage and the contaminants associated with it have been described as the biggest environmental problem facing the mining industry. Commonly referred to as acid rock drainage (ARD) or acid mine drainage (AMD), it may be generated from mine waste rock or tailing dumps or mine structures, such as pits and underground workings.

Acid generation can occur rapidly, or it may take years or decades to appear and reach its full potential. For that reason, even a long-abandoned site can still intensify its environmental impacts.

The severity of, and impacts from, AMD/ARD are primarily a function of the mineralogy of the rock material and the availability of water and oxygen. While acid may be neutralized by the receiving water, some dissolved metals may remain in solution (U.S. EPA, 2000).

Metal contamination of ground and surface water: mining operations can affect ground water quality in several ways. The most obvious occurs in mining below the water table,

either in underground workings or open pits. This provides a direct conduit to aquifers. Ground water quality is also affected when waters infiltrate through surface materials (including overlying wastes or other material) into ground water. Contamination can also occur when there is a hydraulic connection between surface and ground water. Any of these can cause elevated pollutant levels in ground water. On the contrary, contaminated ground water may discharge to surface water down gradient of the mine, as contributions to base flow in a stream channel or springs.

Dissolved pollutants at a mine site are primarily metals but may include different products used for metallurgic treatment. These contaminants, once dissolved, can migrate from mining operations to local ground and surface water. Elevated concentrations of metals in surface water and ground water may preclude their use as drinking water. Low pH levels and high metal concentrations can have acute and chronic effects on aquatic life/biota.

While AMD/ARD can enhance contaminant mobility by promoting leaching from exposed wastes and mine structures (cfr. § 1.5), releases can also occur under neutral pH conditions. Dissolution of metals due to low pH is a well known characteristic of each acid drainage. Anyway low pH is not always necessary for metals to be mobilized and to contaminate waters; there is increasing concern about neutral and high pH metal mobilization (U.S. EPA, 2000).

1.4.2 Geotechnical risks

Slope failure: slopes at mine sites fall into two categories, 1) cut slopes and 2) manufactured or filled slopes. The methods of slope formation reflect the hazards associated with each. *Cut slopes* are created by the removal of overburden and/or ore which results in the creation of or alteration to the surface slope of undisturbed native materials. Changes to an existing slope may create environmental problems associated with increased erosion, rapid runoff, changes in wildlife patterns and the exposure of potentially reactive natural materials. Dumping or piling of overburden, tailings, waste rock or other materials creates *manufactured or filled slopes*. These materials can be toxic, acid forming, or reactive. Slope failure can result in direct release or direct exposure of these materials to the surrounding environment. Saturation of waste material can also trigger slope failure.

Structural stability of tailings impoundments: the historic disposal of tailings behind earthen dams and embankments raises a number of concerns related to the stability of the units. In particular, tailings impoundments are nearly always accompanied by unavoidable and often necessary seepage of mill effluent through or beneath the dam structure. Such seepage results from the uncontrolled percolation of stored water or precipitation downward through foundation materials or through the embankment. Failure to maintain hydrostatic pressure within and behind the embankment below critical levels may result in partial or complete failure of the structure, causing releases of tailings and contained mill effluent to surrounding areas.

Subsidence: mining subsidence is the movement of the surface resulting from the collapse of overlying strata into mine voids. The potential for subsidence exists for all forms

of underground mining. Subsidence may manifest itself in the form of sinkholes or troughs. *Sinkholes* are usually associated with the collapse of a portion of a mine void (such as a room in room and pillar mining); the extent of the surface disturbance is usually limited in size. *Troughs* are formed from the subsidence of large portions of the underground void and typically occur over areas where most of the resource has been removed. Effects of subsidence may or may not be visible from the ground surface. Sinkholes or depressions in the landscape interrupt and/or redirect surface water drainage patterns. In developed areas, subsidence has the potential to affect building foundations and walls, highways, and pipelines (Craig et al., 1996; U.S. EPA, 2000).

1.4.3 Landscape deterioration

The absence of adequate controls over some mining activities in the past has left numerous scars on the surface of Earth. When an open pit mine closes, a large hole remains and sometimes neither waste rock nor water table are available to fill it. In other AML it is possible to find mounds of waste material (Craig et al., 1996).

Erosion: Because of the large land area disturbed by mining operations and the large quantities of earthen materials exposed at sites, erosion is a primary concern at mine sites (U.S. EPA, 2000).

Structures: Abandoned structures at mining sites damage panorama if they were built without any consideration about environmental impact and if they are in a crumbling state (Trinder, 1987; Alfrey & Clark, 1993; Deshaies, 2002).

1.5 Acid Drainage

ARD or AMD are the names of a set of processes developing when meteoric, superficial or ground waters come into contact with sulphide-bearing material in an oxidizing environment. The oxidation of sulphide minerals generates acid waters containing high concentrations of sulphates and metals.

1.5.1 Reactions

According to the reviews in AMD given by Nordstrom and Alpers (1999) and Blowes et al. (2003), pyrite oxidation must be considered the main cause of ARD or AMD processes. Even if pyrite is not the most reactive mineralogical phase (Jambor & Blowes, 1994), it is however the most common mineralogical sulphide phase in ore deposits.

Pyrite oxidation is a complex process that can involve chemical, biological and electrochemical reactions. The simple pyrite oxidation by atmospheric oxygen and water is:

$$2\,FeS_{2\,(s)} + 7\,O_{2\,(g)} + 2\,H_2O_{\,(l)} \rightarrow 2\,Fe^{2+}{}_{(aq)} + 4\,SO_4^{2-}{}_{(aq)} + 4\,H^{+}{}_{(aq)} \qquad \text{Eq. 1}$$

The Fe^{2+} thus released may be oxidised to Fe^{3+}:

$$4\,Fe^{2+}{}_{(aq)} + O_{2\,(g)} + 4\,H^{+}{}_{(aq)} \rightarrow 4\,Fe^{3+}{}_{(aq)} + 2\,H_2O_{\,(l)} \qquad \text{Eq. 2}$$

Fe^{3+} oxy-hydroxides may precipitate:

$$Fe^{3+}_{(aq)} + 3\ H_2O_{(l)} \rightarrow Fe(OH)_3 + 3H^+ \qquad \text{Eq. 3}$$

Adding equations 1-3 yields the overall reactions:

$$4\ FeS_{2\ (s)} + 15\ O_{2\ (g)} + 14\ H_2O_{(l)} \rightarrow 8\ SO_4^{2-}{}_{(aq)} + 4\ Fe(OH)_3 + 16H^+ \qquad \text{Eq. 4}$$

1.5.2 Factors

However the factors that affect ARD or AMD processes are numerous and concern site features (location, climate, geology), physical features of reactive material (porosity, permeability, grain size) and chemical features of reactive material (mineralogy, weathering).

1.5.3 Sources

Prior to mining, oxidation of these minerals and the formation of sulphuric acid is a function of natural weathering processes. The oxidation of undisturbed ore deposits followed by the release of acid and mobilization of metals is slow. Natural discharge from such deposits poses little threat to receiving aquatic ecosystems except in rare instances. Mining and mineral processing operations greatly increase the rate of these same chemical reactions by removing large volumes of sulphide rock material and exposing increased surface area to air and water. Materials and wastes that have the potential to generate ARD as a result of metal mining activity include mined material, such as spent ore from heap and dump leach operations, tailings, and waste rock units, as well as overburden material. AMD generation in the mines themselves occurs at the pit walls in the case of surface mining operations and in the underground workings associated with underground mines (Nordstrom & Alpers, 1999; U.S. EPA, 2000).

Surface and ground waters contamination is strictly related to the ARD/AMD processes, since 1) all the mineralogical phases that are oxidised release metals as cations and 2) many mineralogical phases are more soluble under acidic conditions (Smith and Huyck, 1999).

1.6 Environmental legislation

1.6.1 International

Nowadays only few nations have a specific legislation, policy and guidance about risks related to AML. USA, Canada and Australia have faced this problem in different ways.

In the USA the first blueprint for responding to both oil spills and hazardous substance releases, called *National oil and hazardous substances pollution Contingency Plan* (NCP – US EPA, 1994) was developed and published in 1968. This plan provided the first comprehensive system of accident reporting, spill containment and cleanup, and established a response headquarters, a national reaction team and regional reaction teams. Following the passage of *Superfund legislation* in 1980 (in US EPA, 2008), the NCP was broadened to cover releases at

hazardous waste sites requiring emergency removal actions. Superfund is 1) an environmental program established to address abandoned hazardous waste sites and 2) a fund established by the Comprehensive Environmental Response, Compensation and Liability Act (CERCLA) of 1980 (in US EPA, 2008). Into the abandoned hazardous waste sites a specific program look after AML. During this program that followed the policy and guidance of EPA (1997) an additional handbook was developed focusing on problems of AML (EPA, 2000). The two main problems are related 1) to the autonomy of the different states that sometimes do not have the same policy and 2) to the very high number of AML occurring on the national area.

Canada has a complex mining and environmental legislation since it is managed at the federal, provincial, and territorial levels (Castrilli, 2007). Even if an unambiguous and final policy and guidance is present, however the AML issue has been analysed since 2001, when a multi-stakeholder workshop was held to review this issue and identify approaches for cleaning up these sites. This workshop provided recommendations and guiding principles that resulted in 1) an "Action Plan" that received the support of the Mines Ministers, 2) the establishment of an Advisory Committee on Orphaned/Abandoned Mines charged with undertaking the Action Plan. The Action Plane was called "National Orphaned/Abandoned Mines Initiative" (NOAMI) and included mining industry, federal/provincial/territorial governments, environmental non-government organizations and First Nations. The Advisory Committee created several Task Groups designed to address different aspects of the orphaned/abandoned mine problem. Actually guidelines have been designed to facilitate completion of a review of legislation (Acts, regulations, and instruments such as permits, licences, approvals) and related policies, programs, and practices that relate to orphaned/abandoned mine sites as well as contaminated and operating sites where there is demonstrated relevance to legacy issues. The ultimate goal is to ensure that approaches across jurisdictions are themselves consistent, certain, transparent, coordinated, and efficient.

Further information about this topic is hardly traceable since many states are not interested in this field or are starting now.

1.6.2 European Union

At the present no specific legislation about AML has been published. Some projects started, among these the most important are: the Land Restoration Trust (2004), the European Mining Heritage Initiative (2006) and the Eden Project.

1.6.3 Italian

Before that article n.17 of D.Lgs 22/97 took effect and became operative with D.M. 471/99, the environmental Italian legislation faced the question of the potential contaminated sites in a fragmentary way, examining each case one at a time. D.Lgs 22/97 and D.M. 471/99 established a standard procedure for the identification and characterisation of contaminated sites, the identification of toxic substances and the threshold concentration for contamination. Following the procedure proposed by this law the owner of a location

that shows clues of a probable contamination must communicate it to the organisations (Province, Region, Environmental Agency). According to the organisation the owner must execute the characterisation of the site, the sampling and the analyses of the environmental matrices (waters, soils and air). The site is defined as "contaminated" even if only one of concentration values of pollutant substances is higher than threshold concentration established by D.M. 471/99. Taking into account that these threshold concentrations for contamination (CSC) were calculated supposing that in the site occur the worst conditions, sometimes must be started useless remediation procedures throwing away money (owner) and time (organisations).

With D.Lgs 152/06 risk assessment is introduced to calculate threshold concentrations of contamination for each site (CSR). The first step is to identify the waste components at the source, including their concentrations and physical properties. After the source has been characterised, the pathways of the hazardous chemicals are analysed by quantifying the rates at which the waste compounds volatilise, degrade and migrate from the source. Finally, if the pathway analysis shows that the contaminant will come into contact with receptors; the hazard must be assessed with the aid of toxicological data (NAS, 1983; US EPA, 1989; Watts, 1998). Nowadays a lot of software allows developing risk assessment: Giuditta 3.1 (Provincia di Milano & URS Italia, 2006), Rome 2.1 (ANPA & Environ Italy, 2002) and RBCA (GSI Environmental Inc., 2008) are generic for "contaminated sites" while Mindec (BGS, 2002) was prepared for AML. All the software are characterised by the same procedure both for the hazard identification and for the risk characterisation. On the contrary, exposure assessment depends on used equations and toxicity assessment depends on used database. If only one of concentration values of pollutant substances is higher than threshold concentration calculated after the risk assessment procedure a remediation project must be edited. **Fig. 2** summarises the legislation process of D.Lgs 152/06.

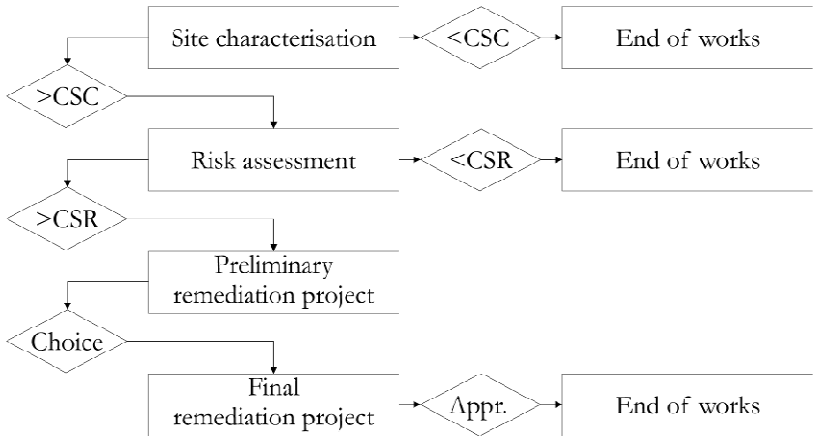

Fig. 2 - Flowchart of the procedure to assess the contamination state of a site according to D.Lgs 152/06. CSC = contamination threshold, CSR = risk threshold, Appr. = Approval

However there is no specific legislation about the management of "abandoned mining sites" but only general legislation about "contaminated site remediation" or "waste disposal". Isolate enterprise has been developed by Sardinia region which wrote guidelines for remediation and reclamation of AML (Regione Sardegna, 2003).

There are several problems related to the management of AML. The first problem is related to the identification of the person or the company who is liable to pollution. This subject must pay for remediation. For legislation in force the liable of pollution is "who caused the exceeding of threshold concentration". But now, after thirty years or more since closure of mining districts, it is very difficult to find who is liable to pollution. The second problem is related to the concentration of heavy metals into all the environmental matrices since a mining site is a natural geochemical anomaly (cfr. § 1.1), so it is a mistake to classify an AML as a potentially contaminated sites or as a contaminated sites taking into account only metal and metalloid concentrations into environmental matrices. Moreover, for AML it is very difficult to calculate metal and metalloid background concentration values (EPA, 2002b; Provincia di Milano & UNIMI, 2003; APAT & ISS, 2006b). The last problem is related to the cultural and historical heritage of AML. The remediation methodologies must be Chosen not only for their efficiency but also for their impact on morphology and structures of the AML that are considered cultural and historical heritage (D. Lgs. 42/04).

1.7 Remediation methodologies and technologies

Below are reported in succession the main technologies for mitigation of AMD processes (Johnson & Hallberg, 2005):

1.7.1 Water treatment

The objective o to restore the water quality after it has been polluted.

Wetlands: areas that are inundated or saturated by surface or ground water at a frequency and duration sufficient to support bacterial life to inhibit AMD reactions and that vegetation typically adapted for life in saturated soil conditions to metal bio-accumulation. Wetlands have the ability to remove metals from mine drainage and to neutralize AMD. Since wetlands are self-sustaining ecosystems, they may be able to remediate contaminated mine drainage as long as it is generated. Thus, they may represent a long-term solution to AMD, and to contaminated mine drainage in general. There are also sobering examples of failed designs of wetland treatment systems. There is not a single "shining example" which demonstrates that wetlands uniformly ameliorate degraded mine drainage. On the contrary, there are small examples from many sources generally supporting this idea. (Gazea et al., 1996; Sobolewski, 1997 and references therein; Von Der Heyden, 2005).

Permeable Reactive Barrier: in recent years, the difficulties of treating ARD (and other) contaminated groundwater has led to greater focus on the development of permeable reactive barriers (PRB). These passive treatment systems reduce or (potentially) eliminate on-going treatment costs and are designed to act as conduits for contaminated groundwater flow (U.S. EPA, 1998). Contaminants can be contained (immobilized) and/or transformed

(into non-toxic forms) within a PRB by adsorption, absorption, precipitation, redox, or biological processes (Puls, 1998) and represent a novel progression from inefficient groundwater pump and treat systems (National Academy of Sciences, 1994). Remediation of ARD with PRB generally relies on raising pH, and/or chemically- or biologically-induced sulphide precipitation (see Naftz et al., 2002). Relying on a single process limits the suite of metals that can be effectively removed, so multi-stage PRB are commonly employed for ARD remediation (Munro et al., 2004 and references therein).

1.7.2 Water drainage control

The objective is to prevent contact between the reactive minerals and the water.

Dry cover – Soil cover systems: this technology consists in creating a "sealing layer" that covers the spoil that is usually constructed from clay. Dry covers used for surface storage of reactive mineral spoils may also incorporate an organic layer (MEND, 2000; Swanson et al., 1997).

Water cover system: underwater storage has been used for disposing and storing mine tailings that are potentially acid-producing (Li et al., 1997). Again, the objective is to prevent contact between the minerals and dissolved oxygen. Shallow water covers may be used, and their effectiveness may be improved by covering the tailings with a layer of sediment or organic material, which has the dual benefit of limiting oxygen ingress and affording some protection against resuspension of the tailings due to the actions of wind and waves (MEND, 2000).

Groundwater depression: this methodology consists in placement of sumps and pumping systems that allow the droop of water table under sulphide material.

1.7.3 Sulphides oxidation control

The objective is to prevent the acidifying reaction due to the contact between sulphide and oxidising waters.

Flooding: as much as both oxygen and water are required to perpetuate the formation of AMD, it follows that by excluding either (or both) of these, it should be possible to prevent or minimise AMD production. A way in which this may be achieved is by flooding and sealing abandoned deep mines. The dissolved oxygen (DO2) present in the flooding waters (ca. 8–9 mg/l) will be consumed by mineral-oxidising (and other) microorganisms present, and replenishment of DO2 by mass transfer and diffusion will be impeded by sealing of the mine. However, this is only effective where the location of all shafts and adits is known and where influx of oxygen-containing water does not occur.

Neutralisation: Another suggested approach for minimising AMD production is to blend acid-generating and acid-consuming materials, producing environmentally benign composites (Gazea et al., 1996; Mehling et al., 1997; MEND, 2000).

Coating: A variant on this theme is to add solid-phase phosphates (such as apatite) to pyritic mine waste in order to precipitate iron (III) as ferric phosphate, thereby reducing its

potential to act as an oxidant of sulphide minerals. However, inhibition of pyrite oxidation using this approach may only be temporary, due to the process of "armouring" of the added phosphate minerals (Evangelou, 1998). Application of soluble phosphate (together with hydrogen peroxide) is one of the "coating technologies": the peroxide oxidises pyrite, producing ferric iron, which reacts with the phosphate to produce a surface protective coating of ferric phosphate. An alternative technique involving the formation of an iron oxide/silica coating on pyrite surfaces has also been described.

Chapter 2

Geo-environmental characterisation of AML

2.1 Geo-environmental models

The first step, moving towards the mitigation of the AML related risks, is the characterisation of the AML. It consists in the complete and ordered collection of the whole geological and environmental data about the AML.

The following steps, that are the organisation and the elaboration of the collected data, are known as "conceptual modeling of the site". When the site is a mining district these operations are called "geo-environmental modeling". Even if the geo-environmental modeling was created to support the exploration and the exploitation phases, nowadays it is also used for the evaluation and the management of the AML related risks. The major part of the technicians and the scientists that work in this field thinks that this is a fundamental step that allows to choose the best remediation methodology and to bind the remediation area.

In this chapter the geo-environmental model and their main applications are briefly described togheter with the fundamental parameters necessary to their building. Moreover the deficiencies of the used guideline for the compilation of a geo-environmental model and our proposals to overtake and to improve the methodology are pointed out.

2.1.1 Definition

Geo-environmental models are a compilation of geologic, geochemical, geophysical, hydrologic and engineering information pertaining to the "environmental behaviour" of geologically similar mineral deposits prior to mining and resulting from mining, mineral processing and smelting (Plumlee & Nash, 1995).

2.1.2 Uses

The main purpose of the geo-environmental models is to provide impartial geosciences information that can be used to better understand, anticipate, minimize, and remediate the environmental effects of mineral deposits and mineral-resource development. Land managers can use the models to develop perspectives concerning historical and potential future environmental impacts related to mineral deposits. In addition, the models should be of some assistance in developing mitigation strategies and for ecosystem-based land management plans. Many of the models include data, such as natural pre-mining

environmental baselines, which can be suitably applied during post-mining remediation endeavours. The models include objective information that is available to all concerned; they potentially benefit industry, regulators, land managers, and the general public. Some of the models present not only the potential environmental concerns likely to be associated with particular mineral deposit types, but also present information concerning how mineral-deposit-related environmental impact can be avoided, minimized, or remediated.

Establishment of pre-mining baseline conditions: it is more cost-effective, technologically feasible and realistic to remediate mine sites to baseline (typically somewhat contaminated) conditions that existed in mineralised areas prior to mining, rather than to conditions that prevail in unmineralised areas. When possible, the geo-environmental models include data on environmental signatures prior to mining or disturbance; such data are crucial to establish reasonable baseline conditions for diverse deposit types in various climates. Then these baseline models can then be used to establish analogues for pre-mining conditions in mining districts where historic mining activities have obscured pre-existing baseline conditions.

Mine planning and development: improved predictive capabilities provided by environmental models will enable mine planners to better anticipate, plan for and mitigate potential environmental problems, rather than to treat (with much greater technical difficulties and costs) environmental problems after they occur. Similarly, inherent geologic characteristics of a particular deposit can be exploited to help mitigate subsequent potential environmental problems. For example, carbonate-bearing wall-rock alteration commonly present on the fringes of deposits, or carbonate sedimentary rocks near some deposits, may be useful in acid drainage mitigation.

Remediation**:** the geo-environmental models summarize crucial geologic, geochemical and hydrologic information (such as geologic controls on ground water flow, ore mineralogy and materials geology) needed by engineers to develop effective remediation plans at mine sites. Some remedial plans currently in implementation ignore or dangerously oversimplify important geologic information. For example, adit plugging has been used or is proposed to reduce acid drainage from a number of mine sites. The geo-environmental models can be used to identify deposit types in which faults or other hydrologic conduits might be common, thereby reducing the effectiveness of adit plugging as a remedial solution. In addition, the models can be used to help identify likely types and orientations of faults and other hydrologic conduits present at remediation sites.

Abandoned mine lands issues: although mineral resource extraction has been carried out for several millennia, minimizing associated environmental effects, nevertheless it has received relatively little attention until the last decades. As a result, a very large number of historic mining and mineral processing sites (those operated prior to the last decades), that were abandoned once profitable ore was exhausted, are now potential sources of environmental contamination. In Italy, land management agencies are currently faced with the daunting task of identifying and prioritizing for remediation all abandoned mine sites on public lands. The geo-environmental models provide land managers with a low-cost

screening technique to help identify, prioritize for study and develop remediation plans for hazardous mine sites on public lands.

2.2 Fundamental parameters

Fundamental components that control the environmental conditions existing in naturally mineralised areas prior to mining and conditions that result from mining and mineral processing are accounted in succession.

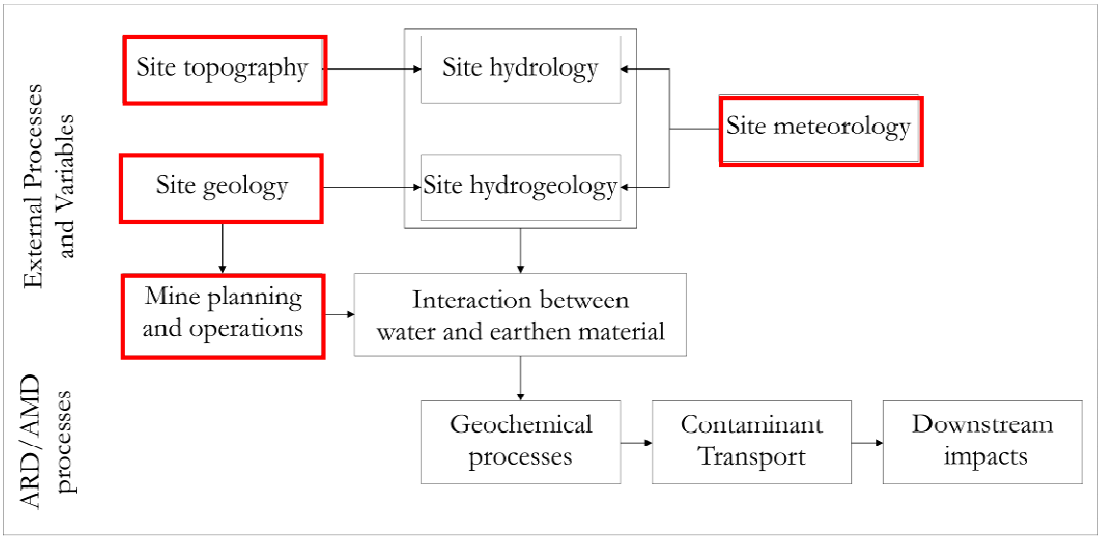

Fig. 3 - ARD modeling of waste rock piles (MEND, 2000c)

2.2.1 Topography

Topography and physiography affect the position and shape of ground water tables, which in turn control the extent to which mines or mineral deposits, are exposed to significant ground water flow. Moreover, in regions with steep topography, high mechanical erosion rates can greatly exceed chemical weathering rates such that new fresh sulphide minerals in highly altered rocks are continually exposed.

2.2.2 Geology

Ore and gangue mineralogy: the minerals present are the predominant control on environmental signatures.

Many sulphide minerals, including pyrite, marcasite, pyrrhotite, chalcopyrite and enargite generate acid when they interact with oxygenated water. Other sulphide minerals, such as sphalerite and galena generally do not produce acid when oxygen is the oxidant. However, aqueous ferric iron, which is a by-product of iron sulphide oxidation, is a very aggressive oxidant that, when it reacts with sulphide minerals, generates significantly greater quantities of acid than those generated by oxygen-driven oxidation alone. Thus, the amount of iron

sulphide present in a mineralised assemblage plays a crucial role in determining whether acid will be generated (Kwong, 1993; Plumlee, 1999).

Some non-sulphide minerals, such as siderite and alunite, can also generate acid during weathering if released iron or aluminium precipitates as hydrous oxide minerals. In contrast to acid-generating sulphide minerals, carbonate minerals, whether present in ore or in host rocks, can help to consume acid generated by sulphide oxidation. Other materials that may react with acid, though less readily than carbonate minerals, include aluminosilicate glasses or devitrified glasses (as in volcanic rocks) and magnesium-rich silicate minerals such as olivine and serpentine.

The relative rates, at which minerals react, play a crucial role in environmental processes, including acid-drainage generation and release of metals into the environment from solid mine or mineral processing wastes. Although the relative weathering rates of various sulphide minerals, as determined in laboratory, vary considerably from study to study (Jambor & Blowes, 1994; Smith et al., 1994), a general sequence of "weatherability" has been established (listed here in order of decreasing reactivity): pyrrhotite > chalcocite > galena > sphalerite > pyrite > enargite > marcasite > cinnabar > molybdenite.

As is well known to most field geologists, carbonate minerals are the most reactive of the acid-consuming minerals; among these, calcium carbonate minerals (calcite, aragonite) react most readily with acidic water, whereas iron, magnesium, or manganese carbonate minerals (dolomite, magnesite, siderite and rhodochroisite) tend to be the least reactive with acidic water. Aluminosilicate minerals tend to react much more weakly with acid water than carbonate minerals; Fe-, Mg-silicate minerals (such as olivine and serpentine) are the most reactive of the aluminosilicate minerals, whereas feldspars and quartz are the least reactive.

In the case of some industrial minerals such as fibrous silicate minerals, mineralogy plays a well-known, key role in determining adverse health effects associated with the intake of these minerals (Ross, in press). For example, chrysotile asbestos, the most common form of asbestos used in industrial applications in the United States, apparently has negligible effects on human cancer incidence, whereas crocidolite and amosite asbestos varieties are clearly linked to greatly increased human mortality rates from certain types of cancer.

Ore and gangue geochemistry: the major- and trace-element composition of mineral deposits and their host rocks strongly influence the suites of elements dispersed into the environment from given deposit types.

Major-element compositions (of iron, aluminum, carbon, etc.) influence, for example, types of precipitates formed in drainage water and can therefore influence trace metal transport mechanisms such as complexing.

Metal and trace element suites in ore are commonly reflected in environmental signatures of soil, water, and smelter emissions; for example, most copper-rich ore produces drainage water and smelter emissions with copper as the dominant trace element.

Ore and gangue texture: mineral textures and trace element contents influence the rate at which minerals weather and oxidize (Kwong, 1993; Plumlee et al., 1993). The grain size, which is the most important texture feature, seemed to be an efficient factor in controlling the speed of the AMD processes. Despite a decrease in porosity with decreasing particle size, thus limiting or inhibiting the water–rock interaction, the clayey and silty fractions represented a minor component of the material studied, which consisted of gravel- and sand-dominated sediments. Consequently, the other factor directly correlated to the decrease in the grain size (i.e. the increase in the surface/volume ratio) strongly favoured reactivity and rapid interaction with the circulating waters. Other texture features (i.e. habitus, micro-fractures, coating) could be related to AMD processes, but their analysis are much more expensive and their results much more difficult to interpret in objective way.

Secondary mineralogy: as deposits are exposed at the Earth's surface to processes such as weathering and erosion, new, more chemically stable, mineral suites develop.

Pre-exploitation: as weathering and erosion expose sulphide-bearing mineral deposits, associated potential environmental impact may be reduced as a consequence of sulphide mineral oxidation; some metals contained therein may be subsequently incorporated in relatively less soluble minerals from which metal mobility is limited. These less soluble minerals include hydroxides of iron (such as goethite and limonite), manganese, aluminum, and other metals, some sulphate minerals (such as anglesite, jarosite, plumbojarosite, and alunite), carbonate minerals (such as smithsonite, malachite and azurite) and phosphate minerals (such as turquoise and hinsdalite). The extent and mineralogical products of pre-mining oxidation are a complex function of deposit geology, hydrology, topography, and climate (Guilbert and Park, 1986 and references therein).

Post-exploitation: in contrast to secondary minerals formed by pre-mining mineral deposit weathering, many secondary minerals formed from weathered, sulphide-bearing ore and tailings wastes are quite soluble and can play an important role in controlling metal mobility from mine sites. Of these secondary minerals, the most common and environmentally important are metal sulphate salts of calcium (gypsum), iron (jarosite, melanterite, copiapite, rhomboclase, and many others), copper (chalcanthite, brochantite, and others), zinc (goslarite), magnesium (pickeringite), and other metals. These salts form efflorescent coatings on rocks, fractures, and mine workings, and are produced by evaporation of sulphate-rich drainage water during dry periods or in areas sheltered from water runoff. The salts have variable compositions, and serve as solid storage reservoirs for both metals and acid. Due to their high solubility, the salts dissolve rapidly during rainstorms or snowmelt; metals and acid released by salt dissolution can lead to temporary but significant degradation of surface- and ground-water quality. Water remaining after storm or snowmelt events can itself become a highly reactive fluid that enhances sulphide mineral oxidation; eventually, these fluids evaporate completely and reinitiate the salt precipitation-dissolution cycle. The particular secondary salts formed depend strongly upon deposit geology, climate, and the extent of evaporation.

Structural setting: the access of weathering agents such as ground water and atmospheric oxygen are controlled by the structural and physical characteristics of mineral deposits. For example, faults can focus groundwater flow, thereby promoting water access to sulphide-rich material and inhibiting contact with potential acid-buffering agents in wall rocks. On the contrary, clay layers have low permeability and inhibit ground-water flow; consequently, sulphide minerals under clay layers can remain unoxidized, even when they are well above the water table.

2.2.3 Climate

Also the climate affects the "environmental behaviour" of mineral deposits. The amount of precipitation and prevailing temperatures influence the amount of water available as surface runoff, the level of the water table, rates of reaction, amounts of organic material, and other parameters that affect weathering of mineralised rocks and ore.

In general, water tables are shallow in wet climates and deep in semi-arid climates. However, depths to the water table can be highly variable across short distances within a mining district.

Deep weathering (oxidation) profiles tend to develop in semi-arid climates.

Leaching of elements tends to be intense in humid tropical climates and modest in arid deserts. In humid to semi-arid climates, leaching and transport tends to be downward, whereas in arid climates upward movement of water by capillary action becomes a significant process.

As described below, mine-drainage water associated with sulphide-mineral-bearing deposit types, which generate acid mine water, tends to have lower pH and higher metal contents in dry climates than in wet climates due to evaporative concentration of acid and metals. However, dry-climate mine drainage water with low pH and high metal content may have less environmental impact than in a similar deposit in a wet climate setting because of the relatively small volume of surface drainage water. Evaporative processes can also operate in wet climate settings characterised by seasonal wet and dry periods. Relative shifts in pH and metal content for a given deposit type in different climate settings are still very much less than shifts due to differences in geologic characteristics, however.

Very cold climate can have several consequences for environmental processes. First, weathering rates decrease substantially in very cold climates; unweathered sulphide minerals may be abundant at the surface where climate favours permafrost formation. However, during short summer seasons in areas dominated by cold climate, weathering of exposed sulphide minerals can lead to formation of highly acidic water (again depending upon the mineral-deposit geology). Freeze-concentration of acid water can also lead to increased acidity and metal contents.

Climate effects on environmental impact downstream from mineral deposits can be significant. For example, downstream dilution (and therefore environmental mitigation) of acid mine water by dilute water draining unmineralised areas is much more efficient in wet

climates than in dry climates. In contrast, downstream mitigation is enhanced in dry climate settings by the increased buffering offered by solid material in stream beds.

Systematic studies of environmental geochemistry as a function of climate are in their infancy. In detail, the subject is complex, but some generalizations can be made by considering element mobility, deposition, and adsorption in soil and ore deposit supergene zones (Rose et al., 1979).

2.2.4 Mine planning and operations

Mining and milling methods employed are typically influenced strongly by the geologic characteristics of deposits. A wide variety of mining and mineral processing methods are currently in use; even more have been used over the course of historic mineral extraction activities. Both may change significantly over the life of a mine as technology evolves.

As with climate, also mining and mineral processing methods have effects on most environmental signatures In most cases, abundances of acid and metals in mine water draining deposits with similar geologic characteristics progressively increase from water draining underground workings, to that draining mine dumps, to that draining mill tailings, and finally, to that collecting in open pits. This trend reflects increasing access to weathering agents (water and atmospheric oxygen); increased surface area of sulphide minerals exposed to weathering and increased opportunities for evaporative concentration. In addition, the size of particles produced by milling and beneficiation processes can dramatically influence the extent of environmental impact. Finely milled ore and tailings, which enhance metal adsorption while enhancing sulphide oxidation, can more rapidly generate acid and are more likely to be distributed by wind and water than their more coarse-grained equivalents.

One important way in which mineral processing techniques are of primary importance relates to techniques that introduce potentially problematic chemicals. For example, mercury amalgamation was widely used as a gold extraction technique in the last century. As a result, soil and sediment may be mercury contaminated at many sites where amalgamation was practiced historically, but would not otherwise be characterised by elevated mercury abundances.

2.2.5 Hydrology and hydrogeology

Hydrology is mainly influenced by topographic features of the site. Anyway the mine operations can deeply modify the natural setting both through the change of the topographic features due to excavation and dumping works and the building of artificial drainage canals.

Hydrologeology is strongly controlled by geologic characteristics of deposits, including whether ore is present as veins or lenses, both of which can focus ground water flow, or whether low-permeability barriers to ground water flow, such as clay-altered wallrock, are present.

Both hydrology and hydrogeology have an environmental key role since they drive the water-earthen material interaction.

2.2.6 Geochemistry

As mentioned above AMD processes are the main cause of environmental pollution related to AML. The development of AMD processes begins when earthen material containing sulphides reacts with water in oxidant conditions.

For this reason the evaluation of AMD potential of earthen material is of primary importance. At the present time two methodologies are available for the evaluation of this parameter and are classified as "static tests" and "kinetic tests".

The first methodology is based on 1) the calculation of sulphuric acid that the earthen materials can produce starting from the analytic determination of S content of the earthen materials and the stoichiometry of the Eq. 4 reaction and 2) the calculation of sulphuric acid that the earthen materials can neutralize starting from titration tests. After the analytic determination of S content of the earthen materials, it is usually assumed that a) all the S is in the form of sulphide, b) all the sulphide is in the form of pyrite and c) the Eq. 4 reaction is quantitative. The results are expressed in H_2SO_4/t that the earthen materials can produce and the samples are plotted in a binary diagram and are grouped into 3 classes: "AMD possible but not persisting in time due to low S content", "AMD possible and persisting in time due to high S content", " AMD impossible".

Kinetic tests founds on the reproduction of the natural processes in laboratory. They consist in the leaching of a known quantity of earthen material by a known quantity of water. The result is a coming out water that represents a surrogate of the surface or ground waters that pass through the mine dumps. The advantage of this methodology is the possibility to obtain direct information about the chemical and the physical properties of the drainage waters. On the contrary these tests could need too long time compared to the attending time and it is very difficult to reproduce the real weather conditions.

2.3 Case history

Even if the Italian AML census is already available (APAT, 2006) and some of these sites were included into the lists of sites that need a priority remediation, only few of them have already undergone an assessment was done.

For the majority of AML nothing has been done, for a few dozens of them a process of conservation, protection and promotion is in progress (The Geominerary Park project – ISPRA, 2008) while only for some AML belonging to "Parco Tecnologico e Archeologico delle Colline Metallifere Grossetane" (Regione Toscana, 2002) and to "Parco Geominerario Storico e Ambientale della Sardegna" (RAS & Comune di Villaputzu, 2003, 2004; MATT et al., 2003a, 2003b, 2004 and 2006) the environmental assessment has been done.

The case history is confined to these reports since the quality of the geo-environmental modeling is as good as the world-wide reports.

The fundamental parameters are well-examined, so these geo-environmental models built following the previous guidelines, provide a preliminary idea about 1) the activity or

inactivity of AMD processes in the whole area, 2) the elements or the substances that exceed the law limits and 3) the potential targets of the pollutants.

However some remarks can be made to these works:

- the identification of the pollution sources was performed in an approximate way by means of field survey, while the evaluation of their geometry (morphology and volume) is missing;
- the evaluation of the heavy metal contents in the earthen materials was done by means of a raw geostatistical elaboration based on core drilling sampling. Even if the geostatistical elaboration is more than that requested by law, however the number of samples and their location do not allow a complete and correct characterisation of earthen materials;
- the occurrence of AMD processes was deduced only by the water analyses;
- nothing is said about the persistence in time of processes.

2.4 Innovative components

The previous information can be improved with 1) the mine dumps characterisation, 2) the spatial analysis of the earthen materials features, 3) the geochemical risk assessment and 4) the estimation of the persistence in time of AMD processes.

2.4.1 Mine dumps characterisation

Mine dumps are the waste products of exploitation, composed mainly of rocks with metal concentration too low to be economic but rather high to be a source of environmental pollution. This feature, joined with the loose sediment composition of the mine dumps, makes them the main source of pollution of AML.

At present day the mine dumps can be identified and characterised by remote image analysis, field investigations or stratigrafic correlation of core logs.

Remote image analysis has the advantage of cheapness since now the aerial view pictures are available free for the major part of the national area (Google Earth – Live Search) and/or it is possible to purchase the high definition ones at low cost. The problem of this methodology is that the little experience of the operator can lead to wrong identification of the mine dumps. The most common mistake is to associate the mine dumps with the unvegetated areas. This mistake can involve an overestimation of the mine dumps when the unvegetated areas, like the excavation fronts, are associated to the occurrence of mine dumps or, vice versa, an underestimation of the mine dumps when they are vegetated and so are not identified. Another lack of the remote image analysis is the inability to determine the thickness of the mine dumps and their chemical and physical features.

The field investigation (geological survey) allows honing the results obtained by remote image analysis. Only with a direct observation of the earthen materials it is possible to

distinguish the outcropping rocks from disaggregated earthen materials that typically compose the mine dumps. The weak spot of this methodology is the difficulty to distinguish between some disaggregated deposits, like landslide deposit, and the anthropic ones. Moreover, in the same way as by the remote image analysis, there is the inability to determine the thickness of the mine dumps if vertical cross sections do not occur. The most common mistake is to overestimate the volume if the waste materials take up only few centimetres above the outcropping bedrock. A subordinate problem can be related to the occurrence of thick vegetation on the mine dumps.

The evaluation of the thickness of the mine dumps can be done starting from a well-planned core drilling survey and the following stratigraphic interpretation. This is the only one methodology that allows the sampling of deep earthen material for the analysis of the chemical and physical features. Moreover the execution of core drilling allows the determination of geotechnical and hydrogeological parameters. The biggest problems related to this methodology are the high costs and the restriction that the data are representative of a line.

A preliminary low-cost identification of mine dumps could be done by means of digital elaboration of topographic maps. This operation allows to identify and to evaluate the morphology and dimension of mine dumps having bibliographic data (topographic maps of different years) and CAD software (Servida et al., 2009).

Mine dumps characterisation could be completed and refined by Electrical Resistivity Ground Imaging (ERGI) investigations (Mele et al., 2007) that enable to reduce direct investigation number and, consequently, to reduce costs and acquisition time. Moreover ERGI investigations supply 3D information concerning a more extended area.

2.4.2 Variables spatial analysis

Often geo-environmental models are built with a great number of geological and environmental data, collected further to field sampling and laboratory analysis that are not well-utilised. Some of these variables are the contaminant concentrations, the mineralogical composition, the grain-size and the acidic potential of earthen materials that are of primary importance for the characterisation and the risk analysis related to the AML.

In different guidelines for the execution and redaction of geo-environmental models there is a minimum number of environmental matrix samples to collect (usually proportional to the surface of the AML to characterise) and the indication of the geometrical distribution to use during the sampling (**Fig. 4**a). However, most of the guidelines suggest associating the point value of the variables to the surrounding area without a spatial analysis (**Fig. 4**b).

Considering the high costs and the long time necessary to the data acquisition, it is useful to spend a little bit of time more to improve the spatial analysis. This allows to estimate the value of any variable in all the points that were not sampled (**Fig. 4**c) to obtain a contour map that covers the whole investigated area (**Fig. 4**d).

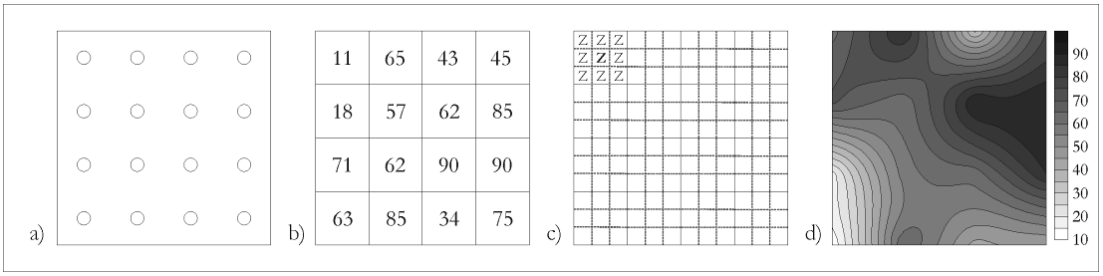

Fig. 4 - a) possible location of samples for the characterisation of a squared area, b) association of the analytical value to the area surrounding the sampling position, c) discretization of the area in sub-units and estimation of the variable value z, starting from the whole georeferenced analytical results and a suitable interpolation method that considers the spatial relation of the variable value z, d) graphical display of the estimation

The spatial analysis allows 1) to round in the best way the geo-environmental model preserving the investment, 2) to quantify the area that is characterised by a variable into a range, above or below a threshold value and 3) to lay the foundations for a more solid and realistic hydrogeologic and geochemical modeling.

The only flaw related to the spatial analysis made by interpolation is that the distribution of the variables will be always more homogeneous than in the reality.

2.4.3 Geochemical hazard assessment

Geochemical hazard related to sulphide-bearing AML could not be evaluated taking into account only the metal and metalloid concentrations of terrains, since it is high by nature. For these reason it was proposed to calculate the natural background of different contaminants into the earthen materials of each site and then to use this value as CSC (EPA, 2002b; Provincia di Milano & UNIMI, 2003; APAT & ISS, 2006b).

It is suggested to evaluate geochemical hazard starting from the combination of high metal and metalloid concentrations and of the acid production or neutralising potential of terrains by AMIRA procedure (IWRI & EGI, 2002). Hazard evaluation was performed by geostatistical analyses, resulting from 1) the interpolation of the terrain chemical features on the whole area, 2) the overlapping of previous results and 3) the adding of the topographic setting. This approach allows to identify the areas where the presence of metal and metalloids is really hazardous. It also supports the choice of areas that need any treatment.

2.4.4 AMD time persistence evaluation

Since AMD processes have a key-role in environmental damages from mining pollution, it is important to know their persistence in time. The fate of these processes is the natural attenuation, even if it happens more or less quickly.

Considering that the works for the characterisation, the safe keeping and the remediation of an AML can last from a year to some years and can cost millions of Euros it is clear the

importance to know before the beginning of the works the persistence in time of the AMD processes.

No studies about this topic have been done yet. In a preliminary step, the persistence of AMD processes could be calculated starting from common data as yearly rainfall, mining waters pH and acid production or neutralising potential of terrains.

These few input data allow to obtain a number of years indicative of the potential persistence in time of the processes. Even if this number could be refined, the mere order of magnitude is useful to classify the persistence of the processes into 3 classes: low (<10 years), middle (<100 years) and high (>100 years).

Starting from the persistence class it is possible to decide if the remediation activity is useful or not. In an AML belonging to the low persistence class the time for the natural attenuation and for the remediation works are comparable, so in some cases it could be better to do nothing. On the contrary the other classes need remediation. The estimation of the persistence is useful also to calculate the costs of the different remediation strategy.

Chapter 3

Methodology

To develop a geo-environmental model to AMD hazard evaluation the following steps were performed:

- collection of the available scientific and technical data about the sites;
- field collection of the lacking or "incomplete" data;
- sampling of waters and earthen materials;
- chemical and physical analyses of earthen materials and waters;
- data processing.

3.1 Historical data

Besides the routine bibliographic research about the AML under investigation, also a historical data research was accomplished.

The main purpose of this research was to find topographical maps reproducing the different physiography of the AML to the elapse of time and mining works. These maps were at the base of the topographic elaboration (cfr. § 3.5.1) that allows to have a first idea about the location of the excavation and of the disposal area to plan the following investigations.

Moreover sketch maps of the mining work and annual reports about the mining activity were considered useful to integrate the preliminary data.

The problems related to the collection of historical data about AML are that:

- not all the AML have a historical archive;
- if an AML has a historical archive, this is not often in the same place of AML;
- if an AML has a well-known historical archive, this rarely contain all the data or the data are in disorder.

However, the time dedicated to search historical data is a little loss in the worst case, while it is a great improvement in the best case.

3.2 Field investigations

3.2.1 Electrical Resistivity Ground Imaging (ERGI)

Near surface direct current electrical resistivity method (Dahlin, 2001) is a geophysical tool routinely used under a variety of field conditions and geological settings in environmental geology (Guerin et al, 2004; Godio & Naldi, 2003; Vichery & Hobbs, 2003; Beresnev et al., 2002).

A 2-D electrical resistivity survey (**Fig. 5**) requires the use of several electrodes driven into the ground surface at constant offset (electrode separation) along a straight line and it consists in measuring subsurface apparent resistivity by injection of an electrical current (current dipole) and measurement of the voltage drop between two electrodes (potential dipole) due to the current flow. The measurements are made by increasing the separation between current dipole and potential dipole in order to obtain information at increasing depths along the survey line. Generally, exploration depth is a function of the electrical properties of the investigated terrains and of the technical arrangements; in low contrast terrains, for a 48-electrodes Wenner-Schlumberger array (**Fig. 5**), resistivity data to a maximum depth of 1/5 of the total length of the array can be obtained.

Processing of field resistivity data is performed through finite-difference inversion routines (Loke & Barker, 1995) to invert the field apparent resistivity data set in order to obtain a 2-D model of subsurface real electrical resistivity distribution. For this study RES2DINV software (Loke, 1999) was used. The 2-D geoelectrical model consists of a large number of blocks with different resistivities whose spatial extent (survey resolution) depends on electrode spacing. The inversion routine works with a least-square optimization method (Loke & Barker, 1995; 1996) in order to minimize the root mean square (survey accuracy; RMS% error) between field apparent resistivities and the theoretical apparent resistivities simulated for an arbitrarily shaped 2-D subsurface geoelectrical model.

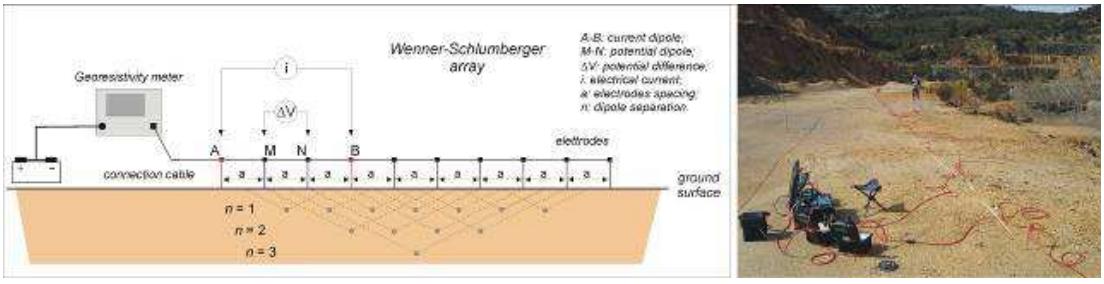

Fig. 5 - 2-D electrical resistivity imaging: acquisition scheme (left) and field arrangements (right)

In order to calibrate the instrumentation it is necessary to perform at least a 2-D resistivity section located on an outcrop that shows both waste rocks and bedrock, or at least one of them. In most cases this is a condition easily achievable, since in AML there are often

abandoned open pits with exposed quarry bench. This allows to associate the geological bodies with a range of electrical resistivity.

3.3 Sampling

3.3.1 Earthen materials

A grid sampling was selected to a preliminary collection of earthen material samples. This strategy allows an uniform coverage of the area, it is easy to use and also enables the estimation of spatial correlations, the identification of patterns and the increase in size of samples (US EPA, 2002). The choice between a central aligned square and an unaligned grid was only related to the AML logistic.

<table>
<tr><td colspan="4">ABANDONED MINE LAND:</td></tr>
<tr><td colspan="2">Sample identifier:</td><td colspan="2">Sampler:</td></tr>
<tr><td colspan="2">Date:</td><td colspan="2"></td></tr>
<tr><td colspan="4">Geographic coordinates:</td></tr>
<tr><td colspan="2">X (GPS):</td><td colspan="2" rowspan="3">Sketch map of location:</td></tr>
<tr><td colspan="2">Y (GPS):</td></tr>
<tr><td colspan="2">Z (pressure altimeter):</td></tr>
<tr><td colspan="4">Physical features:</td></tr>
<tr><td colspan="4"><u>Nature of earthen material:</u></td></tr>
<tr><td>□ Tailings</td><td>□ Waste rocks</td><td>□ Landslides dep.</td><td>□ Soil</td></tr>
<tr><td colspan="4"><u>Grain size:</u></td></tr>
<tr><td>□ Cobbles</td><td>□ Gravel</td><td>□ Sand</td><td>□ Silt and mud</td></tr>
<tr><td colspan="4"><u>Moisture:</u></td></tr>
<tr><td>□ Wet</td><td>□ Humid</td><td>□ Dry</td><td></td></tr>
<tr><td colspan="4"><u>Vegetation:</u></td></tr>
<tr><td>□ Wood</td><td>□ Brushwood</td><td>□ Meadow</td><td>□ Absent</td></tr>
<tr><td colspan="4">Pictures:</td></tr>
<tr><td colspan="2">Sampling site:</td><td colspan="2">Sample:</td></tr>
</table>

Tab. 2 – Field card for identification and description of earthen materials

Planned samples were collected at 0.25-0.50 m depth after removing the superficial part. They were put into a plastic bag and labelled. At the same time two pictures, one of the sample site and one of the collected sample, were made and a preliminary description of the samples was done following **Tab. 2**, which contains the main measures and field observations.

3.3.2 Waters

The superficial water sampling was planned considering both the topography and the weather features.

ABANDONED MINE LAND:			
Sample identifier:		Sampler:	
Date:			
Geographic coordinates:			
X (GPS):		Sketch map of location:	
Y (GPS):			
Z (pressure altimeter):			
Hydrological features:			
Nature of water			
□ Superficial	□ Underground	□ Spring	□ Adit
Discharge (l/s)			
Chemical and physical features			
Temperature (°C)		Eh (mV)	
pH		Conductivity (μS/cm)	
Anions			
Alkalinity ($CaCO_3$ mg/l)		Sulphate (mg/l)	
Chloride (mg/l)			
Pictures:			
Sampling site:		Sample:	

Tab. 3 - Field card for identification and description of waters

The first information allows the sampling of:

- upstream waters, that have not yet interacted with AML earthen materials;
- "central" waters, that are interacting with AML earthen materials;
- downstream waters, that have already interacted with AML earthen materials.

The second information allow to have water samples at least after a dry period and after a wet period to evaluate the variation with changing weather features.

After field measurements, the water samples were collected as:

- filtered samples (using 0.45 μm Millipore filters) for anion analyses;
- filtered samples acidified with 7M ultrapure HNO_3 for major, minor and trace element analyses.

3.4 Analyses

3.4.1 On-site water analysis

Temperature, pH, Eh and conductivity were determined in the field with a WTW Multiline P3 Set equipped with:

- combined pH-temperature electrode "SenTix41", range of measure from -2.00 to 16.00, precision ± 0.01;
- redox electrode "Sentix ORP", range of measure from -1999 to 1999 mV, precision ± 0.3 mV in a range of temperature between 15°C e 35°C;
- connect conductivity cell TetraCon 325®.

The filtered rates were analysed by spectrophotometric technique to determinate chlorides, sulphates and nitrates. For these analysis Orbeco-Hellige Model 975MP Portable Analyst was used.

3.4.2 Off-site water analysis

The filtered and acidified rates were analysed by FAA spectrophotometry (Perkin Elmer 2380) to determine Na^+, K^+ Ca^{++} and Mg^{++}. The spectrometer works with Hollow Catode Lamps in an air-acetylene flame. For the whole element determinations a La-chloride - Cs-chloride buffer of 100 ppm was used.

3.4.3 Grain size analysis

The particle size distribution was obtained by dry sieving. Since earthen materials are often characterised by coarse fractions, the analysis was split into two steps: the first step on-situ and the second step in laboratory. This allowed to work with a representative quantity of

earthen materials, that for samples with particles bigger than 5 cm is of about 25 kg following CNR UNI 10006 prescriptions.

The first part of the analysis was conducted on-site separating the fractions >20 mm, 20-12 mm, 12-4 mm and <4 mm. This work was performed by hand using sieves built on purpose. After this analysis about 2 kg of <4 mm fraction was sampled and brought to laboratory.

Here, the second step of grain size analysis was conduced: through dry sieving with a Controls D411 Automatic Sieve Shaker, fractions of 4-2 mm, 2-1 mm, 1-0.5 mm, 0.5-0.025 mm, 0.25-0.125 mm, 0.125-0.0625 mm and <0.0625 mm were separated.

3.4.4 X-ray diffraction (XRD)

The XRD analyses were carried out using a Philips PW3710 diffractometer equipped with a Co-anode (CoKa radiation; current 40 mA, voltage 40 kV) and interfaced with PC-APD software for data acquisition and processing. Phase identification of the <2 mm fraction was performed under the following conditions: angular range 5–120° 2θ, step 0.020° 2θ, sampling time 1-2 s per step.

3.4.5 X-ray fluorescence (XRF)

Earthen material fraction <2mm were ground in an agate mill to a fine powder for subsequent geochemical analyses.

Rock-forming elements and S_{tot} composition for each sample were determined by XRF analysis on powder discs using an automated Philips PW 1400 spectrometer.

Rock-forming elements: since the geochemistry of samples varies greatly, the XRF calibration straight line was built using a suitable set of standard materials.

For earthen materials coming from acid rocks, the calibration line was built adding to acid rock standards some standard rocks with low SiO_2 and high Fe_2O_{3tot} contents. The lower detection limit was put at 35.00 wt % for SiO_2 and upper detection limits were put at 30.00 wt % for CaO, 10.00 wt % for MgO and 50.00 wt % for Fe_2O_{3tot}.

For earthen materials coming from basic and ultra-basic rocks the calibration line was built adding to basic rock standards some standard rocks with high Fe_2O_{3tot} contents.

Total Sulphur: since the peculiarity of the environmental matrix, the XRF calibration straight line was built using different samples of S-rich mine dumps previously analysed.

3.4.6 Inductively Coupled Plasma - Atomic Emission Spectroscopy (ICP-AES)

Trace element concentrations were determined by ICP-AES (Jobin Yvon JY24) on solutions obtained by acid digestion (0.25 g powder leached with 6 ml 30% HCl Suprapure and 2 ml 65% HNO_3 Suprapure) in a closed microwave oven (Milestone 1200 Mega). The analyses were performed in two phases, following the usual analytical procedures.

In the first step, selected samples were analysed for 25 elements: Ag, As, Au, B, Ba, Bi, Cd, Co, Cr, Cu, Ga, Hg, La, Mo, Ni, Pb, Sb, Sc, Se, Sr, Th, U, V, W and Zn.

In the second step, the trace elements that 1) had shown the highest variability, 2) are known to be toxic and 3) have a geo-environmental meaning were selected for further analyses on the whole samples of the square grid.

3.4.7 AMD evaluation

The AMD evaluation of earthen material samples was based on the AMIRA procedure (IWRI & EGI, 2002) which is a revision of the Sobek procedure (Sobek, 1978). The Acid-Base Account values (ABA, that involves static laboratory procedures to evaluate the balance between acid generating processes and acid neutralising processes) are referred to as the Maximum Potential Acidity (MPA) and the Acid Neutralising Capacity (ANC), respectively.

MPA is an estimate of the amount of acid that the sample can release by complete oxidation of sulphides, expressed as kg H_2SO_4/t. The evaluation of MPA by the AMIRA standard procedure is based on the conservative assumption that all S is present as pyrite. This simplification may overestimate the AMD as other sulphides with higher Me/S ratio have lower acid generation potential than pyrite. Moreover, such an overestimation can give marked and unrealistic results where high portions of S are present as non-acid generating phases (i.e. sulphates). For this reason, in addition to the standard MPA assessment using total S, a second MPA value was calculated using sulphide S instead of total S. The determination of sulphate was performed by Leco analysis at the ACME Laboratory of Canada.

ANC is an estimate of the buffering capacity of the sample expressed as kg H_2SO_4/t that the sample is able to neutralise. It was experimentally determined by titration preceded by a "fizz test" as described by Sobek et al. (1978). When a negative value of ANC is obtained, it is reported in as 0.00, indicating the sample incapacity of neutralisation.

The difference between MPA and ANC is referred to as the Net Acid Producing Potential (NAPP). NAPP is a theoretical value commonly used to indicate if earthen material has potential to generate AMD. The NAPP is also expressed in units of kg H_2SO_4/t and when negative it indicates that a sample may have sufficient ANC to prevent acid generation. Conversely, if the NAPP is positive a material may be acid generating.

3.5 Data processing

3.5.1 Topographic modeling

To simulate the topographic evolution of the studied areas, topographic maps of AML were digitalised and were georeferenced with AutoCAD 2004 software; moreover, a Digital Terrain Model (DTM) of each map was computed.

The mining maps relative to different AML and different periods were covered with an appropriate square grid and the nodes of which were quoted. The data was gridded with

kriging interpolation method by SURFER 8 software. This method has allowed the obtaining of a 3D topographic map of the area relative to different periods. The best conditions occur when at least 3 maps are available:

- a map previous to the beginning of the exploitation works;
- a map subsequent to the end of the exploitation works;
- a map subsequent to the end of the reclamation works.

To assess the amount of ore material removed during the exploitation period and earthen materials piled up, these maps have been processed with SURFER 8 software. Above all, the subtraction between the topographic surfaces relative to the different periods has been made, followed by the calculation of the volumes both of removed and piled up material.

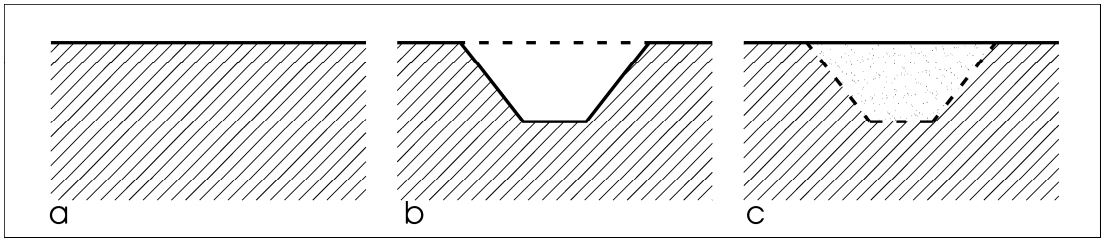

Fig. 6 - Sketch representing the evolution of topographic surface of an AML: a) before exploitation, b) after exploitation and c) after piling up of waste rock material

3.5.2 Statistical and geostatistical analyses

Major element concentrations, heavy metal contents and AMD values were processed by means of statistical and geostatistical methods in all the investigated area.

At first, an univariate descriptive analysis of chemical data was performed to describe the populations of the data and to identify outlier values.

Geostatistics was based on the theory of a regionalized variable (Matheron, 1963), which is distributed in space (with spatial coordinates) and shows spatial autocorrelation such that the samples close together in space are more alike than those that are further apart.

The geostatistical approach uses the technique of variogram (or semi-variogram) to measure the spatial variability of a regionalized variable, and provides the input parameters for the spatial interpolation of kriging (Krige, 1951; Webster and Oliver, 2001). It relates the semi-variance, half the expected squared difference between paired data values Z(x) and Z(x+h), to the lag distance h, by which locations are separated:

$$\gamma(h) = \tfrac{1}{2} E [Z(x) - Z(x+h)]^2$$

For discrete sampling sites, such as earthen material samples, the function is estimated as:

$$\gamma(h) = \frac{1}{2} N(h)^{-1} \sum_{i=1}^{N(h)} [Z(x_i) - Z(x_i+h)]^2$$

where $Z(x_i)$ is the value of the variable Z at location of x_i, and N(h) is the number of pairs of sample points separated by the lag distance h.

The variogram plot is fitted with a theoretical model which provides information about the spatial structure as well as the input parameters for kriging interpolation.

Kriging (Krige, 1951) is regarded as the Best Linear Unbiased Estimator (BLUE), which is a process of a theoretical weighted moving average:

$$\hat{Z}(x_0) = \sum_{i=n}^{n} \lambda_i Z(x_i)$$

where $\hat{Z}(x_0)$ is the value to be estimated at the location of x_0, $Z(x_i)$ is the known value at the sampling site x_i. Altogether there are *n* sites used for the estimation, and the number *n* is selected based on the size of the moving window and user definition. Contrary to other methods (such as inverse distance weighted), the weighting function λ_i is no longer arbitrary, and it is calculated based on the parameters of the variogram model. To ensure that the estimate is unbiased, the weights need to sum to one:

$$\sum_{i=n}^{n} \lambda_i = 1$$

and the estimation errors (or kriging variances) need to be minimised.

Natural neighbour gridding method was sometimes used for representing areal distribution of any variables even though a spatial relation was assessed with variogram analysis. This choice was supported by negative concentration areas, which have no physical significance, resulting by kriging interpolation without outlier removal.

3.5.3 Geochemical hazard mapping

To evaluate the contamination not only the heavy metal contents but also reciprocal relation between NAPP and heavy metal contents were considered. Consequently, any earthen material area can be classified into one of these 6 classes, characterised by:

1. NAPP>0 and at least one heavy metal concentration higher than "Commercial or Industrial Area (CIA)" limits defined by D.Lgs 152/06;
2. NAPP>0 and at least one heavy metal concentration higher than "Residential Area (RA)" limits defined by D.Lgs 152/06;

3. NAPP>0 and heavy metal concentrations lower than RA limits;
4. NAPP<0 and at least one heavy metal concentration higher than CIA limits;
5. NAPP<0 and at least one heavy metal concentration higher than RA limits;
6. NAPP<0 and heavy metal concentrations lower than RA limits.

The geostatistical analysis of these parameters allows the evaluation of areas belonging to the different classes and the delimitation of them. Mathematical interpolation, based on geostatistical refining of data, has allowed the subdivision of each square, representative of one sample, in 9 subareas and to attribute each of them to one of the classes defined above.

As a result of the overlaying of heavy metal map and NAPP map by means of GIS method it is possible to obtain the area belonging to different classes and their spatial distribution.

AMD processes produce a geochemical hazard when acid waters interact with heavy metal rich-materials. Such hazard also depends on the mobility of heavy metals, that, in this area, has been assessed by geochemical analyses of waters. So, it is possible to say that:

- the worst environmental situation occurs in the areas that belong to class 1 or 2 because these earthen materials are characterised by NAPP>0 and heavy metal concentrations that exceed RA or CIA law limits and AMD processes can start;
- a negative environmental situation occurs in the areas that belong to class 3 because these earthen materials can produce acid waters;
- a variable environmental situation occurs in the areas that belong to class 4 or 5 because these earthen materials can neutralize waters but, at the same time, they can be sources of heavy metals;
- a positive environmental situation occurs in the areas that belong to class 6 because these earthen materials can neutralize waters.

This analysis is static while a quantitative approach to hazard evaluation should consider NAPP values and spatial relationships between cells.

For example, when an area with NAPP>0 (class 1, 2 or 3) is located upstream of an area with NAPP<0 and heavy metal concentrations higher than RA or CIA law limits (class 4 or 5), this could be a hazardous situation if $|NAPP_{upstream}|>|NAPP_{downstream}|$ as the acid waters produced upstream are not completely buffered downstream and they can then leach heavy metals from the area located downstream. On the other hand, if $|NAPP_{upstream}|<|NAPP_{downstream}|$ the acid water produced upstream can be neutralised from the earthen materials located downstream.

So, these results are a starting point for a quantitative approach that is being developed through a dedicated software (Servida et al., in progress).

3.5.4 AMD time persistence evaluation

The input data to the evaluation of the time persistence of AMD processes were:

- yearly rainfalls and temperatures (subdivided into months);
- area of drainage basin;
- pH of rainfall and drainage water;
- acidic potential, reactive thickness and density of earthen material;

The fist step attends to calculate the volume of water that react with the earthen material. A general water balance equation is:

$$P = Q + E + \Delta S$$

where P is precipitation, Q is runoff, E is evapotranspiration and ΔS is the change in storage (soil or bedrock). Assuming that the AMD processes involved only the superficial waters (because this is the earthen material that interacts more with atmospheric agents and is the depth at which earthen material samples were collected), it is necessary to subtract the evapotranspiration and the infiltration rate from precipitation to obtain the runoff.

The evapotranspiration rates were calculated according to Thornthwaite (1948) starting from monthly rainfall and temperature values, while the infiltration rates were evaluated by means of Soil Conservation Service Curve Number (USDA-SCS, 1972).

The product of "rainfall that runoff" per "area of drainage basin" gave the volume of water that react with the earthen material.

The pH value of rainfall water (assumed to be 5.66 where direct analysis were not available) and the pH of drainage water allowed to calculate the request of H^+ to keep this pH value constant for all the rain water falling on and running off in the studied area. As a consequence it was converted in kg H_2SO_4/y needed.

The knowledge of the acidic potential of earthen materials (NAPP) expressed as kg H_2SO_4/t and the tonnage of the same estimate as:

(area of drainage basin)*(reactive thickness)*(density)

allows to calculate the production of H_2SO_4.

So, assuming that the environmental and climatic conditions do not change, dividing the total amount of H_2SO_4 equivalent that can be released by the total amount of H_2SO_4 equivalent necessary to maintain the current pH values of waters, the time persistence of AMD processes is obtained.

Chapter 4

Application 1: Rio Marina mining district

Rio Marina mining district was chosen as pilot site for the application of the new methodologies of geo-environmental modeling since:

- Elba Island was one of the most important Italian mining sites, where the iron exploitation lasted till 1981;
- the intense mining activity in Tuscany has left many abandoned mines and waste dumps that represent a potential source of heavy metal pollutants (Benvenuti et al., 1999; Mascaro et al., 2001);
- the site is characterised by the occurrence of a great amount of sulphides as pyrite and of coloured ponds that are clue of AMD processes (cfr. § 4.1);
- there are targets for a possible contamination: aquifer that provides drinking water to the island, swimming seawater, workers, tourists, etc.

The present application investigates the northern portion of the Rio Marina mining district which includes Rosseto, Valle Giove, Falcacci, Zuccoletto, Antenna and Pozzi Fondi mining works (**Fig. 7**a) and is the report of previous publications (Servida et al., 2009; Mele et al., 2007).

This mining area, west of Rio Marina village, has a surface of 1 km^2 and is characterised by hematite + pyrite ore association occurring in strata, lens or vein deposits (Zuffardi, 1990; Tanelli et al., 2001).

It was exploited till 1981 (ARPAT, 2004) and a great amount of material was removed. Conversion of the area into a historical and touristic site began in the nineties with the projects "Elba Island Mineralogical and Mining Park" (1991) and "Tuscan Archipelago National Park" (1996).

However, the intense mining activity and the lack of any management of the earthen materials have left deep marks in the landscape behind Rio Marina and on the eastern coast of Elba Island because sulphide-bearing ore has been exploited and processed at the same site. The accumulation and the exposure to the atmospheric agents of the sulphide-bearing earthen materials without adequate management triggered the AMD processes.

Fig. 7 - a) Aerial view of Rio Marina mining district (modified after Live Search Map, 2007). Names correspond to different mining sites exploited during the activity of mining district. The smaller red square identify the mine dump investigated with 2D-ERGI methodology, the bigger red square identify the boundary of the investigated area b) Valle Giove open pit, c) Antenna and Zuccoletto mine dumps

4.1 Environmental assessment

The geo-environmental modeling starts with the characterisation of the superficial waters of the site.

Fig. 8 - a) Location of surface water sampled, b) yellow sea water just over the Rio Marina mining district, c) yellow-brownish pond (sample 2), d) orange stream (sample 1), e) red pond (sample 4), f) dark red pond (not analysed).

Rio Marina mining district is well-known for the occurrence of coloured ponds (**Fig. 8**) that are described as a particular environmental feature. The colour of these waters (ranges from yellow to orange, from red to purple) is a clue of the AMD processes occurrence. It could be mainly related to high Fe content that it soluble only in low pH waters.

Nine points of the superficial water network were selected for surface water sampling (**Fig. 8**a). Surface waters were sampled both after a dry period (October 2006) and after a wet period (March 2007). These sampling points are representative, from upstream to downstream, of:

- surface drainage waters that flow through waste rock deposits on the Antenna and Zuccoletto mine dumps (sample 7 and 9);
- surface drainage waters that, after flowing through waste rock deposits on the Antenna and Zuccoletto mine dumps, form coloured pools (sample 2 and 4, respectively in **Fig. 8**c and e);
- surface drainage waters that flow through debris deposits on open pit benches of Valle Giove (sample 1 -represented in **Fig. 8**d-, 6 and 8);
- groundwaters that form a spring at drift entrance in Valle Giove (sample 3);
- surface drainage waters that reach the settling basin before drainage to the sea (sample 5).

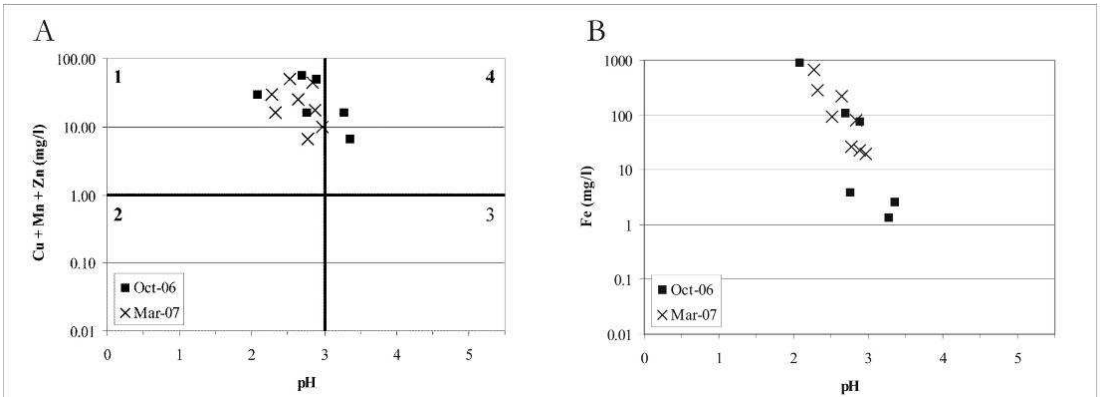

Fig. 9 - a) Ficklin diagram (after Ficklin et al., 1992): field 1 "extremely acid with high metal content" waters; field 2 "extremely acid with low metal content" waters; field 3 "acid with low metal content" waters; field 4 "acid with high metal content" waters b) Fe vs pH diagram.

The occurrence of ongoing AMD processes is confirmed by the chemical and physical features of surface waters (App. A.1), that are characterised by low pH, ranging from 2.08 to 3.35, and high heavy metal contents that reaches 903.16 mg/l for Fe, 45.02 mg/l for Mn,

10.08 mg/l for Zn and 1.75 mg/l for Cu. Moreover they are characterised by high conductivity, low chloride and nitrate contents and very high sulphate concentrations (App. A.1).

According to Ficklin et al. (1992) and Plumlee et al. (1999), waters collected in the studied area are classified in two classes as "extremely acid with a high metal content" or as "acid with high metal content". All the samples belong to the first class except samples 2 and 5 collected in the dry period (**Fig. 9**).

Diagrams in **Fig. 9** point out that there is no significant variation in pH and metals in solution between the waters collected after a dry period and the waters collected after a wet period. This could mean both "acid-producing phases" and "metal-releasing phases" are enough to saturate the rainfall waters also in the wet period.

4.2 Topography

The mining district is located around the Giove valley and is surrounded by low hills, close to the seashore (**Fig. 7**a). The nowadays topography is strictly related to the past mining activity.

The northern area is characterised by the occurrence of an open pit (**Fig. 7**b) extending on a 200,000 m² area between 100 and 210 m a.s.l.. It is composed by 11 half-circle concentric benches with an average height of 10 m and an average width of 15 m with the exception of the three innermost benches that form wide squares.

The southern area is characterised by the occurrence of 3 plains (**Fig. 7**c) extending on a 100,000 m² area between 150 and 200 m a.s.l..

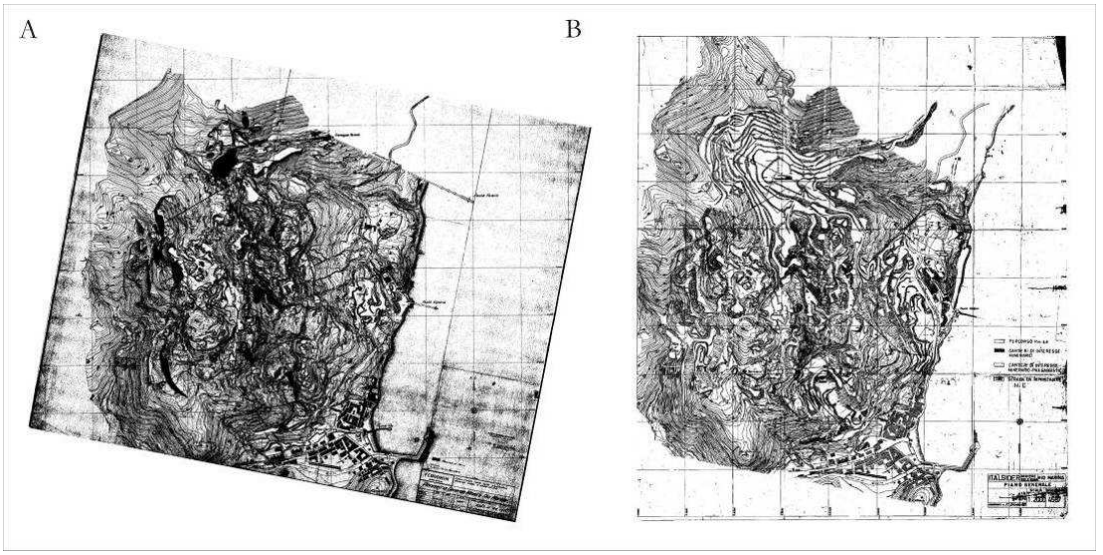

Fig. 10 - Topographic maps of Rio Marina mining district in a) 1954 and b) 1979

Topographic maps showing Rio Marina mining district in different years were found c/o the "Archivio storico delle miniere dell'Isola d'Elba" (**Fig. 10**), while the nowadays topographic map was provided by D'Oriano (2007).

4.3 Geology

Elba Island is the southwesternmost outcrop of the northern Appennine chain. It consists of several east-verging thrust sheets, belonging to Tuscan, Ligurian and Piemontese domains, emplaced between Late Cretaceous and Pliocene. The following extensional phase produced the thinning of the Tuscan crust, the uplifting of the Moho and the beginning of the Tyrrhenian basin opening. The emplacement of Miocene-Pliocene granitoid bodies and the formation of ore deposits and skarn are linked to this phase (Benvenuti et al., 2001 and references therein).

In the studied area only rocks of the Tuscan domain (Trevisan, 1950), belonging to two main tectonic units: Monticiano-Roccastrada Unit and Tuscan nappe Unit (Bortolotti et al., 2001) crop out. As shown in **Fig. 11**, from the bottom to the top of Monticiano-Roccastrada Unit in the studied area the following formations are present:

- Rio Marina Formation (Stephanian-Autunian): graphitic phyllites and meta-siltstones, quarzitic meta-sandstones, locally with quartzitic meta-conglomerates;
- Verrucano Group (?Ladinian-?Carnian): violet and greenish phyllites, violet and grey quartzites and meta-siltstones, with light grey and pinky quartzitic meta-conglomerates;
- Monte Serra Quartzites (?Carnian): quartzitic, sometimes graded meta-conglomerates and white-pink quartzites, with scarce phyllitic interbeds (White-pink Quartzites Member) and cross bedded light grey and greenish quartzites with phyllites (Green Quartzites Member);
- Calcare di Valle Giove (unknown age): grey, pinky and grey-green crystalline limestones with phyllites. At the top calcareous phyllites and varicoloured calcschistes.

The only outcropping formation of the Tuscan nappe Unit is:

- Calcare Cavernoso (?Norian-?Rhaetian): massive, brecciated or vacuolar, crystalline, more or less dolomitic limestones.

Quaternary cover was strongly modified by anthropic action. Mining activity almost completely removed the original alluvial and detritus deposits. On the other hand it generated widespread and thick waste rock disposals, that are present in three main areas (westward and eastward of Valle Giove mining area and on Antenna and Zuccoletto mining areas). Where mining works did not modify the original surface, soils show a lithological control: carbonate soils are situated in the W area, silicate soils are located in the N area.

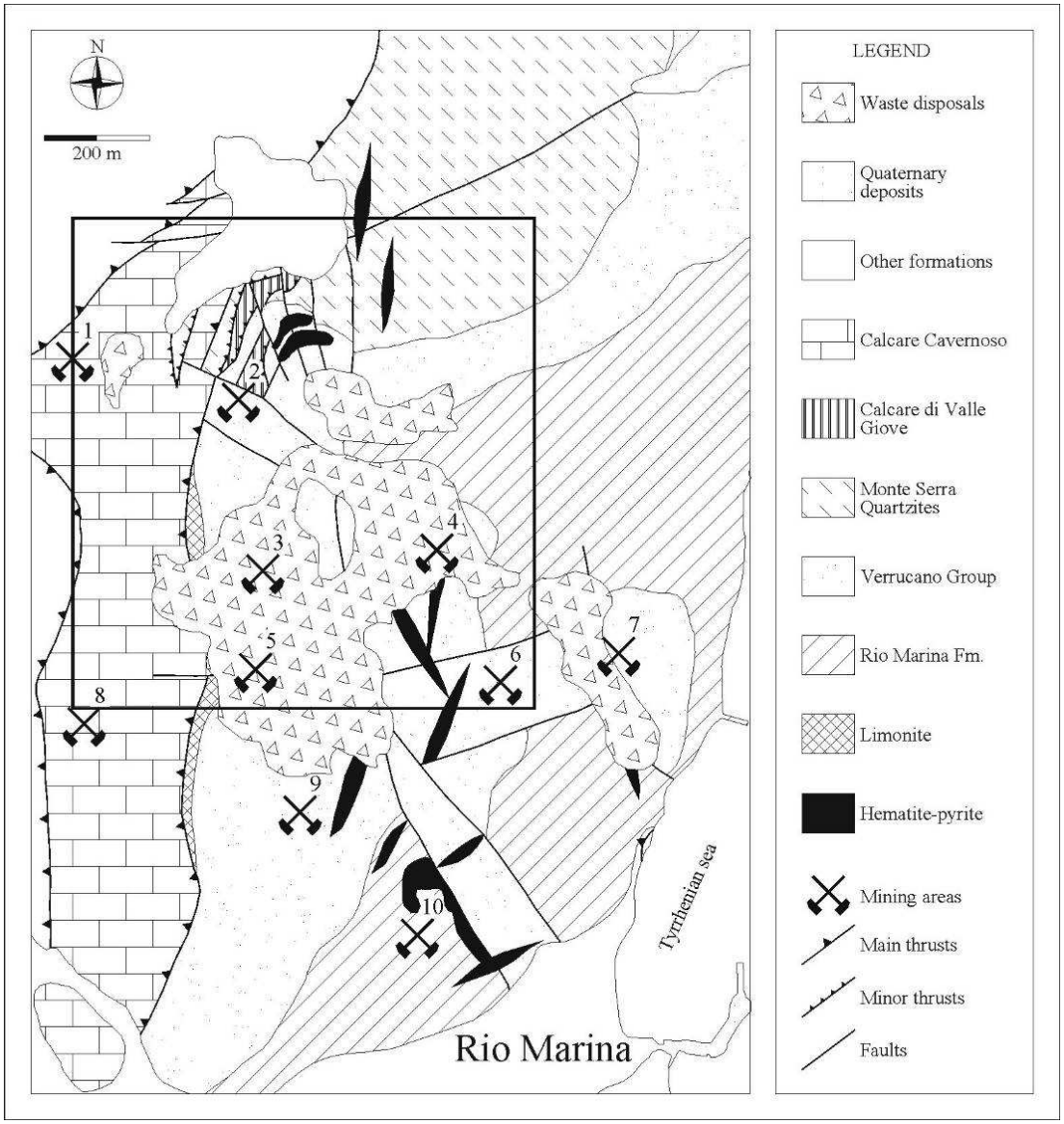

Fig. 11 - Geological map of the Rio Marina mining district (after Deschamps, 1983a and Bortolotti et al., 2001). The studied area is outlined. Mining areas are represented by numbers: 1) Rosseto, 2) Valle Giove, 3) Falcacci, 4) Zuccoletto, 5) Antenna, 6) Pozzi Fondi, 7) Vigneria, 8) Valle di Catone, 9) Filon Basso and 10) Bacino.

The main structural lineament is a N-S fault that separates Monticiano-Roccastrada Unit to the east from Tuscan nappe Unit to the west. It has been differently interpreted either as a E verging thrust plane (Deschamps et al., 1983a and 1983b) or a W dipping low angle normal fault (Bortolotti et al., 2001). Moreover Monticiano-Roccastrada Unit is characterised

by NNW-SSE to N-S trending axis folds and E 30-60 dipping faults. A later set of NW-SE to NE-SW step gravity faults, dipping 45-70 either NW or SW, cut both Monticiano-Roccastrada and Tuscan nappe Units (Deschamps et al., 1983a and 1983b; Zuffardi, 1990; Bortolotti et al., 2001).

Iron ore occurs as massive hematite ± pyrite bodies or as limonite-rich layers. Hematite-pyrite ore normally occurs as lenticular and strata-bound bodies within the Rio Marina Formation and Verrucano Group, while limonite ore as layers at the contact between Monticiano-Roccastrada and Tuscan nappe Units. Two hypotheses are presented for the genesis of ore deposits (Tanelli & Lattanzi, 1986 and references therein):

- an epigenetic genesis of the mineralisation related to metasomatic and hydrothermal events that occurred during monzogranite intrusions.
- a syngenetic genesis related to an ore sedimentary horizon involved in a thermo-metamorphic event.

Other mineralogical phases that occur in ore deposits, but never abundant, are magnetite ± sphalerite ± chalcopyrite ± galena ± bismuthinite ± anglesite ± cerussite ± native sulphur.

4.4 Hydrogeology

Elba Island is poor in alluvial bodies which could host groundwater reservoirs. Moreover, most of the rock formations are impermeable (Barberi et al., 1969).

The quaternary deposits occurring in the studied area are characterised by permeability ranging from 10^{-3} to 10^{-4} m/s, carbonatic rocks from 10^{-3} to 10^{-5} m/s, other rocks from 10^{-5} to 10^{-7} m/s (Comune di Rio Marina, 2003).

The Calcare Cavernoso hosts some relevant aquifers. It is characterised by vacuum and fracture related porosity ranging from 2% to 10% and, therefore it is the main groundwater reservoir of the island with a capacity of 10^{6}-10^{7} m^3 (Studio Chines, 1999). The Calcare Cavernoso outcrops to the west of the Rio Marina mining district, from Porto Azzurro to Cavo for a length of 8 km.

The studied area is characterised by a periodical occurrence of surface water flow related to rainfall periods (cfr. water balance at § 4.11). A fraction of the waters that flow on the surface run along the mining area slopes without channelling, another fraction converges into the Giove creek bed, while the last fraction converges into the artificial canals and passes through a system of 5 settling basins before flowing into the sea. Anyway, yellow and red pools (**Fig. 8**) generated by rainfall events persist in the mining district most of the year.

4.5 Climatic features

Elba Island is characterised by an average annual temperature of 16.5°C, ranging from average winter temperature of 10.5°C to average summer temperature of 23.0°C (Trianet Projcet, 1999 - **Fig. 12**a).

The annual precipitations, recorded in the 1961-1970 period, range from a minimum of 387.0 mm to a maximum of 842.0 mm (Landi, 1972). The highest precipitations are on Monte Capanne in the western inland of the island, the lowest on the central-eastern coast. The seasonal trend of rainfall is characterised by a dry summer (31.6 mm/month) and a wet autumn (72.7 mm/month). The average rainfall in Rio Marina was 663 mm/y, from 1922 to 1981 (Bencini et al., 1986) and 630 from 1961 to 1990 (Trianet Projcet, 1999 - **Fig. 12**b).

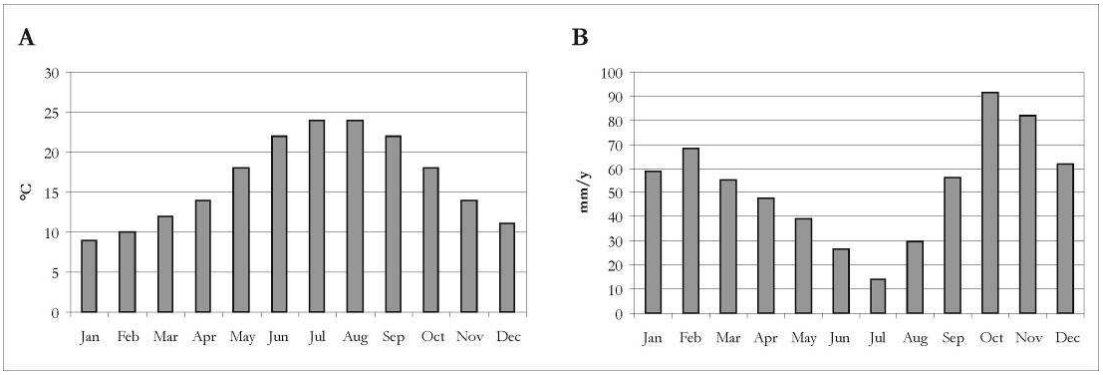

Fig. 12 - Diagrams of a) monthly average temperature for the period 1931-1989 and b) monthly average precipitations for the period 1931-1989 (Trianet Projcet, 1999)

4.6 Mining activity

The site underwent a deep anthropogenic transformation due to ore exploitation. The mining works occur in ten distinct areas, which are Rosseto, Valle Giove, Falcacci, Zuccoletto, Vigneria, Antenna, Pozzi Fondi, Valle di Catone, Filon Basso and Bacino (**Fig. 7**).

The studied area includes the following mining sites from N to S (ARPAT, 2004):

- Rosseto: exploited between 1850 and 1955 for limonite;
- Valle Giove: exploited between 1950 and 1981 for hematite;
- Falcacci: exploited between 1890 and 1962 for hematite and limonite;
- Zuccoletto: exploited between 1860 and 1950 for hematite;
- Antenna: exploited between 1900 and 1950 for hematite and limonite;
- Pozzi Fondi: exploited between 1850 and 1955 for hematite and limonite.

In all areas of the district the mining activity was characterised by three steps: the first one consisting in underground prospecting by means of log drilling, the second one

consisting in underground prospecting by means of drifts and pits and the last one that consisted in open pit exploitation.

At present only some hundreds of meters of tunnel occur because most of them were destroyed during the previous exploitation step.

The main works are in the Giove creek basin creating an overshadowing open pit (**Fig. 7**b). From this open pit, a lot (tens of millions tons) of material was removed and wasted in the contiguous ones at the mining sites reported above (**Fig. 7**c) mainly composed by rock forming minerals (quartz and muscovite, calcite and dolomite, serpentine and talc) and non valuable metallic minerals (pyrite), in minor amount by ore minerals (hematite) and alteration phases (chlorite, jarosite, gohetite and copiapite).

As a consequence of mining activity, the natural water flow was modified: at present rainwater flows to the sea along the mining area slopes or is drained to settling basins before pouring out in seawater (cfr. § 4.7).

4.7 Mine dump characterisation

4.7.1 Topographic modeling

The 1953 map (**Fig. 10**a) and the 1979 map (**Fig. 10**b) were chosen for the topographic elaboration since the first period is close to the beginning of exploitation of Valle Giove, and the second period is close to the closure of the mine works. It is worth to point out that Valle Giove is the latest site which was exploited and also the biggest one in Rio Marina mining district.

Besides these two historical maps also the 2007 map (D'Oriano, 2007) was processed to obtain the topographic variation at present.

The Digital Terrain Models (DTM) of the studied mining area relative to 1954, 1979 and 2007 (**Fig. 13**a, b and c) show that deep modifications occurred in the mining site.

In **Fig. 13** (d, e and f) the excavation areas, where surface elevation decreased, are in yellow and the piling up areas, where elevation increased, are in blue. The main excavation area corresponds to Valle Giove open pit, where the exploitation works removed up to 40 m of material (**Fig. 13**f). There are also two subordinate areas of excavation that correspond to Valle di Catone – Falcacci (SW) and to Vigneria (SE). **Fig. 13**f shows also that there are three main waste rock disposal areas, the first situated upstream of Valle Giove open pit, the second located downstream of Valle Giove open pit, the third corresponding to Antenna and Zuccoletto planes.

From the open pit roughly $2.96*10^6$ m^3 of material were scavenged from 1954 to 1979, the period of major activity of the Valle Giove mine working. Only $1.38*10^6$ m^3 of material were removed, while the other $1.57*10^6$ m^3 were piled up in the mining area.

Further $1.41*10^6$ m^3 of material were scavenged from 1979 to 2007, due to 1979-1981 period of activity, but at least $2.89*10^6$ m^3 were piled up in the mining area. It implies that in

the latest period a great amount of material was moved during the reclamation works to fill the old mining works and that at least $4.46*10^6$ m^3 of material are mine wastes.

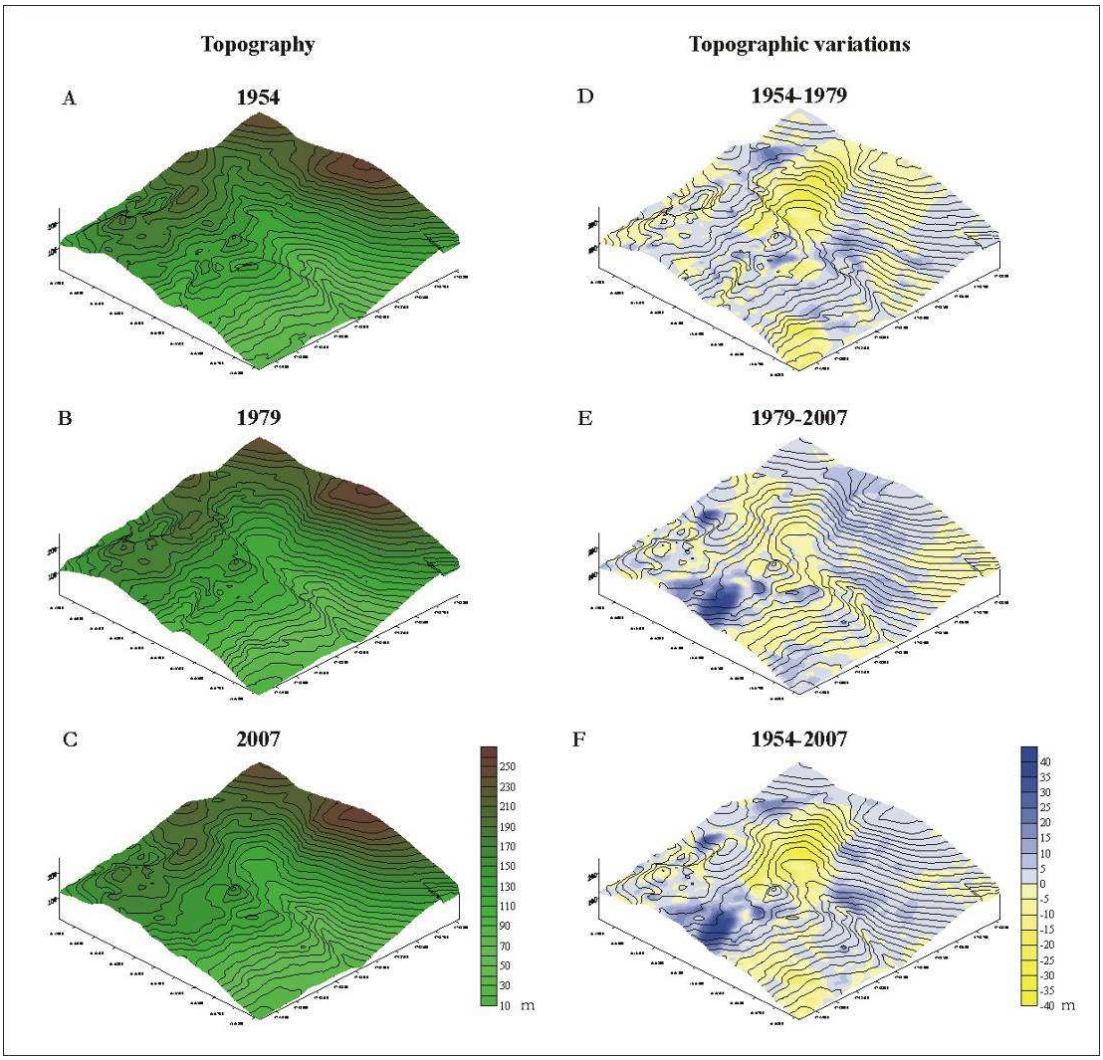

Fig. 13 - Topographic evolution of Rio Marina mining district: DTM of a) 1954, b) 1979 and c) 2007; topographic variations occurred in d) 1954-1979, e) 1979 – 2007 and f) 1954 – 2007. Removed material areas are shown in yellow, piled up material areas in blue.

The amount of mine waste material piled up in the studied area was checked and adjusted with additional field investigations since the first-mined open pits next to Valle Giove were used as mine waste dumps. To this purpose, a geophysical survey was performed (cfr. § 4.7.2).

The identification of mine dump deposits by topographic elaboration was compared with the identification performed by Bortolotti et al. (2001) and by Comune di Rio Marina (2003).

Fig. 14shows the boundary of mine according to different works and point out that the previous Authors identified as mine dumps the northern area which is an exploiting site and underestimated the extension of mine dumps in the southern area.

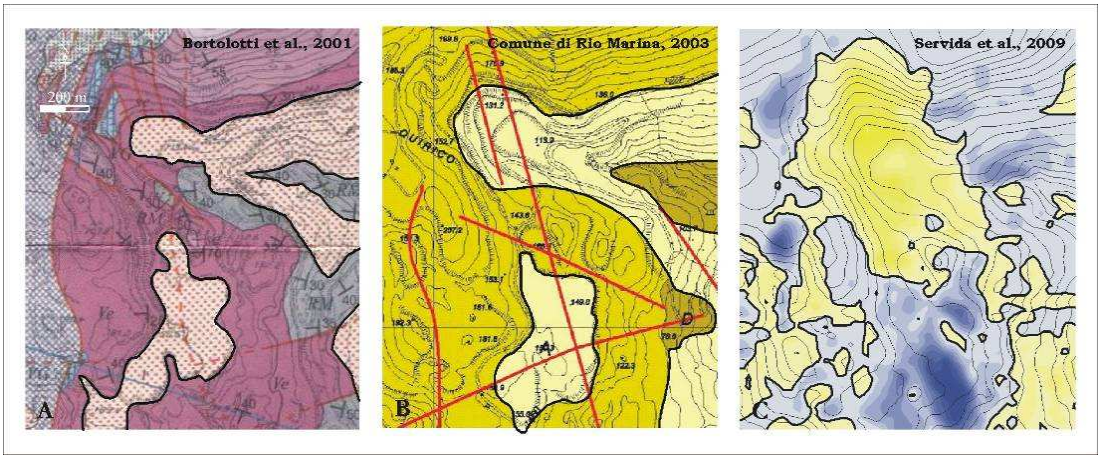

Fig. 14 - Identification of mine dump deposits in a) geological map of eastern Elba (Bortolotti et al., 2001), b) "Piano Strutturale" of Rio Marina (Comune di Rio Marina, 2003) and c) present topographic elaboration (Servida et al., 2009)

4.7.2 Geophysical modeling

This pilot-study investigates Antenna mine dump (Mele et al., 2007; Mele & Servida, submitted). This area was chosen since it is the greatest waste rock disposal of Rio Marina AML.

In order to perform a direct-calibration of the electrical resistivity class-values on the bedrock, a single 2-D resistivity section (**Fig. 15**a down) located on a quarry bench of Valle Giove open-pit was performed. The investigated quarry benches (**Fig. 15**a up) are characterised by the occurrence of 2 north-dipping hematite veins, up to 7 m thick, outcropping between 15 and 45 m and by the occurrence of an irregular pyrite body, up to 5 m thick, outcropping between 65 and 75 m. These mineralised bodies lie within unweathered metamorphic rocks. A 2-D resistivity section was collected by a Wenner-Schlumberger array, provided by 30 electrodes with 2.5 m electrodes spacing. The final RMS error after 5 iteration was 5.39%. The inverted resistivity section shows two high-conductive bodies within a homogeneous resistive unit. Comparing the geological outcrop with the ERGI profile acquired, it is possible to point out the good correlation of these resistivity anomalies

with the different geological bodies. This comparison allowed to estimate the class-values of electrical resistivity both for resistive bedrock (from 40 to 150 **Ω**m) and for the conductive mineralised ore bodies (from 5 to 30 **Ω**m).

Geoelectrical exploration of Antenna plains was planned in order to obtain evenly spaced electrical resistivity measurements within a 40,000 m² survey area (**Fig. 7**a). Five apparent resistivity sections were acquired (**Fig. 15**b) with up to 48 electrodes with Wenner-Schlumberger array and electrodes spacing ranging from 3 up to 5 m. Geoelectrical sections were oriented on a square grid in order to map subsurface electrical resistivity distribution and to trace the buried interface between the waste deposits and the bedrock over the whole survey area. Five crossover points (control points) between cross-sections were analyzed to integrate and evaluate reliability of subsurface structure.

Inverse model resistivity sections on Antenna plains were obtained after 5 iterations with RMS error ranging from 4.30% to 10.60%, with a maximum depth of investigation of 30 m below acquisition surface. Subsurface electrical resistivity distribution (**Fig. 15**c) was interpreted, in a first step, in terms of different conductive or resistive homogeneous bodies. In each section it is possible to recognise: 1) high conductive bodies, characterised by electrical resistivity ranging from 3 to 10 **Ω**m, 2) conductive bodies, characterised by electrical resistivity ranging from 10 to 50 **Ω**m, 3) resistive bodies, characterised by electrical resistivity ranging from 50 to 160 **Ω**m.

In a second step these electrical resistivity bodies (**Fig. 15**d) were associated to geological bodies in the following way: 1) high conductive bodies associated to waste rocks, 2) conductive bodies associated to ore deposits, 3) resistive bodies associated to metamorphic rocks.

Interpretation and associations are based on:

- the identification of resistivity classes obtained from direct calibration (**Fig. 15**a) that allowed the distinction between metamorphic basement and ore bodies;
- the knowledge of exploitation morphologies (open pit with ramp-and-flat shape) and methodologies (exploitation and re-filling) that allow to trace straight boundaries;
- the high conductivity of waters and the assumption that metamorphic basement and ore bodies are impermeable (lower water content: resistive), while waste rock are permeable (higher water content: conductive). Following this assumption and taking into account that a water with an average conductivity of 7.4 mS/cm correspond a resistivity value of 1.3 **Ω**m, near surface electrical body with resistivity lower than 10 **Ω**m must be wet waste rock.

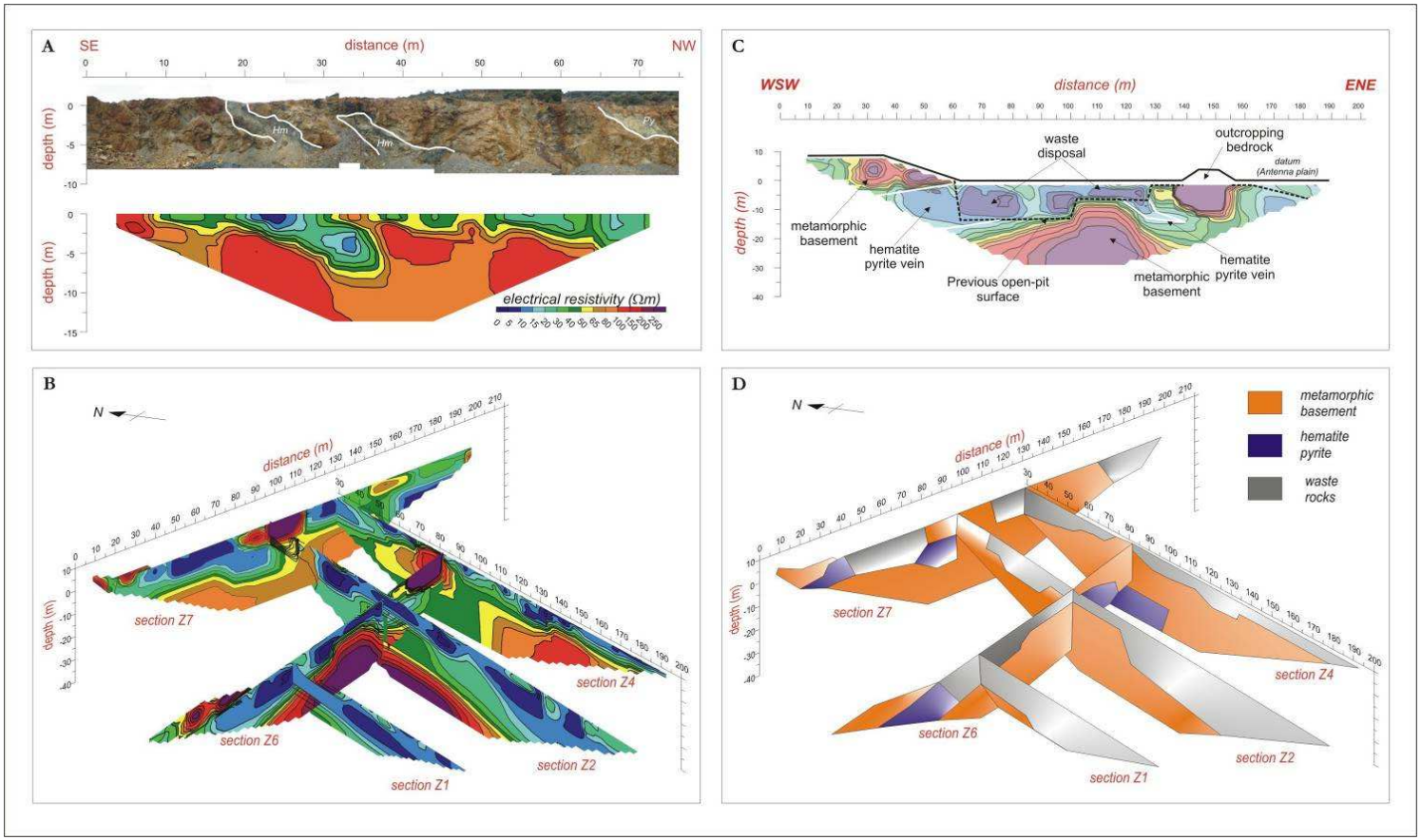

Fig. 15 - a) Calibration was performed comparing electrical resistivity profile (down) on an quarry bench of Valle Giove open pit (up), b) 2-D electrical resistivity sections, c) example of interpretation of subsurface electrical resistivity distribution, d) interpretation of 2-D electrical resistivity sections

To evaluate the geometrical features of the mine dump (morphology and principal dimensions) a geostatistical analysis of the high conductivity bodies depth (waste rocks) referred to the local z-datum plane was made. In each resistivity section the depth of the buried interface was picked up with an average distance of 5 m. A gaussian kriging interpolator (range: 90 m; sill: 60; anisotropy ratio: 2/1, anisotropy direction: N120-300) with a discrete nugget effect was used in order to reproduce the real shape of the buried surface.

The interpolated surface is typical of an open pit, with a funnel morphology. In particular the dip is characterised by a NW-SE major axis and NE-SW minor one. The dip increase from NE to SW and is characterised by a first floor located at 15 m below actual topographic surface and a second floor at 35 m below actual topographic surface. The bench structure of the buried surface was already identified by the analysis of the single 2D electrical resistivity profiles. However the occurrence of 2 benches for a depth development of 35 m seemed to be underrated, since the mining methodologies of the last century count one bench for about 10 m of vertical development of open pit. This could be related not to the absence of more benches but to a noise effect and to the closeness between electrical resistivity values of waste rock and hematite-pyrite bodies.

The comparison between mine dump morphology and volume obtained from digital elaboration of 1954 and 2007 topographic maps ($\sim 3.11*10^5$) and from ERGI investigation ($\sim 2.02*10^5$) outlines the similarity of them. So it is possible to assert that neither exploitation nor piling up workings were made outside the mapped mining reports.

4.8 Earthen material features

All the features of earthen materials were defined starting from collection of 54 samples (**Fig. 16**) and laboratory analyses following the relative guidelines, and then interpolated by geostatistical elaboration.

4.8.1 Grain size

Earthen materials are characterised by an homogeneous grain size composition. Using the Gravel – Sand – Mud diagram (**Fig. 17**) created by Gradistat software (Blott, 2000) they could be classified as "sandy gravels" with the exception of two samples, one included into the "gravels" and one included into the "gravelly sands". The percentage of mud is always under 5%, while the sand and the gravel range from about 30 to 80%.

From this result it could be deduced that all the earthen materials have a permeability value ranging from 10^{-3} to 10^{-4} m/s, in agreement with the available hydrogeological data. Moreover it is reasonable to think that the waste material underwent only the first stage of mineral processing on-site, while the grinding/milling and the mineralurgical processing were made off-site.

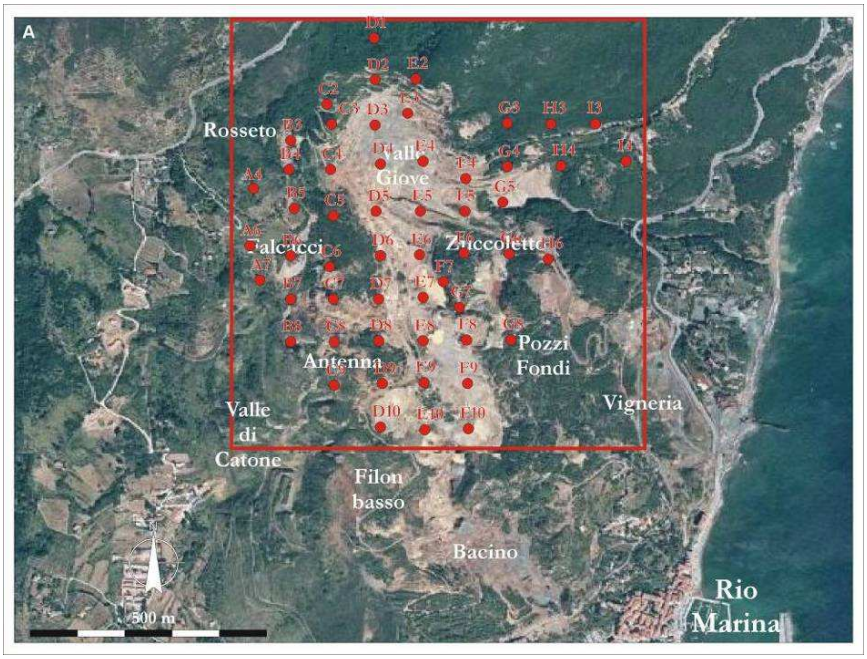

Fig. 16 - Location of earthen material samples

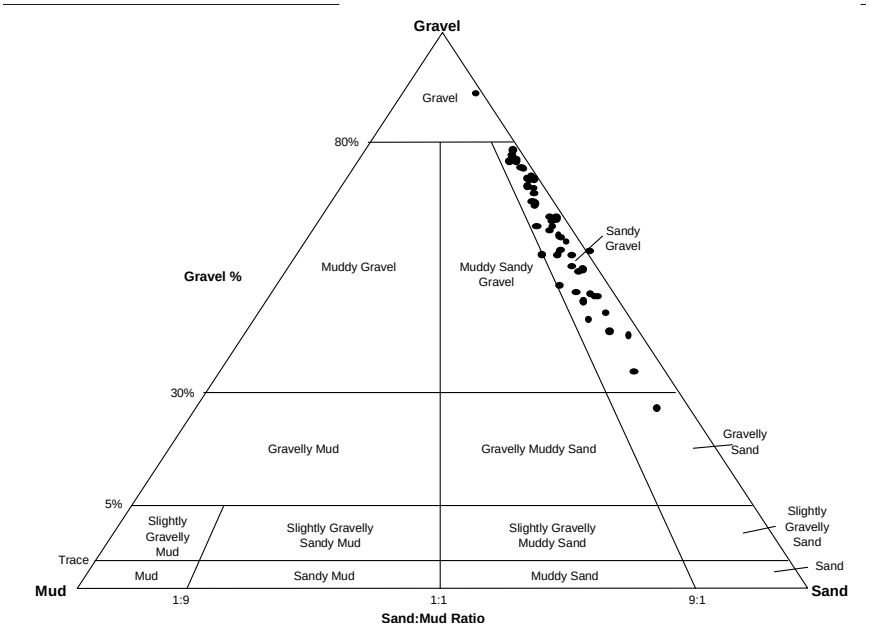

Fig. 17 - Plot of the grain size composition of Rio Marina mining district earthen materials into the gravel – sand – mud diagram

4.8.2 Mineralogy

The XRD analyses were performed on 28 samples (App. A.4). Among "gangue and host rock minerals" quartz and muscovite are always present, often with chlorite and k-feldspar. In 17 samples there is occurrence of serpentine and talc besides the previous minerals, while in 4 samples there is occurrence of calcite and dolomite. Hematite and magnetite are the ore minerals, pyrite is the only mineral detected as unalterated sulphide. The secondary minerals occurring are both silicates (illite, sepiolite, kaolino), oxides (goethite) and sulphates (jarosite and gypsum).

All the mineralogical compositions agree with the geological setting (cfr. § 4.3) and with the geochemical analyses (cfr. § 4.8.3). It must be pointed out that jarosite, a phase occurring in 50% of the analysed samples, is a typical product of AMD processes (Murad and Rojik, 2004).

4.8.3 Geochemistry

Chemical data of bulk elemental composition of earthen materials are reported in App. A.5 and A.6 and summarised in **Tab. 4**.

The 4 classes distinguished by field investigation and topographic analyses showed some particular features:

1. Soils on carbonatic or dolomitic bedrock are characterised by high CaO (median: 30.00, range: 14.96 ÷ >30.00 wt%) and MgO (median: 8.26, range: 2.76 ÷ 8.29 wt%) contents and low Al_2O_3 (median: 9.67, range: 6.42 ÷ 13.44 wt%) and SiO_2 (median: 35.00, range: <35.00 ÷ 38.33 wt%) contents. The Fe_2O_{3tot} (median: 6.04, range: 4.77 ÷ 44.21 wt%) content show both the lowest and the highest contents, on the contrary the S contents are constant and always under XRF detection limit (0.10 wt%).
2. Soils on siliceous bedrock are characterised by low CaO (median: 0.50, range: 0.03 ÷ 1.36 wt%) and MgO (median: 1.94, range: 0.98 ÷ 5.24 wt %) contents and high Al_2O_3 (median: 14.61, range: 10.03 ÷ 19.79 wt%) and SiO_2 contents (median: 56.83, range: 42.13 ÷ 77.04 wt%). The Fe_2O_{3tot} is generally low (median: 12.26, range: 5.50 ÷ 25.92 wt %), as well as the S contents (median: 0.05, range: <0.10 ÷ 0.27wt%). Sample A07 show a bulk elemental composition out of this range, with exceptional high Fe_2O_{3tot} values.
3. Waste rocks related to mining activity are characterised by average composition similar to silicate rocks for CaO (median: 0.17, range: 0.03 ÷ 3.46 wt %), MgO (median: 2.43, range: 0.86 ÷ 8.75 wt%), Al_2O_3 (median: 15.43, range: 6.49 ÷ 25.34 wt%) and SiO_2 (median: 46.40, range: 36.19 ÷ 57.89 wt%) contents. The Fe_2O_{3tot} (median: 22.54, range: 11.79 ÷ 40.39 wt%) and the S (median: 1.87, range: <0.10 ÷ 4.42 wt %) contents are high. Sample C08 shows a bulk elemental composition out of this range.

4. Debris deposits related to erosion and superficial water transport, located in the open pit area, are characterised by heterogeneous contents of CaO (median: 0.23, range: 0.01 ÷ 9.44 wt%), MgO (median: 2.11, range: 0.93 ÷ >10.00 wt%), Al_2O_3 (median: 16.20, range: 4.87 ÷ 20.96 wt%), SiO_2 (median: 48.26, range: <35.00 ÷ 64.79 wt%), Fe_2O_{3tot} (median: 17.88, range: 7.79 ÷ >50.00 wt%) and S (median: 0.24, range: 0.05 ÷ 8.46 wt%).

SAMPLE	CaO wt%	MgO wt%	Al2O3 wt%	SiO2 wt%	Fe2O3 wt%	S wt%	Cu ppm	Mn ppm	Pb ppm	Zn ppm
Carbonate soils										
min.	14.96	2.76	6.42	35.00	4.77	0.05	18	1076	28	323
I quartile	26.24	6.88	6.46	35.00	5.69	0.05	22	1464	33	351
med.	30.00	8.26	9.67	35.00	6.04	0.05	34	2626	46	440
III quartile	30.00	8.28	13.01	35.83	15.61	0.05	632	3677	146	1824
max.	30.00	8.29	13.44	38.33	44.21	0.05	2396	3727	407	5734
Silicate soils										
min.	0.23	0.98	6.70	35.00	5.50	0.05	22	301	33	277
I quartile	0.35	1.43	11.35	45.48	9.58	0.05	30	1012	89	568
med.	0.50	1.94	14.61	56.83	12.26	0.05	48	2006	113	755
III quartile	0.82	2.30	17.36	62.51	19.23	0.05	59	2257	159	869
max.	1.36	5.24	19.79	77.04	50.00	0.27	6169	6381	460	10211
Waste rocks										
min.	0.03	0.86	4.64	36.19	11.79	0.05	1	87	28	140
I quartile	0.07	1.92	12.92	41.57	17.76	0.64	32	147	56	273
med.	0.17	2.43	15.43	46.40	22.54	1.87	53	251	100	402
III quartile	0.32	3.30	17.39	49.25	30.20	2.59	97	496	205	824
max.	3.46	10.00	25.34	57.89	40.39	4.42	313	1370	6250	2897
Debris deposits										
min.	0.01	0.93	4.87	35.00	7.29	0.05	0	53	27	223
I quartile	0.07	1.80	14.41	43.83	10.74	0.05	34	166	63	363
med.	0.23	2.11	16.20	48.26	17.88	0.24	52	541	78	575
III quartile	0.97	3.59	18.71	56.59	24.47	2.90	89	931	116	740
max.	9.44	10.00	20.96	64.79	50.00	8.46	1037	3088	510	2789

Tab. 4 - Statistical report of geochemical features of earthen materials

Bulk elemental composition of carbonate and silicate soils is strictly related to bedrock composition. Bulk elemental composition of mine waste rocks and debris deposits are more similar to silicate soils than to carbonate ones. These two kinds of earthen materials differ in Fe_2O_{3tot} and S contents that are, on average, higher and more homogeneous in mine waste rocks than in debris deposits, which are characterised by lower median values and by

minimum and maximum values. This could be explained by pyrite and hematite occurrence: while in waste rocks this occurrence is rather homogeneous, the contrary occurs in debris deposits where it is related to occurrence of mineralisation.

The analyses of trace elements performed in the first step on fifteen samples show that, As, Cd, Co, Cr, Cu, Hg, Pb, Sb, Se, Tl and Zn have concentration that could be interpreted as environmental pollution. In the second step, the trace elements that had shown the highest variability and are known to be toxic (Cu, Pb and Zn) were selected for further analyses on all the samples (App. A4 and **Fig. 18**, second row).

Copper average concentration is 230 ppm (σ = 877). The concentration limit for RA is 120 ppm Cu and for CIA is 600 ppm. Cu concentration exceeds RA limit in 8 samples and CIA limit in 3 samples.

Lead average concentration is 336 ppm (σ = 957). The concentration limit for RA is 100 ppm Pb, while for CIA is 1000 ppm. Pb concentration exceeds RA limit in 22 samples and CIA concentration limit in 2 samples.

Zinc average concentration is 919 ppm (σ = 1554). The concentration limit for RA is 150 ppm Zn and for CIA is 1500 ppm. Zn concentration exceeds RA limit in 42 samples and CIA limit in 6 samples.

In conclusion, heavy metal content could be related to several factors: bedrock nature, mining exploitation area setting, mineralurgical ore working methodology and piling up strategy. The presence of a spatial relation of heavy metal distribution allows an evaluation of heavy metal content at any point within the area.

4.8.4 Acid Mine Drainage

AMD static test results (App. A.5) show that in Rio Marina mining district potential for AMD generation is widespread. Indeed, 30 samples have MPA higher than 1.5 kg H_2SO_4/t, which is the lowest MPA value related to the S detection limit of 0.10 wt %. Only one soil sample has MPA value higher than 1.5 kg H_2SO_4/t, while 50% of debris samples have MPA values higher than 1.5 kg H_2SO_4/t and further 80% of waste rock samples show MPA values higher than 1.5 kg H_2SO_4/t. Nevertheless, the highest MPA values (reaching 258.9 kg H_2SO_4/t) are associated with debris deposits, followed by waste rocks (135.3 kg H_2SO_4/t). This could be explained by a more homogeneous composition of waste rocks compared to debris deposits.

Sulphates/Total S ratio is lower than 10% in 11 samples with S higher than detection limit, it is included between 10 and 50% in other 14 samples while it varies between 50 and 100% in only 4 samples. The average value of earthen material MPA, evaluated starting from S determination, is 43.4 kg H_2SO_4/t, while considering only the S sulphide is 37.0 kg H_2SO_4/t.

ANC values are positive in 33 samples: all the carbonate and silicate soil samples have positive ANC values, while 70% of debris deposit samples and only 35% of waste rock

samples have positive ANC values. Moreover, the highest ANC values (880.8 kg H_2SO_4/t) are associated with carbonate or dolomitic soils. ANC values of waste rocks and debris deposits are much lower, with maximum of 57.9 kg H_2SO_4/t and 169.5 kg H_2SO_4/t respectively.

Frequently, samples that have MPA values higher than 1.5 kg H_2SO_4/t have not positive ANC value (19 samples) or samples that have positive ANC value have not MPA value higher than 1.5 kg H_2SO_4/t (22 samples). Only in 10 samples positive ANC is associated with positive MPA to produce a buffer effect on acid production. Only 3 of these samples (C05, C06 and E10) can buffer more than 10% of acid production. Consequently, the buffering effect on AMD processes is very low and the samples with the greatest MPA value correspond on average to the samples with the greatest NAPP values.

4.9 Spatial analysis

By the semi-variogram analysis the spatial relation of each element and AMD parameter was assessed. The variogram parameters are reported in APP. A.7.

Contour maps relative to major element concentrations (**Fig. 18**) and S (**Fig. 19**) show that:

- SiO_2 has an inverse distribution respect to CaO and is strictly related to the geological setting. CaO shows the highest values in the western area, where Calcare Cavernoso crops out, while SiO_2 shows the highest values all around Valle Giove open pit ;
- Fe_2O_{3tot} and S have a peculiar distribution not related to those of SiO_2 and CaO.
- Fe_2O_{3tot} concentration shows the highest values in Valle Giove open pit, where the mineralised veins are still exposed, and in Antenna area, marking a NW-SE enriched zone probably related to an unexploited mineralisation.
- S concentration shows the highest values in the Valle Giove open pit, where the mineralised veins are still exposed, and at Antenna mine dumps, where the waste materials were piled up.

The contour maps of the selected heavy metal concentrations show that:

- Cu and Pb have a similar areal distribution, while Zn has an homogeneous distribution all around the mining district;
- Cu reaches the highest values (over than 6000 ppm) in the area between Antenna and Falcacci. This values could be related to limonite veins hosting chalcopyrite, in agreement with the geological setting;
- Pb reaches the highest values (over than 6000 ppm) in Antenna mine dumps. These values could be related to the occurrence of Pb-bearing material in the waste rocks;

– Zn reaches the highest values (over than 10000 ppm) in Valle di Catone mining area. This values could be related to high local background, since the Zn concentration is high in the whole earthen material, even where there is no the evidence of Zn minerals.

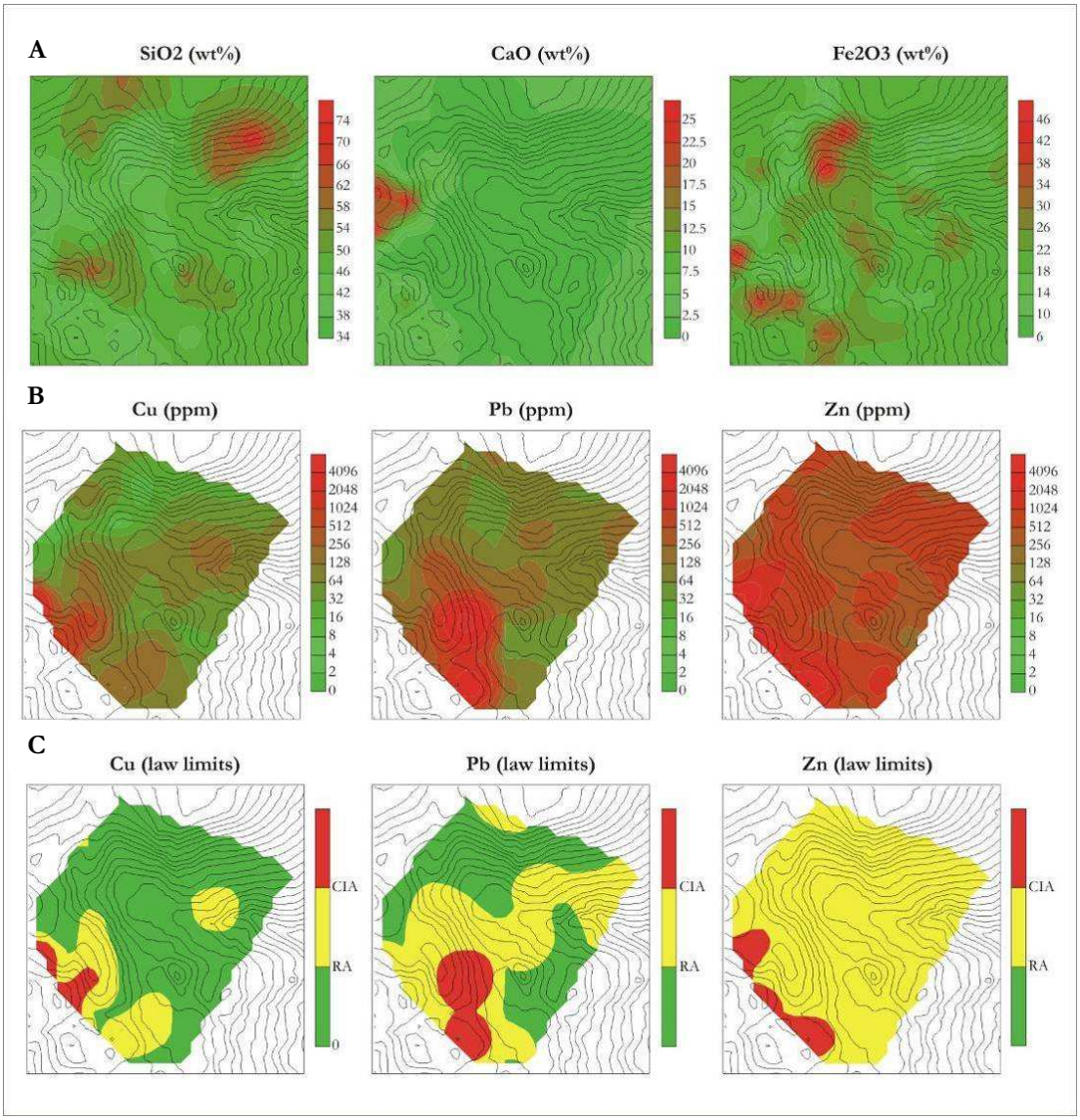

Fig. 18 - Contour maps of a) selected major element (first raw), b) selected heavy metals potentially toxic (second raw) and c) selected heavy metals compared with Italian law limits (CSC of D.Lgs 152/2006)

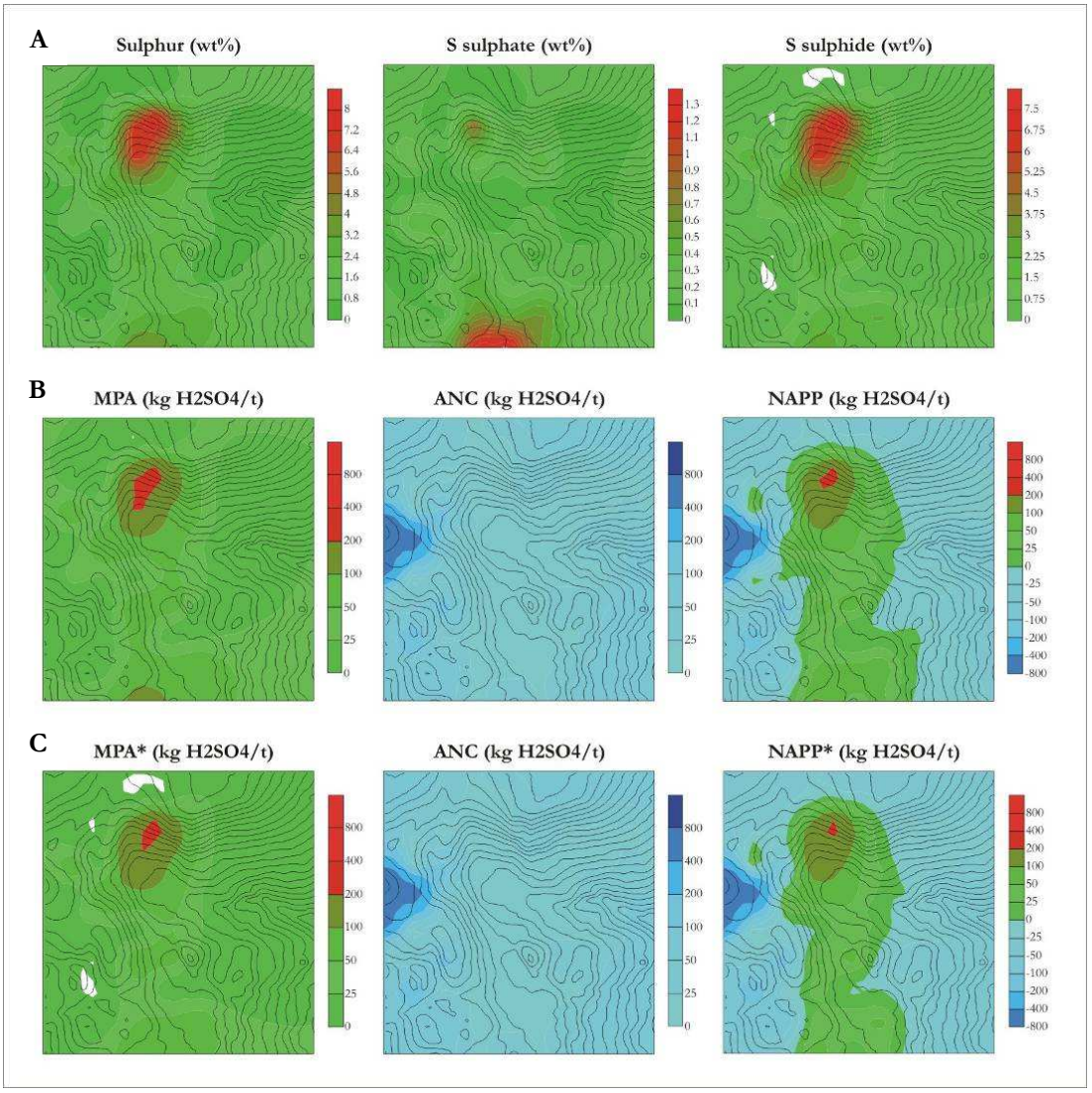

Fig. 19 - Contour maps of AMD parameters in the investigated area

The contour maps of Cu, Pb and Zn were then compared with Italian law limits, established by D.M 471/1999 and D.Lgs. 152/2006 both for residential area (RA) and for commercial or industrial area (CIA) because the future destination of the area is actually unknown (**Fig. 18**c).

The contour maps of AMD parameters (**Fig. 19**) show that:

- all the Valle Giove open pit and Antenna mine dump earthen materials could produce more than 25.0 kg H_2SO_4/t. The areas that have not undergone mining works (exploitation or piling up) show lower MPA values together with the western area characterised by carbonate rocks.
- only the western upstream earthen material could buffer more than 25.0 kg H_2SO_4/t.
- NAPP, obtained subtracting ANC contour map from MPA one, is positive in the Valle Giove and in Antenna areas, while is negative in the remaining areas of the mining district.

4.10 Geochemical hazard assessment

AMD risk evaluation was performed creating a synthesis maps of heavy metal contents compared to law limits and a simplified map of NAPP of earthen materials.

The synthesis contour map for the overlapping of Cu, Pb and Zn content is shown in **Fig. 20**a. Where at least one of these heavy metals exceeds CIA limits the area has been coloured with red, whilst where at least one of these heavy metals exceeds RA limits the area has been coloured with yellow. Nowhere the considered heavy metals are contemporaneously all under RA limits.

The simplified contour map of NAPP is shown in **Fig. 20**b. It was obtained changing the coloured scale and assigning red to NAPP>0 areas and blue to NAPP<0 areas.

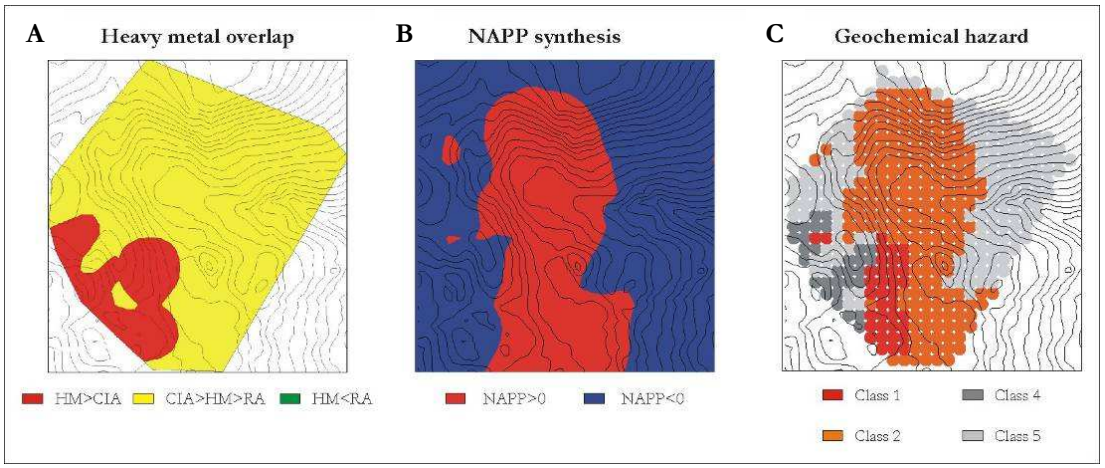

Fig. 20 – a) overlaying of heavy metal map, b) simplified NAPP map and c) geochemical hazard classes distribution. See text for definition of the classes

As a result of the overlapping of heavy metal map (**Fig. 20**a) and NAPP map (**Fig. 20**b) by means of GIS method:

- $3.99*10^4$ m² of the area belong to class 1 (Falcacci and Antenna mining area);
- $2.20*10^5$ m² to class 2 (Antenna and Zuccoletto planes and Valle Giove open pit);
- $3.23*10^4$ m² to class 4 (area westward Antenna and Falcacci);
- $1.76*10^5$ m² to class 5 (to the W and to the E of Antenna planes and Valle Giove open pit);
- no area pertains to classes 3 and 6 (**Fig. 20**c).

It is possible to point out that a fraction of the area which, following the law, must be reclaimed also in the case of industrial restorement, is characterised by high metal concentrations but, on the other hand, by a negative NAPP. This implies a low probability of mobilisation of metals, hence a low reclamation priority.

On the contrary, a fraction of the area which, following the law, must be reclaimed only in the case of residential requalification, is characterised by "medium" metal concentrations but positive NAPP. This implies a high probability of mobilisation of metals, hence a high reclamation priority.

4.11 Persistence of AMD processes

Starting from monthly rainfall and temperatures (cfr. § 4.5), evapotranspiration and surface flow rates were calculated. Evapotranspiration affects water balance for 66% as annual average and reaches 100% of precipitation value from April to September, while it is at the lowest in January (30%). The rest of meteoric waters could flow on surface (16%) or infiltrate into the ground (18%).

Assuming that 630 mm/y of rain waters fall on Rio Marina catchment, 414.4 mm/y were lost through evapotranspiration, 102.9 mm/y flow on surface and 112.8 mm/y infiltrate in the ground.

Considering that the Rio Marina catchment has an area of $1.2*10^6$ m² and that only $8.2*10^5$ m² are upstream of NAPP>0 area, it is possible to calculate that $8.4*10^4$ m³/y of meteoric water are available for AMD generation processes.

The average surface water pH value in the studied area is 2.67. This pH value implies an H^+ concentration of 2.14 mg/l. To keep this pH value constant for all the rain water falling on the studied area, $8.83*10^3$ kg H_2SO_4/y are needed.

Since average NAPP value of earthen materials is 67.00 kg H_2SO_4/t, and assuming a reactive thickness of 0.25 m (because this is the earthen material that interacts most with atmospheric agents and is the depth at which earthen material samples were collected) and an average density of 3.50 g/cm³, these earthen materials could produce as much as $1.93*10^7$

kg of H_2SO_4. So, if the environmental and climatic conditions do not change, dividing the total amount of H_2SO_4 equivalent that can be released by the total amount of H_2SO_4 equivalent necessary to maintain the present pH values of waters, a duration of present conditions of $2.18*10^3$ years is obtained.

Instead, assuming that all the piled up earthen materials determined by topographic modeling react and keeping constant the other variables, they could produce up to $1.56*10^{10}$ kg of H_2SO_4 and AMD processes could last for the next $1.18*10^5$ years.

4.12 Conclusions

Environmental assessment of Rio Marina mining district regarded only the surface earthen materials and the surface waters. This restriction was made since the processes considered for transport and diffusion of pollutants are active on the boundary between soil and air. It must be also pointed out that in this application CSC of D.Lgs. 152/06 were used as limits to determine the contamination of earthen materials and waters. It would have been better to calculate CSR by dedicated software but this is not the aim of this work and the developed methodologies leave the chosen values out of consideration.

Metal concentrations in earthen materials exceed RA limits of D.Lgs. 152/2006 for some metals like Cd, Co, Cr, Hg, Sb, Se and Tl and CIA limits of D.Lgs. 152/2006 for other heavy metals like Cu, Pb and Zn. These high concentrations must be identified, in environmental mean, as a source of contamination. However, they could be due both to natural anomalies and to exploitation and piling up processes. Since neither historical geochemical data are available nor all the mineralised area was completely or partially exploited, it is now impossible to calculate the natural background values for these elements in the earthen materials.

The surface waters are characterised by Cu, Fe, Mn and Zn values that exceed the concentration limits of D.Lgs. 152/2006. The surface waters are a mean of transport for the contamination, since the metal concentrations are over the law limits also downstream the site. The low pH values indicate that the AMD processes are active in this area.

Finally, the occurrence of targets for a possible contamination was assessed.

This information, provided by a normal geo-environmental model, allows to plan two possible remediations:

- removal of the earthen materials characterised by pollutant concentration exceeding the CSC of D.Lgs. 152/06 or the calculated CSR;
- water treatment downstream the site.

Both the solutions are very expensive: the first is senseless for the reasons explained in § 1.1, while the second has been adopted in some AML with different results.

The methodologies proposed as innovative for the geo-environmental modeling allowed:

- the identification and the measuring of mine dumps. It was assessed that no mine dumps are present at Valle Giove open pit. Moreover, the boundaries of the three main waste dumps of the mining district were drawn and their total volume was evaluated in about $4.46*10^6$ m^3;
- the spatial analysis of all the analytical parameter of earthen material on the whole investigated area and the correlation with natural or antropic variables. For example, NAPP values of earthen materials are strongly related to exploitation activities due to the removal of superficial cover of the mineralised areas, allowing for interactions with atmospheric agents. Moreover, the movement of great amounts of earth materials and the exploitation activities created mine waste disposals composed of loose materials with high sulphide contents;
- the geochemical hazard evaluation starting from heavy metal and NAPP distribution in earthen material. Areas characterised by the highest geochemical hazard due to the AMD processes development are located near Antenna area (class I and II) and at Valle Giove open pit (class II);
- to assess a time span from hundreds to thousands of years for the lasting of AMD processes, on the basis of climatic features and characteristics of earth materials. Such values preclude the possibility of natural attenuation of these processes.

Chapter 5

Application 2: Libiola mining site

Libiola mining site was chosen as pilot site for the application of the new methodologies of geo-environmental modeling since:

- it was one of the most important Italian mining sites, where the Cu was exploited almost for a century from 1864 until 1962;
- it is characterised by the occurrence of different sulphides as pyrite, chalcopyrite, sphalerite and pyrrhotite and of coloured waters springing out of adits that are clue of AMD processes (cfr. § 5.1);
- it is included into the list of national sites that must be reclaimed with urgency (Regione Liguria, 1999).

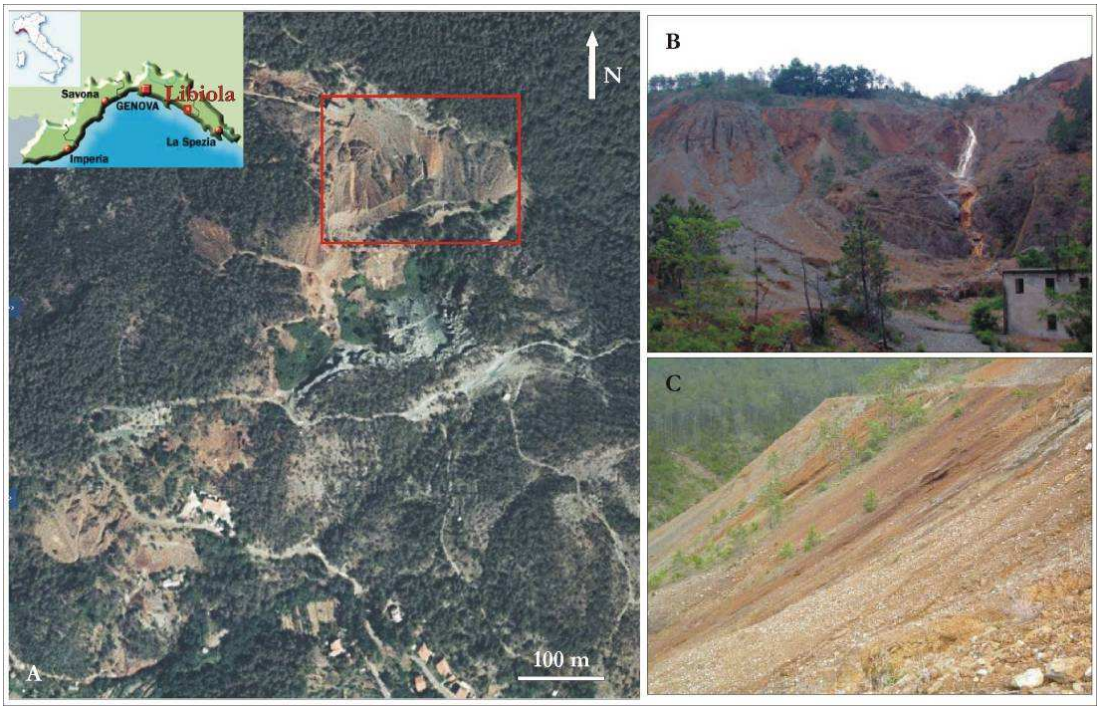

Fig. 21 - a) Libiola mining site aerial view (modified after Live Search Map, 2007), the red square identifies the boundary of the investigated area; b and c) zooms of mine dump.

– its mineralogical features (Carbone, 2002; 2008; Marescotti & Carbone, 2003; Carbone et al., 2005) and water geochemical characters (cfr. § 5.1) were already studied by several Authors.

The area under investigation is one of the biggest waste-rock dumps of the Libiola mine that is located in the northern part of the mining area (**Fig. 21**). It is about 100 m in height and covers a surface of over 3 ha. The area chosen for this application is deliberately restricted to perform detailed investigations on some earthen materials samples relative to variation of their features (grain size, mineralogy, chemistry, AMD parameters, etc.) at metric scale on the surface and with the depth. Results are reported in Azzali et al. (2008), Marescotti et al. (2008; submitted).

Nowadays, the Libiola mine is completely abandoned and presents serious environmental problems due to 1) supergenic sulphide oxidation, 2) erosion of waste deposits, inducing several types of landslides (rockslides, debris avalanches, slumps, etc.), 3) the occurrence of easily accessible mine adits, which continuously discharge strong acid waters and, sometimes, toxic gases (Marescotti & Carbone, 2003).

5.1 Environmental assessment

Recent geochemical analyses (Dinelli et al., 1999 and 2001; Dinelli & Tateo, 2002; Marini et al., 2003; Accornero et al., 2005) have shown that the waters circulating in the Libiola mine area and discharging in the catchment basin of the Gromolo Creek are strongly polluted, being characterised, as shown in **Fig. 22**a-b, by a pH as low as 2.4 and by a dangerous quantity of heavy- and transition-metals (Cr 0.02–2.54 mg/l; Fe 0.03–1115 mg/l; Co 0.018–4.14 mg/l; Ni 0.1–7.78 mg/l; Cu 0.01–221 mg/l; Zn 0.1–55.9 mg/l), and sulphate (57.4–9570 mg/l).

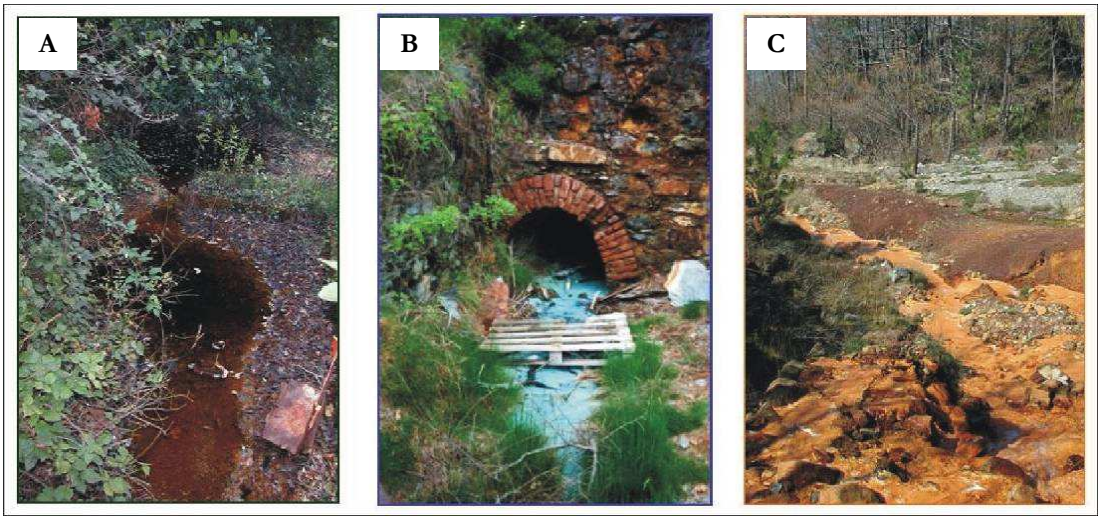

Fig. 22 - a) waters characterised by low pH values, b) waters characterised by high Cu content and c) Fe oxides and hydroxides precipitates

Moreover, extensive precipitation of Fe(III)-bearing muds (**Fig. 22**c) is taking place throughout the whole area as a result of the mixing of acid mine-waters with local streams and ground waters (Dinelli & Tateo, 2002; Marescotti & Carbone, 2003; Marini et al., 2003).

In App. B.1 are reported the results of analyses performed on surface and ground waters (Dinelli & Tateo, 2002; Cortecci et al., 2008) collected close to the studied area, from rills draining the waste dumps and the streams bordering the mining area.

5.2 Topography

The mine site is located about 8 km NE of Sestri Levante (Eastern Liguria, Italy) and extends over an area of about 4 km² within the basin of the Gromolo Creek.

Since the exploitation was carried out mainly underground, the main topographic variations due to mining works are related to mine dumps that occur in the area.

Moreover, no historical topographic maps were found c/o both the property and private or public corporation.

5.3 Geology

Libiola area is located into the northern Appennines. These are characterised by thrusted tectonic units, belonging to four paleogeographic domains (Ligurian, Sub-ligurian, Tuscan and Umbro-Marchigiano).

The whole mining area falls within the Ligurian paleogeographic domains, in particular within the tectonic unit called Vara Supergroup (Abbate et al., 1980) and in the sub-unit Bracco-Val Graveglia (Bortolotti et al., 1994) characterised by an ophiolitic sequence and a sedimentary cover.

The formations that crop out from the bottom to the top of the ophiolitic sequence, as shown in **Fig. 23**, are:

- Ultramafite or Serpentinite: mainly composed by tectonic lherzolite metamorphosed as serpentinite. Olivine and orthopyroxene are often completely alterated, while clinopyroxene and spinel are often preserved (Cortesogno et al., 1978);
- Gabbro (Middle Jurassic): it occur with different textures (from isotropic to cumulitic) and with different mineralogical and chemical compositions (troctolite, olivine-gabbro and gabbro eufotide – Cortesogno et al., 1994);
- Ophicalcite: tectonic monogenic serpentinite breccia cemented by calcite (Principi et al, 1994);
- Case Boeno Breccia: monogenic serpentinite breccia (Principi et al, 1994);

- Basalt (Middle Jurassic): it occurs as massive flows, as pillows and as veins into the basement (ultramafite and gabbro). The mineralogical and chemical composition is typical of MORB (Ferrario, 1973);
- Movea Breccia: poligenic breccia composed by basalt, gabbro and serpentinite fragments (Principi et al, 1994);
- Monte Alpe Chert (Late Jurassic): siliceous sediments of deep sea (Bonatti et al.,1976; Marescotti & Cabella, 1996);
- Palombini Shale (Aptian-Neocomian): succession changing from mudstone and limestone at the bottom to quartz sandstone and siltstone to the top (Principi et al, 1994);
- Monte Gottero Sandstone (Campanian-Paleocene): composed by sandy to muddy turbidite (Principi et al, 1994).

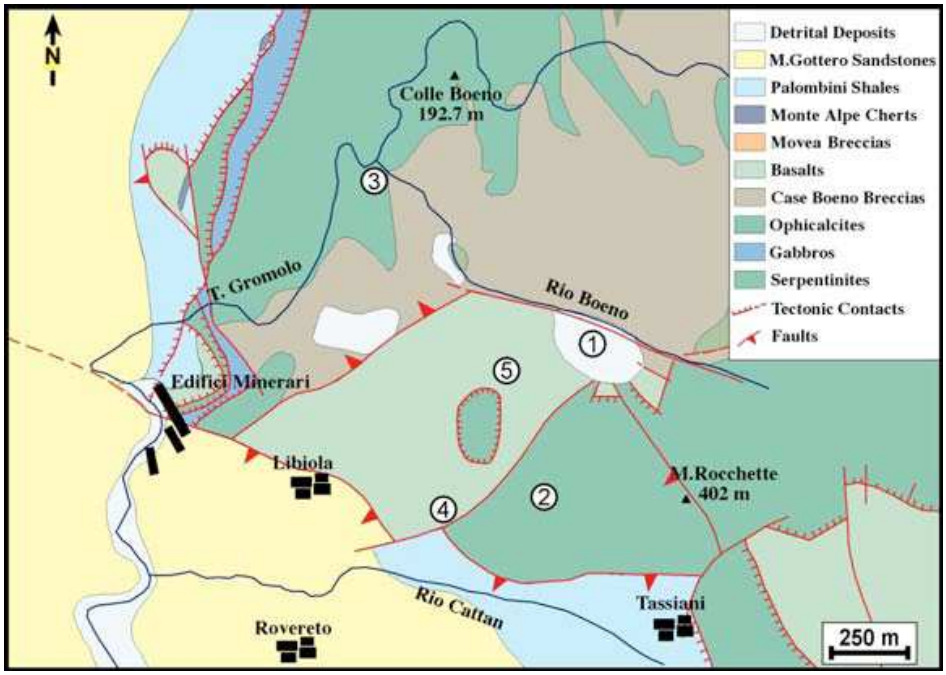

Fig. 23 - Geological map of Libiola mining site (modified after Abbate et al., 1980). The numbers from 1 to 5 indicate the mine dumps

The sulphide ores (pyrite-rich and chalcopyrite-rich mineralisations) mainly occur as massive lenses (25–35 wt% sulphides) and stockwork-like epigenetic veins (<10% sulphides – Garuti & Zaccarini, 2005) near the top of the pillow basalt sequence. Moreover,

disseminated pyrite mineralisations occur in both the pillow basalts and serpentinites. The sulphide ores are the result of a polyphasic evolution that comprised a hydrothermal oceanic stage followed by tectono-metamorphic processes that produced recrystallisation and thickening of the primary mineralisations (Ferrario & Garuti, 1980).

5.4 Hydrogeology

The Gromolo Creek begins at 910 m a.s.l. (Monte Roccagrande) and flows for almost 9 km to its mouth, located in the Sestri Levante bay. It has a catchment basin of about 26 km², with slopes varying from 2.5% to about 15.0%. In the alluvial plain, the Gromolo Creek receives acid and polluted waters from two main tributaries (Rio Boeno and Rio Cattan, **Fig. 23**) that collect most of the Libiola mine waters.

Due to the complexity of the underground setting, this area requires an appropriate investigation to model the ground water flow that are actually in progress.

5.5 Climatic features

Liguria region is characterised by an average annual temperature of 18.7°C, ranging from average winter temperature of 12.3°C to average summer temperature of 25.5°C (Eurometeo, 1995-2008 – **Fig. 24**a).

The average rainfall in Genoa was 802 mm/y, from 1961 to 1990 and the season with the average most abundant precipitation is autumn (109 mm per month) while the season with the average least abundant precipitation is summer (34 mm per month) (Eurometeo, 1995-2008 – **Fig. 24**b).

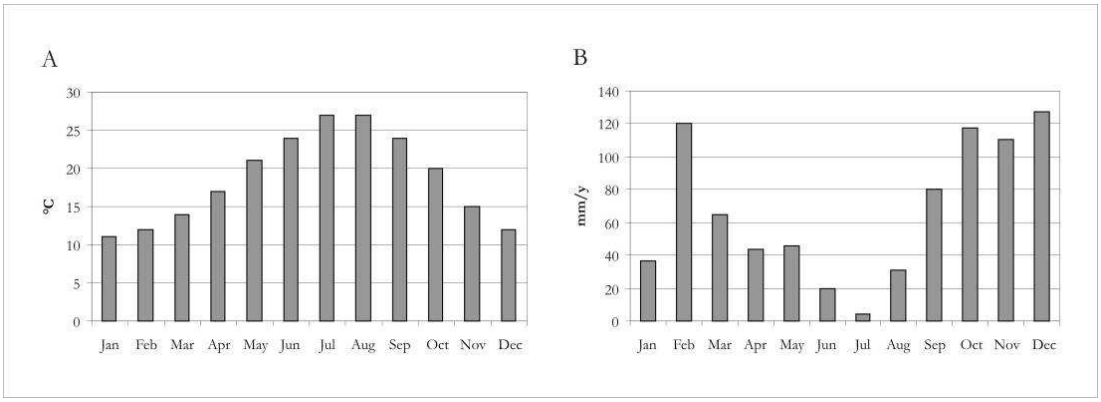

Fig. 24 - Diagrams of a) monthly average temperature for the period 1961-1990 and b) monthly average precipitations for the period 1961-1990 (Eurometeo, 1995-2008)

5.6 Mining activity

Libiola mining site was extensively exploited from 1864 until 1962 and produced over 1 Mt of Fe-Cu sulphides with an average grade ranging from 7 to 14 Cu wt%. The mining area comprises over 30 km of underground excavations (**Fig. 25**) and two open pits (**Fig. 21**a). Mine wastes were dumped in five major piles scattered throughout the mining area and in several minor tailing and waste-rock dumps, mainly located close to the main mine adits.

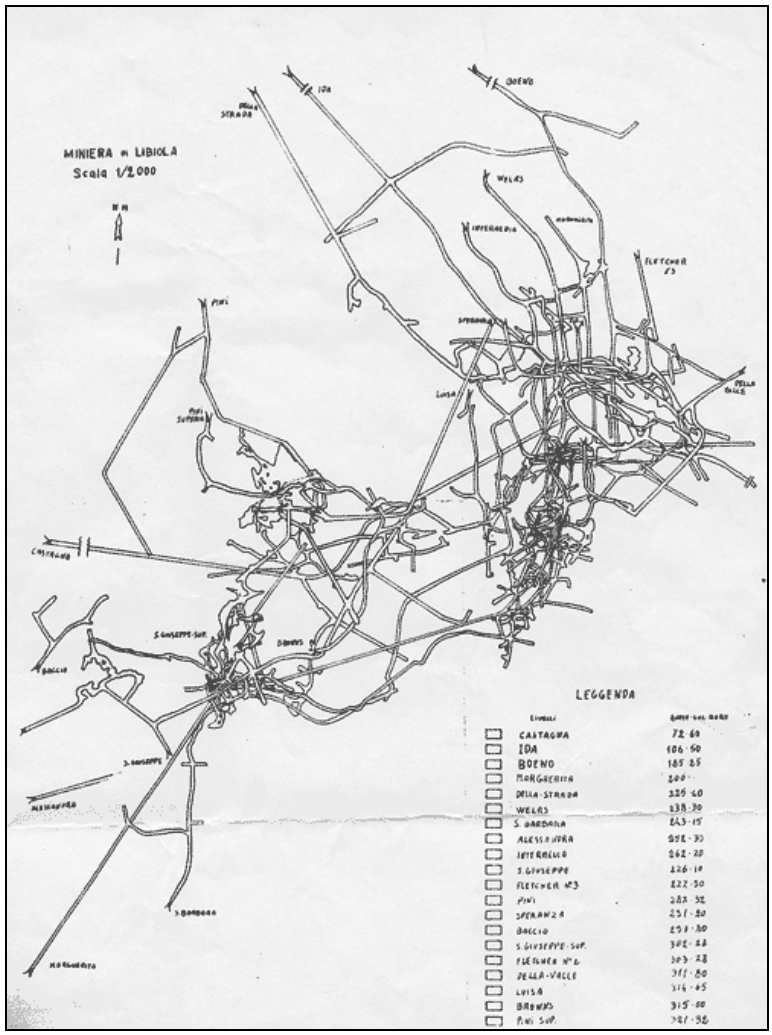

Fig. 25 - Schematic sketch of the underground works in Libiola mining site

The dump mine dumps was constructed in a period of over 50 years during which different techniques of exploitation have been used and different lithotypes and economic

mineralisations have been extracted, either through underground and open-air excavations. The waste materials that were pilled up during exploitation comprise both the host rocks and the non economic mineralisations derived from hand picking, milling and other treatments (Marescotti & Carbone, 2003).

5.7 Earthen material features

Considering that this mine dumps was built over large period of time, significant lateral variations and the vertical heterogeneity are expected.

All the features of earthen materials were defined starting from collection of 21 samples (**Fig. 26**, App. B.2) and laboratory analyses following the relative guidelines, and then interpolated by geostatistical elaboration.

To evaluate the variation of the earthen material features with the depth in the same sites, where samples 20 (bottom of the mine dump) and 21 (top of the mine dump) were collected, two vertical sections of about 1.0 and 1.5 m respectively, outcropping in well-exposed vertical cuts, were sampled every 0.25 m.

All the results of the analyses on this samples are discussed in the spatial analysis chapter.

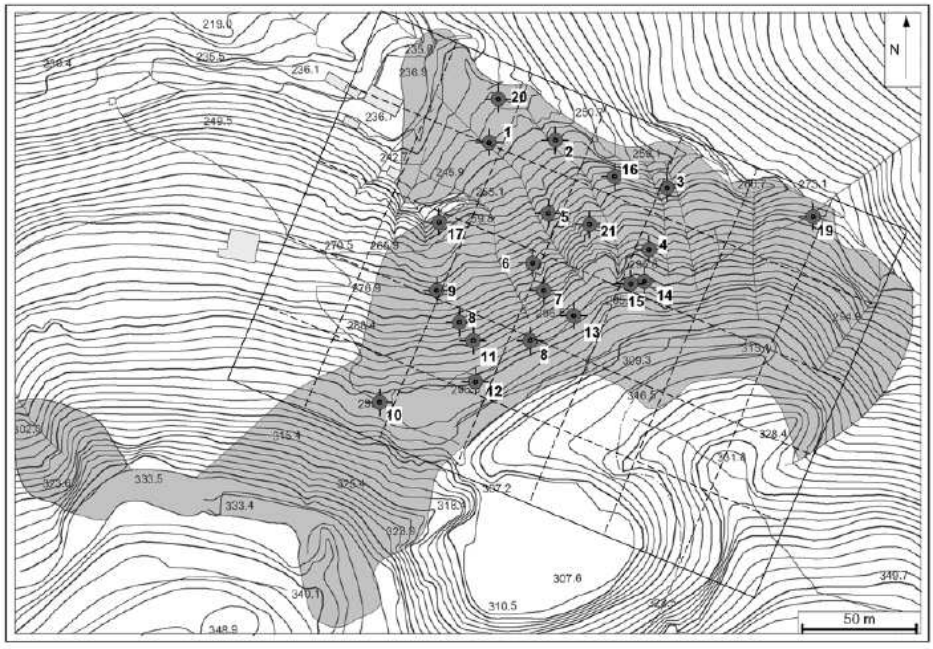

Fig. 26 - Location of the earthen material samples. The shaded area represent the mine dump (Azzali et al., 2008)

5.7.1 Grain size

The results of grain size analysis are shown in App. B.3. All the 21 samples are well-sorted and are classified as "muddy sandy gravel" sediments with the exception of five samples that fall into the "muddy gravel" class and 2 samples that fall into the "gravelly muddy sand" class (Blott, 2000; **Fig. 27**). The silt and the clay fractions (< 0.05 mm) vary from 5 to 26 %.

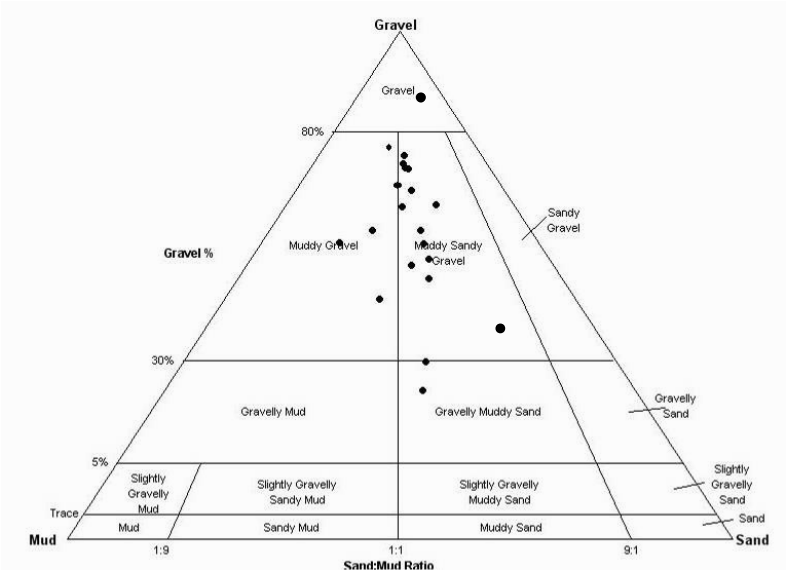

Fig. 27 - Plot of the grain size composition of Libiola mining site surface earthen materials into the gravel – sand – mud diagram of Gradistat (Blott, 2000)

5.7.2 Mineralogy

The results of the mineralogical analysis are shown in App. B.4. The different were distinguished and then classified according to their role in the AMD processes. Following the Jambor and Owens (1993) scheme, they were distinguished: 1) primary minerals (comprising ore- and gangue- mineral assemblages), 2) secondary minerals (comprising all species directly formed within the dump as alteration products of primary phases). Ternary and quaternary minerals were not distinguished minerals because the studied site is an open-air waste-rock deposit.

The waste-rock dumps are characterised by extremely heterogeneous materials since they comprise minerals constituting the gangue and the host rocks, ore minerals with different degree of alteration, and authigenic secondary phases, directly formed on-site, or allocthonous secondary phases, accumulated within the dump.

Gangue and host rock minerals vary from 28.9 to 84.9% of the waste materials and they reflect the two main lithotypes that host the Libiola ore deposit (i.e. pillows and brecciated

basalts and serpentinites). The most abundant minerals are serpentine (lizardite and chrysotile), Ca-plagioclase, magnetite, chlorite, clinopyroxene (augite), clay minerals, albite, and quartz, in decreasing order of abundance. Minor amounts of Cr-spinels, Fe-epidote, ilmenite and zeolites are present in all samples, whereas primary carbonates (calcite, aragonite, dolomite) are generally in trace amounts.

Sulphide ore minerals are represented by pyrite, chalcopyrite, sphalerite and pyrrhotite; other sulphides (such as covellite, chalcocite, pentlandite) and native elements (Au, Ag, and Cu) represent trace constituents. On the whole, they vary from 0.7 to 40.0 % of the waste materials. The lowest and highest contents are anomalous values because they represent sample sites characterised by almost completely inert materials (derived from local open pit excavations in serpentinites) and high enriched sulphide materials (derived from handpicking enrichment operations), respectively.

The secondary minerals are mainly represented by Fe-oxyhydroxides (goethite and minor lepidocrocite) and -oxides (hematite) that represent from 13.8 to 69.3% of the total constituents. Other secondary minerals represent trace constituents and are represented by gypsum, malachite and azurite.

Finally, clay minerals (mainly montmorillonite and other smectite group minerals) are generally widespread, although minor, constituents. Nevertheless, it is still not clear if they derive from AMD processes or from geological processes not directly related to sulphides weathering.

5.7.3 Geochemistry

The analyses and the statistical summaries of the bulk elemental composition of the dumped materials are reported in App. B.5 and are summarized in **Tab. 5** - Statistical report of geochemical features of earthen materials.

The geochemical signatures of the waste rock samples agree well with the qualitative and quantitative results of the mineralogical analyses.

Fe, Si, Mg, and Al are always the main constituents, reflecting the nature of the main lithotypes (serpentinites and basalts) deposited in the dump and the presence of huge quantities of secondary Fe-rich mineral phases.

Sulphur shows wide variations (from 0.01 to 5.71 wt%; table 4) due to the very high variability of sulphide (in particular pyrite) contents in the different sites of the dump. Moreover, the almost complete absence of sulphates and the low S content in the other secondary minerals suggest that the sulphur content of the samples is also controlled, at least in part, by the degree of alteration of sulphides, because most of the sulphur released during sulphide alteration has been removed from the system.

The other metals (such as Cd, Co, Cr, Cu, Mn, Ni, Ti, V and Zn) evidenced a general high concentration and a wide variability, not clearly correlable to the mineralogical

composition of the samples. In fact, these elements can be hosted either within unaltered primary minerals or within secondary Fe-oxides and oxyhydroxides.

SAMPLE	SiO_2	Al_2O_3	TiO_2	Fe_2O_3	MgO	CaO	Na_2O	P_2O_5
	wt%	wt%	wt%	wt%	wt%	wt%	wt%	wt%
min	28.94	1.15	0.17	18.26	2.32	0.13	0.03	0.07
I quartile	33.84	7.32	1.33	27.85	7.75	0.65	0.07	0.13
median	36.6	8.24	1.78	38.98	10.82	0.72	0.16	0.19
III quartile	40.51	10.34	2.27	42.16	21.63	1.115	0.45	0.245
max	46.12	18.08	3.08	51.33	26.73	1.97	0.69	0.29
SAMPLE	**Cd**	**Co**	**Cr**	**Cu**	**Mn**	**Ni**	**V**	**Zn**
	ppm	ppm	ppm	ppm	%	ppm	ppm	ppm
min	1	31	215	160	0.01	93	112	33
I quartile	9	59	541	1258	0.01	224	223	130
median	13	78	846	1887	0.04	435	302	196
III quartile	17	104	1259	3022	0.11	1063	365	317
max	23	408	2524	13347	0.35	3579	541	1126

Tab. 5 - Statistical report of geochemical features of earthen materials

5.7.4 Acid Mine Drainage

AMD static test results (App. B.6) show that in the studied waste-rock dump potential for AMD generation is widespread with MPA values ranging from 0.31 to 174.73 kg H_2SO_4/t. NAPP almost completely coincides with the MPA values because the ANC of all samples is negative with the exception of sample 21.

Since mineralogical investigations have shown that sulphates occurrence is negligible, these AMD values are reliable. So, it was not necessary to analyse samples for S-sulphate to obtain the MPA value calculated starting from S-sulphur. This is also confirmed by the similar trend that we obtained plotting NAPP versus the total S (by bulk chemistry analyses; **Fig. 28**a) and versus the sulphides modal abundance (by point counting; **Fig. 28**b).

Following the Soregaroli and Lawrence (1997) classification, eight samples fall in the "field I", which indicates that AMD is possible but not persisting in time due to the low S content. Twelve samples fall in the "field II" thus indicating that AMD is possible and persisting in time due to the high S content. Only one sample falls in the "field III" (sample 21) which indicates that AMD is impossible; this sample comes from an area where the dumped materials are almost exclusively represented by poorly mineralised serpentinite- and basalt-rich waste rock derived from open pit excavations.

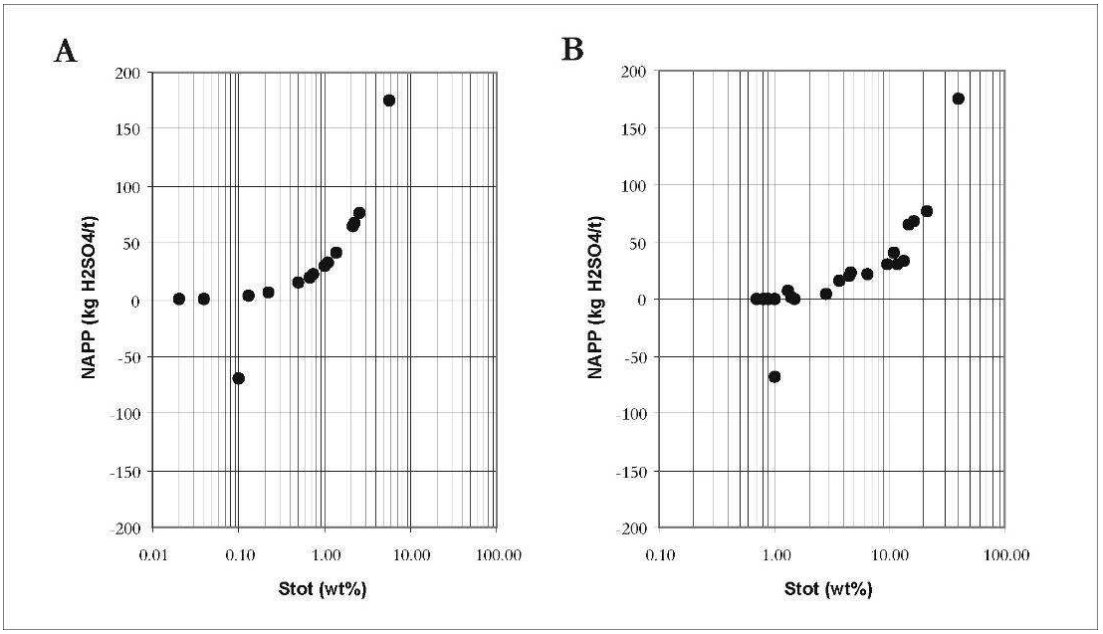

Fig. 28 - a) NAPP values vs. total S content (from Soregaroli and Lawrence, 1997). Field I: AMD possible but non persisting in time. Field II: AMD possible and persisting in time. Field III and IV: AMD impossible. b) NAPP value vs. sulphides modal abundance as determined by point counting

5.8 Spatial analysis

Due to the great heterogeneity of mineralogical, geochemical and AMD data, a spatial analysis was performed to esteem the value of the different variables in the whole mine dump area.

Semivariogram features show that all the variables, with the exception of Cu, have a spatial relation (App. B.7).

After this test, a contour map for each variable was developed with kriging interpolation, whereas contour map of Cu was developed with natural neighbour interpolation. Contour maps (**Fig. 29**) allow to display the different variable distributions of the most significant chemical elements and mineral species and to point out direct and inverse correlations, as well as to confine areas with peculiar characteristics.

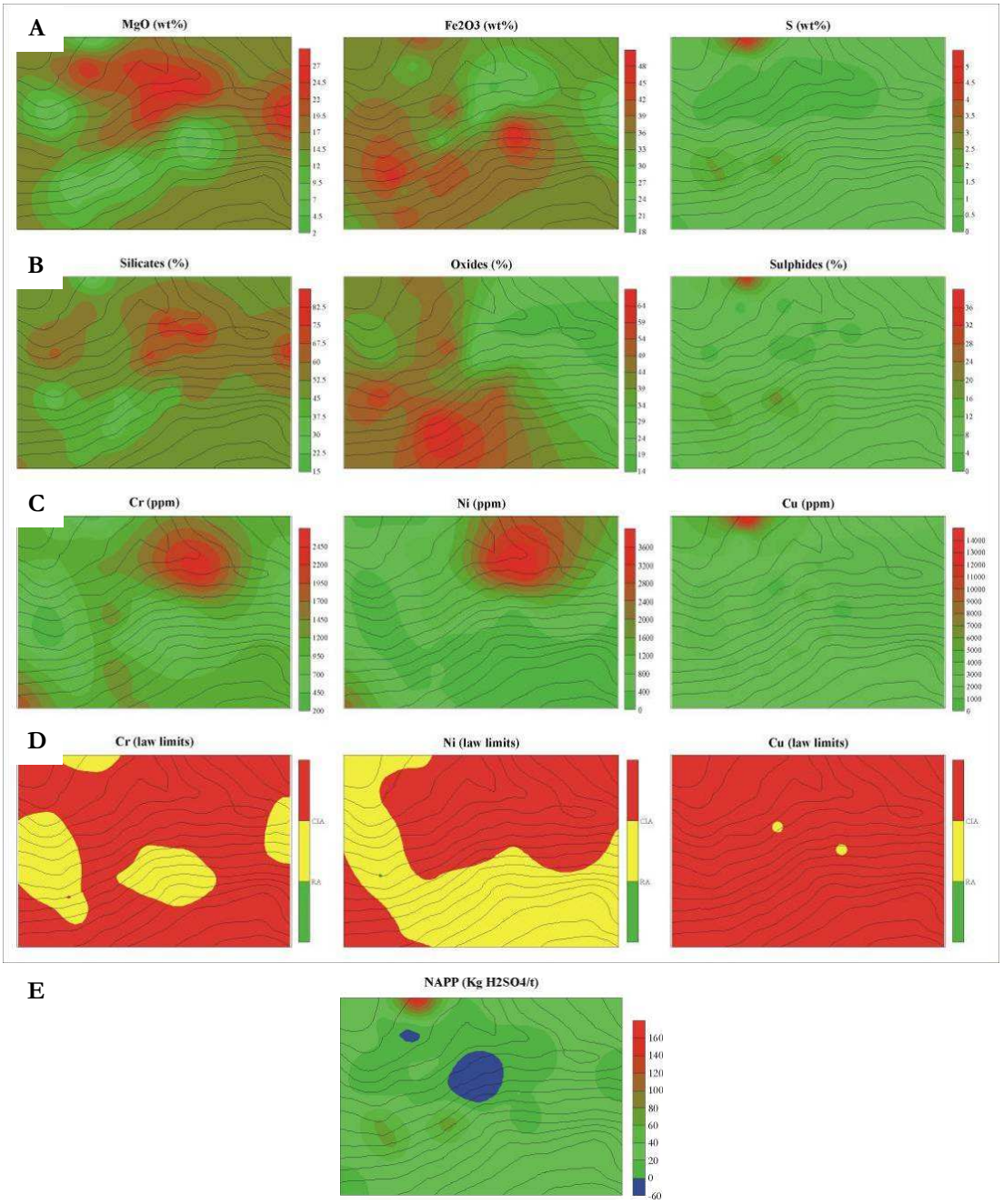

Fig. 29 - Contour maps of a) major element and S concentrations, b) mineral class percentages (Jambor and Owens, 1993), c) heavy metal contents, d) heavy metals compared to law limits and e) NAPP.

On the basis of the contour maps analysis, the studied mine dump can be subdivided into 3 main zones:

1) the first zone, located in the NW sector of the dump, is characterised by a narrow area with high concentrations of total sulphur, Cu, Fe_2O_{3tot}, primary sulphides, as well as by local enrichment in goethite. This results in agreement with historical documents (Marescotti & Carbone, 2003) and with the results of field observations. In fact, this area historically represented the lowest level of the dump where the extracted mineralisations were placed and preliminary treated by means of hand picking and manual selection. The non economic mineralisations were left in place and contain high percentage of pyrite and remnants of chalcopyrite mineralisations. Field observations allowed to recognize the presence in the overall zone of thick ochreous crusts that locally evolve up to centimetric dark reddish hardpans. Moreover, numerous partially unaltered mineralised clasts are easily observable both on the surface of the dump or in the sampled vertical sections.

2) The second zone, located in the SW sector of the dump, corresponds to a topographical plane close to three mine adits and is one of the biggest open pit of the mine area. This zone is characterised by the highest Fe_2O_{3tot} and goethite concentrations with intermediate total sulphur values. The chemical and mineralogical features of this zone can be related to the diffuse presence of non-economic sulphides deposited on-site during the exploitation. As a matter of fact, most of the outcropping rocks in the adjoining area are characterised by the diffuse presence of pyrite-rich stockwork mineralisations. The lowest NAPP values, respect to the NW zone, can be related both to the lower concentration of sulphides in the dumped rocks or by a general more advanced degree of alteration. This is also confirmed by the higher concentrations of secondary minerals (goethite and minor hematite).

3) The third zone, located in the NNE sector of the dump, is characterised by the highest concentration of MgO, Cr_2O_3, Ni and primary silicate minerals. These features are related to the diffuse presence of ophiolitic clasts (serpentinites and basalts) derived from the upper open pit excavations and piled up mainly in this sector of the dump. Other than the above mentioned features, it is important to outline that Cu contents are generally high into the whole mine dump and seem to be independent from the other elements concentrations. Cu distribution is homogeneous with the exception of the zone 1 described above. These features can be related to the scattered distribution of Cu-rich pyrite and chalcopyrite remnants throughout the dump due to the extensive mining activity that affected this site in more than one century.

All the features of sample 20 and 21 show important variation in the first meter of depth.

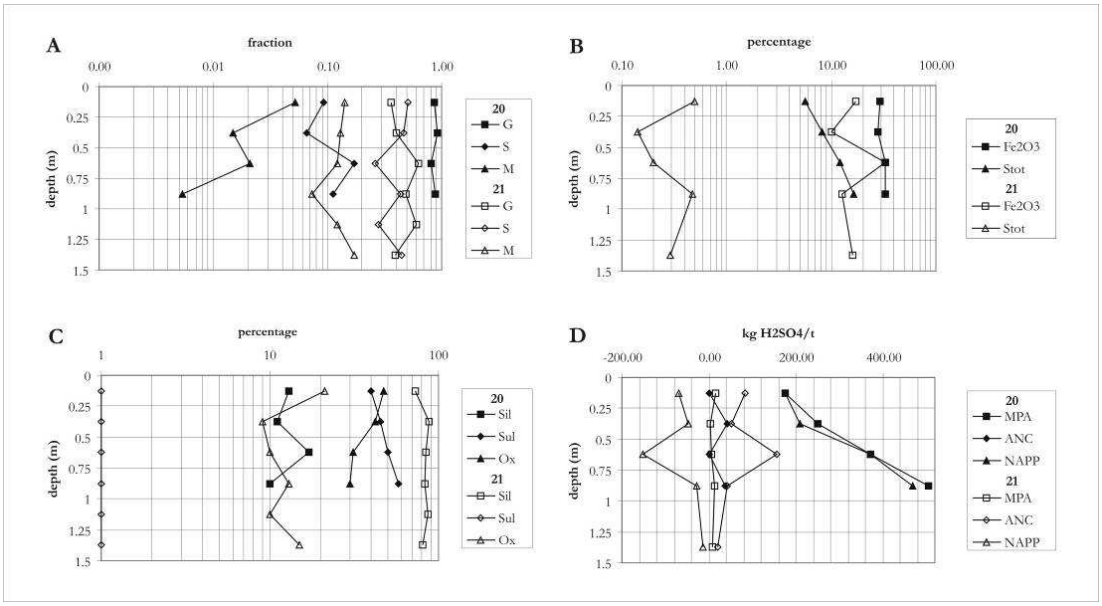

Fig. 30 - Diagrams showing the variation of selected features of samples 20 and 21 with the depth. a) Grain size (G=gravel, S=sand, M=mud), b) Geochemistry, c) Mineralogy (sil=silicate, sul=sulphide, ox=oxide) and d) AMD parameters.

The grain size diagram (**Fig. 30**a) shows an increasing, starting from 1.0 m depth to topographic surface, of the fine fraction in the two sections. Anyway, the grain size of earthen material has a feed-back ralation with the AMD processes, since they perform a chemical alteration that modifie the mineral phases and, at the same time, reduce the grain size.

The chemical composition diagram (**Fig. 30**b) shows that the earthen materials composing the mine dumps are characterised by a compositional layering at centimetric scale. The most important consideration is that sulphur value range from 5.7 to 16.5% in 1.0 m into the section 20 section. Since both the AMD processes are active near the topographic surface, which is always influenced by erosion, the methodology for AMD prevision and prevention may be always considered efficient at least for the earthen materials features down to 1.0 m, or down to an appropriate depth, if the erosion processes are quick.

The mineral species diagram (**Fig. 30**c) shows that oxides duplicate their concentration in the first 0.25-0.50 m from the topographic surface, showing that idea of the thickness of mine dump deposit are influenced by AMD processes.

Finally, the AMD parameters diagram (**Fig. 30**e) shows that the NAPP values of sample 21 are everywhere negative, because ANC values of earthen material are higher than its MPA. On the contrary, the NAPP values of sample 20 increases with the depth.

5.9 Persistence of AMD processes

Starting from monthly rainfall and temperatures (cfr. § 5.5) evapotranspiration and surface flow rates were calculated. Evapotranspiration affects water balance for 54% and reaches 100% of precipitation value from April to September, while it is the lowest in December (16%). The rest of meteoric waters flow on surface (29%) or infiltrate into the ground (17%).

Assuming that 802.0 mm/y of rain waters fall on Libiola catchment (Eurometeo, 1995-2008), 430.6 mm/y were lost through evapotranspiration, 235.1 mm/y flow on surface and 136.1 mm/y infiltrate into the ground.

Considering that the studied mine dump has an area of $4.0*10^4$ m^2 and that only $3.6*10^4$ m^2 are upstream of NAPP>0 area, it is possible to calculate that $9.4*10^3$ m^3/y of meteoric water are available for AMD generation processes.

The average surface water pH value in the studied area ranges from 3.44 to 4.89 (Carbone, 2008). The lowest pH value implies an H^+ concentration of 0.36 mg/l, whereas the highest implies an H^+ concentration of 0.01 mg/l. To keep these pH values constant for all the rain water falling on the studied area, from 6 to 167 kg H_2SO_4/y are needed.

Since average NAPP value of earthen materials is 22.95 kg H_2SO_4/t, and assuming a reactive thickness of 0.50 m (because this is the earthen material that interacts most with atmospheric agents and is the depth at which earthen material samples were collected) and an average density of 2.50 g/cm^3, these earthen materials could produce as much as $1.03*10^6$ kg of H_2SO_4. So, if the environmental and climatic conditions do not change, dividing the total amount of H_2SO_4 equivalent (that can be released) by the total amount of H_2SO_4 equivalent (necessary to maintain the present pH values of waters) a duration of present conditions ranging from $6.17*10^3$ to $1.74*10^5$ years is obtained.

5.10 Conclusions

Environmental assessment of Libiola mining site, alike Rio Marina mining district, regarded only the surface earthen materials and the surface waters and was performed using CSC of D.Lgs. 152/06 as limits to determine the contamination of earthen materials and waters.

The comparison between contour maps of heavy metals concentration and Italian law concentration limits (D.M. 471/99; D.Lgs. 152/2006) allows to outline that the majority of the waste rocks exceed commercial and industrial limit concentrations for Cr, Cu, Ni and V, whereas all the remaining exceed residential limit concentrations. These high concentrations must be identified, in environmental mean, as a pollutant source. In this situation, since the

mining works are mainly underground it will be possible, with a specific field survey, to calculate the natural background values for these elements in the earthen materials.

Also the surface waters are characterised by all the analysed metals that exceed the concentration limits of D.Lgs. 152/2006. The surface waters are a means of transport for the contamination, since the metal concentrations are over the law limits also downstream the site. The low pH values indicate that the AMD processes are active in this area.

Considering that nobody works now at this site and no tourist can enter, the only target for the possible contamination are the surface and the ground waters, even if their use is still not known. For this reason on this site a risk assessment has not been yet done.

The AMD evaluation analysis shows that almost the whole mine dumps can produce acid, up to 67.95 kg H_2SO_4/t.

The spatial analysis of all the analytical parameter of earthen material on the whole mine dump allow to represent the heterogeneities of the waste rocks and then to identify 3 main areas with similar geochemical, mineralogical and acid generating features. This could be very important in a possible future remediation planning, to avoid considering the whole mine dump as a homogeneous object.

Moreover the analysis of vertical sections shows that 1) there are significant variations also with depth and 2) the AMD processes are active mainly between 0.25 and 0.50 from topographic surface. From this arise the necessity to extend the spatial investigation up to a depth related to the erosion processes.

Here, considering that it was assesses a time span of hundreds to thousands of years for AMD processes (0.25-0.50 m earthen material), the erosion rate and the content of sulphides of deeper strata these procedures is fundamental.

Chapter 6

Concluding remarks

On the basis of the presented results the new methodologies here proposed can provide an useful tool to improve the AML characterisation and hence the environmental risk assessment in such sites.

Elaboration of mining areas topographic maps and ERGI investigations are two effective low-cost methodologies that allow identifying and measuring the mine dumps in an objective way. It will be useful to apply the elaboration in the preliminary environmental assessment of every AML that has historical archives with mining maps to plan the following steps of geo-environmental modeling. The ERGI investigations are recommended for the AML where historical data are missing or lacking and, coupled with core drillings, to have an idea of the mine dump geometry and features in 3D.

Application of topographic elaboration in Rio Marina allowed to redefine position, size and shape of the main dumps. Moreover the independent application of the two methodologies on Antenna dump (Rio Marina mining district) has given consistent results that validate the methodology.

Spatial analysis is a valuable tool since it allows to find and display the earthen material heterogeneities in 3D. It showed that to consider each dump as an homogeneous body can be misleading as dumps can show a high degree of both lateral and vertical variability. This analysis is necessary in the following step that concerns the geochemical hazard/risk assessment and could be also useful later, during the remediation planning.

The Libiola mine dump shows how much this analysis is important: there are 3 main areas composed of earthen materials with different features and moreover the waste rocks show strong variations within a meter from topographic surface that should be considered for the management of the site.

Geochemical hazard map is a new suggestion for the judgemental evaluation of the areas that must be prioritarily remediated. Since high metal contents are typical of earthen materials in mining sites, this feature was considered in relation to the capacity of metals mobilisation. In particular the acid production of earthen material has been chosen because the AMD is the most common process that occurs in AML and because there are many procedures to quantify the acid production of earthen materials. However the creation of the geochemical hazard map could be developed 1) using CSR or natural background values instead of CSC, 2) refining the procedures to evaluate the acid production of earthen materials and 3) with the introduction of other parameters to consider (i.e. speciation, availability, etc.). A map of geochemical hazard created in this way allows distinguishing

between earthen materials with a high content of metals and earthen materials with a high content of metals that could be easily mobilised.

Rio Marina is a good example: following the law the majority of the area must be remediated for RA and the remaining for CIA. The examination of the geochemical hazard map shows that about half of the area is composed by earthen material which is not able to produce acid.

As written in § 2.4.3, a quantitative approach to hazard evaluation should consider NAPP values and spatial relationships between cells. For this reason, a dedicated software is under construction (Servida et al., in progress). The input data will be provided by the elaboration of topography (surface water flow) and the spatial analysis of earthen material features. Differently from the available geochemical software, this application will calculate the surface water features starting from earthen material features that interact with them. The purpose is to identify the contamination source area in addition to the assessment of the transport and diffusion of contaminants.

The procedure to assess the persistence in time of the AMD processes is raw but it could be easily applied to any site, since the required input data are often available or could be obtained with standard analyses. This calculation can be useful in remediation planning as it provides information on the possibility of a natural attenuation of the AMD processes.

A persistence in time of the AMD processes higher than a century was assessed both for Rio Marina and for Libiola. It is possible to guess that in these sites naturally attenuation will not occur and, moreover, that a remediation activity could be useful to limit the contamination processes at least in space.

Also this methodology could be improved starting from a more accurate hydrologic balance, supported by hydrogeological analyses, and calculating the persistence value for each area unit with its specific earthen material features.

In conclusion, we think that it will be useful to add these methodologies into the risk assessment procedures for AML, to support their management. The final target will be to provide information for the choice of sites that need priority remediation activities, and within these sites to identify areas responsible for contamination.

Appendix A

Rio Marina mining district data

Appendix A.1 – Water analyses

Sample	pH	Eh	Cond.	Cl^-	SO_4^{--}	NO_3^-	Ca^{++}	Mg^{++}	Na^+	K^+	Fe	Mn	Cu	Zn
		mV	mS/cm	mg/l	mg/l	mg/l	mg/l	mg/l	mg/l	mg/l	mg/l	mg/l	mg/l	mg/l
DRY SEASON														
1	2.1	592	7.54	17.9	7370	0.68	137	484	6.4	1.8	903.20	23.21	0.72	6.18
2	3.3	449	1.63	9.7	875	0.07	76	137	6.8	2.8	1.31	9.89	0.50	5.63
3	2.9	494	6.15	26.1	8860	1.00	160	837	9.7	4.3	77.51	43.72	0.34	6.84
4	2.7	550	6.34	17.1	7400	0.76	215	807	6.6	1.9	110.50	45.02	1.14	10.08
5	3.4	421	2.45	14.7	1900	0.23	468	141	8.6	2.7	2.63	2.88	0.06	3.67
6	n.a.	n.a.	n.a.	n.a.	n.a.	n.a.	n.a.	n.a.	n.a.	n.a.	n.a.	n.a.	n.a.	n.a.
7	2.8	482	7.44	15.2	10100	1.72	106	897	9.6	1.9	3.84	12.03	0.58	3.77
8	n.a.	n.a.	n.a.	n.a.	n.a.	n.a.	n.a.	n.a.	n.a.	n.a.	n.a.	n.a.	n.a.	n.a.
9	n.a.	n.a.	n.a.	n.a.	n.a.	n.a.	n.a.	n.a.	n.a.	n.a.	n.a.	n.a.	n.a.	n.a.
WET SEASON														
1	2.3	528	5.15	15.3	7690	0.22	86	349	4.1	2.88	668.20	23.45	0.40	5.22
2	2.9	503	2.61	22.1	2210	0.25	53	243	6.8	3.43	22.63	12.98	0.55	3.68
3	2.8	517	6.01	24.3	5060	1.30	143	730	9.5	2.33	80.88	38.21	0.26	5.54
4	2.5	573	6.45	24.2	7720	0.45	120	739	7.2	0.39	95.11	41.25	0.96	8.07
5	n.a.	n.a.	n.a.	n.a.	n.a.	n.a.	n.a.	n.a.	n.a.	n.a.	n.a.	n.a.	n.a.	n.a.
6	2.7	531	3.04	28.7	2500	0.14	190	165	17.9	2.52	224.10	22.24	1.75	1.41
7	3.0	497	1.78	10.1	1340	0.65	72	144	4.1	0.31	19.96	8.05	0.38	1.36
8	2.3	550	4.28	22.0	3360	0.15	129	266	4.8	0.97	283.90	12.76	0.69	2.72
9	2.8	535	2.00	28.0	1280	0.15	34	116	3.5	29.70	26.77	5.61	0.18	0.71

Appendix A.2 – Earthen material samples

Sample	X (UTM)	Y (UTM)	Deposit nature	Bedrock*	Sample	X (UTM)	Y (UTM)	Deposit nature	Bedrock*
A04	1615739	4742258	Soil	CV	**E02**	1616119	4742514	Soil	MSQ
A06	1615730	4742125	Soil	CV	**E03**	1616097	4742434	Debris	VG
A07	1615752	4742045	Soil	LIM	**E04**	1616133	4742320	Debris	HEM
B03	1615826	4742371	Waste	CV	**E05**	1616129	4742206	Debris	VG
B04	1615823	4742303	Waste	CV	**E06**	1616126	4742104	Waste	VG
B05	1615835	4742213	Soil	CV	**E07**	1616132	4742002	Waste	VG
B06	1615826	4742102	Debris	CV	**E08**	1616134	4741904	Waste	VG
B07	1615825	4742000	Debris	CV	**E09**	1616135	4741802	Waste	VG
B08	1615825	4741899	Soil	CV	**E10**	1616139	4741697	Waste	VG
C02	1615913	4742452	Debris	CV	**F04**	1616234	4742279	Waste	VG
C03	1615925	4742409	Debris	CV	**F05**	1616231	4742208	Waste	VG
C04	1615920	4742301	Debris	MSQ	**F06**	1616232	4742106	Waste	VG
C05	1615924	4742196	Waste	MSQ	**F07**	1616166	4742009	Waste	VG
C06	1615917	4742076	Debris	LIM	**F08**	1616236	4741905	Waste	HEM
C07	1615925	4741999	Debris	VG	**F09**	1616238	4741804	Waste	VG
C08	1615927	4741900	Waste	VG	**F10**	1616239	4741696	Waste	VG
C09	1615926	4741801	Debris	LIM	**G03**	1616330	4742410	Soil	MSQ
D01	1616020	4742608	Soil	MSQ	**G04**	1616334	4742308	Soil	VG
D02	1616023	4742513	Debris	MSQ	**G05**	1616321	4742225	Waste	VG
D03	1616023	4742405	Debris	VG	**G06**	1616335	4742108	Waste	RM
D04	1616034	4742315	Debris	VG	**G07**	1616219	4741982	Waste	HEM
D05	1616024	4742204	Debris	VG	**G08**	1616340	4741904	Waste	HEM
D06	1616035	4742100	Debris	VG	**H03**	1616434	4742409	Soil	MSQ
D07	1616030	4742001	Waste	VG	**H04**	1616454	4742310	Soil	VG
D08	1616031	4741902	Waste	VG	**H06**	1616426	4742094	Waste	RM
D09	1616038	4741803	Waste	VG	**I03**	1616536	4742407	Soil	VG
D10	1616035	4741701	Waste	VG	**I04**	1616607	4742321	Soil	VG

*RM: Rio Marina Formation, VG: Verrucano Group, MSQ: Monte Serra Quartzites, CV: Calcare Cavernoso, HEM: hematite, LIM: limonite.

Appendix A.3 – Grain size analyses

Sample	G	S	M	D_{10}	D_{60}	C_u	Sample	G	S	M	D_{10}	D_{60}	C_u
	%	%	%	mm	mm	-		%	%	%	mm	mm	-
A04	0.52	0.43	0.05	0.09	4.00	44.44	**E02**	0.62	0.37	0.02	0.30	4.00	13.33
A06	0.49	0.48	0.04	0.15	3.00	20.00	**E03**	0.73	0.26	0.01	0.40	11.00	27.50
A07	n.a.	n.a.	n.a.	n.a.	n.a.	n.a.	**E04**	0.68	0.30	0.02	0.25	6.00	24.00
B03	0.78	0.20	0.01	0.40	11.50	28.75	**E05**	0.34	0.62	0.04	0.10	1.50	15.00
B04	0.64	0.34	0.02	0.25	7.00	28.00	**E06**	0.45	0.51	0.05	0.15	2.50	16.67
B05	0.50	0.47	0.03	0.20	2.70	13.50	**E07**	0.42	0.54	0.03	0.10	2.50	25.00
B06	0.90	0.09	0.01	2.00	12.00	6.00	**E08**	0.65	0.34	0.01	0.35	5.50	15.71
B07	0.74	0.25	0.01	0.50	10.10	20.20	**E09**	0.55	0.43	0.02	0.15	3.50	23.33
B08	0.58	0.40	0.02	0.25	4.00	16.00	**E10**	0.77	0.21	0.01	0.45	10.50	23.33
C02	0.61	0.38	0.02	0.25	4.50	18.00	**F04**	0.55	0.43	0.02	0.15	3.50	23.33
C03	0.66	0.33	0.01	0.40	5.00	12.50	**F05**	0.50	0.48	0.02	0.15	3.40	22.67
C04	0.58	0.39	0.03	0.20	4.50	22.50	**F06**	0.46	0.51	0.02	0.15	2.50	16.67
C05	0.74	0.25	0.01	0.55	10.00	18.18	**F07**	0.56	0.42	0.03	0.15	6.00	40.00
C06	0.76	0.23	0.01	0.40	11.00	27.50	**F08**	0.59	0.38	0.03	0.25	4.50	18.00
C07	0.58	0.37	0.05	0.20	5.50	27.50	**F09**	0.72	0.27	0.01	0.40	8.00	20.00
C08	0.70	0.28	0.02	0.25	11.10	44.40	**F10**	0.79	0.20	0.01	0.40	11.50	28.75
C09	0.49	0.48	0.04	0.10	4.00	40.00	**G03**	n.a.	n.a.	n.a.	n.a.	n.a.	n.a.
D01	0.72	0.26	0.02	0.50	10.00	20.00	**G04**	n.a.	n.a.	n.a.	n.a.	n.a.	n.a.
D02	0.50	0.46	0.04	0.15	3.00	20.00	**G05**	0.73	0.26	0.01	0.15	11.00	73.33
D03	0.66	0.33	0.02	0.30	5.50	18.33	**G06**	0.59	0.41	0.00	0.45	4.00	8.89
D04	0.42	0.57	0.02	0.15	2.00	13.33	**G07**	0.62	0.36	0.02	0.20	5.50	27.50
D05	0.58	0.39	0.03	0.15	3.50	23.33	**G08**	0.55	0.43	0.02	0.25	3.00	12.00
D06	0.69	0.29	0.02	0.35	6.00	17.14	**H03**	0.64	0.33	0.03	0.20	7.00	35.00
D07	0.77	0.22	0.01	0.50	10.50	21.00	**H04**	0.65	0.33	0.02	0.45	4.50	10.00
D08	0.26	0.70	0.04	0.09	1.00	11.11	**H06**	0.76	0.23	0.01	0.30	10.50	35.00
D09	0.50	0.48	0.02	0.15	3.00	20.00	**I03**	0.68	0.30	0.02	0.20	11.00	55.00
D10	0.63	0.35	0.03	0.20	6.50	32.50	**I04**	0.77	0.21	0.02	0.40	11.00	27.50

D_{10} = soil particle diameter at which 10% of the mass of a soil sample is finer, D_{60} = soil particle diameter at which 60% of the mass of a soil sample is finer, $C_u = D_{60} / D_{10}$ is uniformity coefficient. Higher is the uniformity coefficient, more the earthen material is poorly sorted or well-graded.

Appendix A.4 – Mineralogical analyses

Sam	Ab	Cal	Chl	Dol	Gp	Gt	Hem	Kln	Kfs	Jr	Mag	Ms	Py	Qtz	Sep	Tlc
A4		X	X	X								X		X		
A7			X			X	X					X	X	X		
B4			X						X	X		X		X		
B6	X		X							X		X		X		
B8		X	X	X		X		X				X	X	X		
C3			X						X			X		X		X
C5			X				X			X		X		X		X
C8						X					X	X		X		X
C9		X	X	X		X						X	X	X		X
D2			X				X		X			X		X		
D4			X				X			X	X	X		X	X	X
D6			X			X			X			X	X	X		X
D7									X	X		X	X	X		X
D8			X							X		X	X	X		X
D10			X		X		X		X	X		X	X	X	X	X
E3						X	X			X		X	X	X	X	
E5							X		X	X		X	X	X	X	
E7			X				X		X	X		X	X	X	X	
E9			X		X		X		X			X	X	X		X
E10		X	X	X					X	X		X		X	X	X
F4			X				X		X	X		X	X	X	X	X
F6			X				X		X	X		X	X	X		X
F8						X	X	X	X			X	X	X		
F10			X					X	X	X		X		X	X	X
G3							X	X	X			X	X	X		
G5			X				X	X	X			X		X		X
H4			X			X						X	X	X		X
H6			X			X	X	X	X			X	X	X		X

Ab=albite, Cal=calcite, Chl=chlorite, Dol=dolomite, Gp=gypsum, Gt=Goethite, Hem=hematite, Kln=Kaolin, Kfs=k-feldspar, Jr=jarosite, Mag=magnetite, Ms=muscovite+Illite, Py=pyrite, Qtz=Quartz, Sep=Sepiolite, Tlc=Talc+Serpentine

Appendix A.5 – Chemical analyses

Sample	SiO_2 wt%	Al_2O_3 wt%	TiO_2 wt%	Fe_2O_3 wt%	MgO wt%	CaO wt%	Na_2O wt%	K_2O wt%	P_2O_5 wt%	Cu ppm	Mn ppm	Pb ppm	Zn ppm
A04	<35.00	6.42	0.17	6.00	8.25	>30.00	0.15	0.49	0.16	18	3660	28	360
A06	<35.00	6.47	0.15	4.77	8.29	>30.00	0.17	0.77	0.15	44	1593	58	521
A07	<35.00	6.70	0.24	>50.00	1.40	0.32	0.30	0.82	0.06	6169	6381	460	10211
B03	48.81	17.36	0.87	19.80	2.10	0.06	0.23	4.19	0.21	6	357	65	362
B04	41.12	11.30	1.02	29.53	1.84	0.13	0.18	3.34	0.21	5	176	93	143
B05	38.33	13.44	0.36	6.07	8.27	>30.00	0.19	2.58	0.14	23	1076	34	323
B06	51.67	19.28	0.84	14.70	2.57	0.15	0.28	4.39	0.18	35	510	78	2789
B07	58.90	18.69	0.75	10.89	2.17	0.93	0.20	4.23	0.10	57	333	94	527
B08	<35.00	12.87	0.32	44.21	2.76	14.96	0.23	1.17	0.11	2396	3727	407	5734
C02	55.99	18.53	0.75	10.28	4.84	2.55	0.33	3.54	0.09	57	3088	105	356
C03	58.39	15.40	0.68	13.68	3.59	1.10	0.29	3.13	0.08	128	2268	82	754
C04	50.17	18.78	0.68	7.60	>10.00	9.44	0.24	3.10	0.08	18	1578	78	641
C05	40.40	13.28	0.83	26.99	2.55	0.18	0.33	2.99	0.29	156	608	415	1163
C06	45.81	17.02	0.80	23.09	3.59	0.29	0.21	3.57	0.13	159	651	241	623
C07	64.79	18.87	0.74	7.29	1.88	0.04	0.16	3.99	0.10	1037	1317	510	736
C08	41.57	4.64	0.40	40.27	>10.00	0.03	0.19	0.97	0.03	79	90	461	1192
C09	41.82	17.00	0.69	18.28	5.85	8.61	0.26	4.18	0.12	46	802	77	2683
D01	62.48	17.62	1.08	7.46	2.30	0.63	0.47	3.08	0.11	42	4381	102	831
D02	58.95	20.96	0.96	8.86	2.05	0.30	0.25	4.49	0.11	42	687	57	726
D03	36.19	7.90	0.51	38.17	2.03	0.86	0.37	2.76	0.16	46	173	77	226
D04	<35.00	5.12	0.40	>50.00	1.72	0.14	0.14	2.59	0.05	0	53	58	365
D05	46.35	15.14	0.78	22.41	1.68	0.08	0.26	4.30	0.21	80	147	147	254
D06	54.13	15.23	0.71	17.48	1.83	0.16	0.24	3.28	0.09	105	571	366	809
D07	53.39	12.89	1.54	15.61	0.86	0.03	0.29	4.22	0.42	44	87	6250	368
D08	56.39	17.39	1.03	11.79	2.00	0.32	0.24	5.19	0.12	69	280	941	1018
D09	36.19	6.49	0.63	40.39	8.75	0.03	0.23	1.39	0.07	313	310	3718	2897
D10	39.68	12.18	0.70	31.01	3.43	1.00	0.17	4.75	0.16	1	207	36	347

Continue

Sample	SiO_2	Al_2O_3	TiO_2	Fe_2O_3	MgO	CaO	Na_2O	K_2O	P_2O_5	Cu	Mn	Pb	Zn
	wt%	wt%	wt%	wt%	wt%	wt%	wt%	wt%	wt%	ppm	ppm	ppm	ppm
E02	52.47	14.61	1.18	19.05	1.56	0.50	0.37	2.40	0.16	30	1012	159	387
E03	<35.00	4.87	0.63	46.39	1.67	0.01	0.14	3.08	0.08	0	93	36	223
E04	44.50	14.67	0.77	23.23	2.77	0.05	0.23	6.00	0.16	28	114	27	523
E05	45.11	13.64	0.60	28.17	0.93	0.05	0.54	4.21	0.15	83	200	64	479
E06	40.78	16.37	0.91	32.02	2.74	0.17	0.22	3.83	0.08	33	188	191	361
E07	47.84	16.68	0.77	20.55	2.18	0.05	0.28	5.81	0.08	16	126	35	285
E08	46.40	15.43	0.83	23.91	3.13	0.36	0.26	3.95	0.12	230	638	41	572
E09	47.92	12.92	0.54	26.13	2.49	0.91	0.36	3.13	0.09	152	682	191	402
E10	45.02	16.67	0.76	17.39	2.43	3.46	0.30	4.66	0.12	32	147	28	163
F04	45.86	17.45	0.91	22.34	3.37	0.26	0.28	4.71	0.09	97	270	205	655
F05	50.48	19.66	0.77	18.41	1.52	0.07	0.34	4.65	0.08	69	145	114	225
F06	49.25	15.05	0.80	22.54	1.67	0.14	0.38	3.59	0.08	122	496	238	951
F07	40.42	12.67	0.73	33.55	3.30	0.12	0.21	4.19	0.12	44	179	82	824
F08	52.41	21.84	0.95	15.08	1.92	0.11	0.38	4.62	0.06	39	219	56	665
F09	43.97	15.39	0.82	23.64	4.52	0.29	0.20	4.50	0.11	81	404	100	1746
F10	46.58	16.03	0.80	17.76	6.01	0.34	0.22	3.80	0.15	53	928	116	198
G03	62.51	11.35	0.79	9.58	1.43	1.36	0.43	2.28	0.11	28	2006	59	568
G04	65.89	12.76	1.02	10.53	1.97	0.82	0.58	2.22	0.08	59	2209	113	755
G05	44.04	15.09	0.59	30.43	2.60	0.29	0.27	3.10	0.10	268	1370	92	566
G06	48.90	25.34	0.99	16.08	1.63	0.17	0.24	4.20	0.07	45	557	56	273
G07	57.89	14.08	0.69	19.12	1.08	0.35	0.31	2.01	0.06	22	251	52	239
G08	52.75	20.12	0.91	13.13	2.25	0.05	0.30	6.67	0.10	27	103	35	140
H03	77.04	10.03	0.93	5.50	0.98	0.40	0.50	1.90	0.07	22	301	33	277
H04	45.48	19.79	0.86	19.23	5.24	0.35	0.24	3.43	0.13	53	2257	130	883
H06	41.92	19.38	1.04	30.20	2.01	0.10	0.19	4.34	0.09	65	131	106	572
I03	56.83	15.10	0.93	12.26	1.94	1.06	0.42	2.88	0.13	48	1510	89	869
I04	42.13	17.36	0.77	25.92	5.22	0.23	0.22	4.09	0.11	88	971	176	588

Appendix A.6 – AMD static tests

Sample	S	$S_{sulphate}$	$S_{sulphide}$	$S_{sulphate}/S$	S MPA	S^{--} MPA	ANC	S NAPP	S^{--} NAPP
	wt%	wt%	wt%		H_2SO_4 kg/t	H_2SO_4 kg/t	H_2SO_4 kg/t	H_2SO_4 kg/t	H_2SO_4 kg/t
A04	<0.10	na	nc	nc	<1.50	<1.50	880.8	-879.30	-879.30
A06	<0.10	<.03	nc	nc	<1.50	<1.50	715.2	-713.70	-713.70
A07	<0.10	na	nc	nc	<1.50	<1.50	23.0	-21.50	-21.50
B03	0.64	0.20	0.44	0.31	19.58	13.46	0.0	19.58	13.46
B04	3.42	0.31	3.11	0.09	104.65	95.17	0.0	104.65	95.17
B05	<0.10	<.03	nc	nc	<1.50	<1.50	664.4	-662.90	-662.90
B06	1.25	0.45	0.80	0.36	38.25	24.48	0.7	37.55	23.78
B07	<0.10	na	nc	nc	<1.50	<1.50	14.6	-13.10	-13.10
B08	<0.10	na	nc	nc	<1.50	<1.50	178.9	-177.40	-177.40
C02	<0.10	na	nc	nc	<1.50	<1.50	23.0	-21.50	-21.50
C03	<0.10	na	nc	nc	<1.50	<1.50	16.2	-14.70	-14.70
C04	<0.10	na	nc	nc	<1.50	<1.50	129.4	-127.90	-127.90
C05	3.31	0.06	3.25	0.02	101.29	99.45	21.7	79.59	77.75
C06	0.43	0.43	0.00	1.00	13.16	0.00	2.3	10.86	-2.30
C07	<0.10	na	nc	nc	<1.50	<1.50	169.5	-168.00	-168.00
C08	0.15	0.29	nc	nc	4.59	-4.28	0.0	4.59	-4.28
C09	<0.10	na	nc	nc	<1.50	<1.50	100.7	-99.20	-99.20
D01	<0.10	na	nc	nc	<1.50	<1.50	7.1	-5.60	-5.60
D02	<0.10	na	nc	nc	<1.50	<1.50	3.7	-2.20	-2.20
D03	6.95	0.96	5.99	0.14	212.67	183.29	0.0	212.67	183.29
D04	7.58	0.37	7.21	0.05	231.95	220.63	8.2	223.75	212.43
D05	2.76	0.05	2.71	0.02	84.46	82.93	0.0	84.46	82.93
D06	<0.10	na	nc	nc	<1.50	<1.50	2.1	-0.60	-0.60
D07	2.92	0.37	2.55	0.13	89.35	78.03	0.0	89.35	78.03
D08	2.10	0.53	1.57	0.25	64.26	48.04	2.7	61.56	45.34
D09	2.34	0.65	1.69	0.28	71.60	51.71	0.0	71.60	51.71
D10	4.42	1.39	3.03	0.31	135.25	92.72	0.2	135.05	92.52

n.a = not analysed; n.c. = not calculated

Continua

Sample	S	$S_{sulphate}$	$S_{sulphide}$	$S_{sulphate}/S$	S MPA	S^{--} MPA	ANC	S NAPP	S^{--} NAPP
	wt%	wt%	wt%		H_2SO_4 kg/t	H_2SO_4 kg/t	H_2SO_4 kg/t	H_2SO_4 kg/t	H_2SO_4 kg/t
E02	<0.10	na	nc	nc	<1.50	<1.50	2.7	-1.20	-1.20
E03	8.46	0.12	8.34	0.01	258.88	255.20	0.0	258.88	255.20
E04	3.33	0.05	3.28	0.02	101.90	100.37	0.0	101.90	100.37
E05	2.65	0.02	2.63	0.01	81.09	80.48	0.0	81.09	80.48
E06	1.67	0.05	1.62	0.03	51.10	49.57	0.0	51.10	49.57
E07	2.12	0.05	2.07	0.02	64.87	63.34	0.0	64.87	63.34
E08	na	0.14	nc	nc!	0.00	-4.28	2.7	-2.70	-6.98
E09	2.34	0.42	1.92	0.18	71.60	58.75	0.0	71.60	58.75
E10	3.36	1.45	1.91	0.43	102.82	58.45	57.9	44.92	0.55
F04	1.87	0.53	1.34	0.28	57.22	41.00	0.0	57.22	41.00
F05	0.91	0.02	0.89	0.02	27.85	27.23	0.0	27.85	27.23
F06	1.20	0.21	0.99	0.18	36.72	30.29	0.0	36.72	30.29
F07	2.59	0.28	2.31	0.11	79.25	70.69	0.0	79.25	70.69
F08	0.45	0.26	0.19	0.58	13.77	5.81	0.0	13.77	5.81
F09	3.19	0.66	2.53	0.21	97.61	77.42	0.0	97.61	77.42
F10	2.46	0.58	1.88	0.24	75.28	57.53	6.4	68.88	51.13
G03	<0.10	na	nc	nc	<1.50	<1.50	6.6	-5.10	-5.10
G04	<0.10	na	nc	nc	<1.50	<1.50	6.2	-4.70	-4.70
G05	0.25	0.02	0.23	0.08	7.65	7.04	0.2	7.45	6.84
G06	<0.10	na	nc	nc	<1.50	<1.50	0.0	1.50	1.50
G07	<0.10	na	nc	nc	<1.50	<1.50	3.4	-1.90	-1.90
G08	0.80	0.18	0.62	0.23	24.48	18.97	0.0	24.48	18.97
H03	<0.10	na	nc	nc	<1.50	<1.50	1.2	0.30	0.30
H04	<0.10	na	nc	nc	<1.50	<1.50	8.4	-6.90	-6.90
H06	<0.10	na	nc	nc	<1.50	<1.50	0.7	0.80	0.80
I03	<0.10	na	nc	nc	<1.50	<1.50	5.9	-4.40	-4.40
I04	0.27	0.25	0.02	0.93	8.26	0.61	0.7	7.56	-0.09

n.a = not analysed; n.c. = not calculated

Appendix A.7 – Variogram parameters

Variable	Model	Scale	Length	Anisotropy
SiO_2	exponential	108	60	1
CaO	exponential	6.75	50	1
Fe_2O_3	spherical	105	95	1
S	exponential	4.3	110	1
$S_{sulphate}$	exponential	0.08	90	1
MPA	exponential	4250	95	1
MPA*	exponential	3750	115	1
ANC	exponential	1600	50	1

Appendix B

Libiola mining site data

Appendix B.1 – Water analyses

Sample	T	pH	Eh	Cond.	Alk	Cl^-	SO_4^{--}	Ca^{++}	Mg^{++}	Na^+	K^+
	°C		mV	µS/cm	HCO_3 mg/l	mg/l	mg/l	mg/l	mg/l	mg/l	mg/l
1	11.7	3.8	455	1775	-	18.3	1500	289	159	22.1	5.0
10	13.7	5.2	170	940	6.1	7.0	650	101	72	12.1	2.6
13	12.1	5.4	280	536	36.6	7.1	400	50	53	3.6	0.9
11	13.0	4.0	300	722	18.3	7.1	500	92	77	3.3	2.6
11A	11.6	6.6	235	325	24.4	10.7	400	67	52	2.8	1.3
11B	12.1	5.5	245	527	6.1	14.2	550	52	49	2.8	1.9
12	12.0	3.7	220	548	ud	7.1	500	56	46	2.6	1.3
12A	12.0	5.4	142	537	6.1	14.2	500	58	50	2.9	1.7
14	11.3	6.9	na	489	36.6	7.1	300	38	47	3.1	1.1
15	11.8	6.7	na	513	15.3	10.7	450	39	48	3.7	1.2

Sample	Al	Cd	Co	Cr	Cu	Fe	Mn	Ni	Zn
	mg/l	µg/l	mg/l	mg/l	mg/l	mg/l	mg/l	mg/l	mg/l
1	42	-	-	-	32.0	9.8	-	0.7	5.7
10	-	-	-	-	5.9	0.6	-	0.4	1.5
13	nd	1.8	126	0.5	1.8	0.78	0.24	158	0.39
11	nd	4.8	220	2.4	5.5	0.23	0.75	388	1.20
11A	0.01	0.8	16	0.3	0.3	8.00	23.00	40	0.10
11B	nd	2.5	152	0.6	2.5	6.00	0.32	182	0.55
12	nd	1.5	90	2.4	1.1	2.70	0.08	141	0.21
12A	nd	1.9	121	0.5	2.0	0.21	0.23	160	0.39
14	nd	0.5	6	6.2	0.1	16.00	nd	84	0.03
15	nd	1.5	78	0.7	0.5	24.00	0.12	129	0.23

Data about samples 1 and 10 were taken from Dinelli & Tateo, 2002; other samples from Cortecci et al., 2008

Appendix B.2 – Earthen material samples

Sample	X (UTM)	Y (UTM)	Depth (cm)	Sample	X (UTM)	Y (UTM)	Depth (cm)	Sample	X (UTM)	Y (UTM)	Depth (cm)
1	1535823	4905905	-	**11**	1535775	4905791	-	**20b**	1535841	4905818	25-50
2	1535852	4905906	-	**12**	1535816	4905818	-	**20c**	1535841	4905818	50-75
3	1535901	4905885	-	**13**	1535817	4905800	-	**20d**	1535841	4905818	75-100
4	1535893	4905858	-	**14**	1535860	4905829	-	**21a**	1535965	4905872	0-25
5	1535849	4905874	-	**15**	1535891	4905844	-	**21b**	1535965	4905872	25-50
6	1535827	4905924	-	**16**	1535885	4905843	-	**21c**	1535965	4905872	50-75
7	1535842	4905852	-	**17**	1535878	4905890	-	**21d**	1535965	4905872	75-100
8	1535847	4905840	-	**18**	1535867	4905869	-	**21e**	1535965	4905872	100-125
9	1535810	4905826	-	**19**	1535801	4905870	-	**21f**	1535965	4905872	125-150
10	1535800	4905840	-	**20a**	1535841	4905818	0-25				

Appendix B.3 – Grain size analyses

Sample	G %	S %	M %	Sample	G %	S %	M %	Sample	G %	S %	M %
1	0.68	0.26	0.05	**11**	0.68	0.20	0.12	**20b**	0.92	0.07	0.01
2	0.76	0.17	0.07	**12**	0.77	0.16	0.07	**20c**	0.81	0.17	0.02
3	0.56	0.28	0.16	**13**	0.31	0.43	0.26	**20d**	0.88	0.11	0.01
4	0.60	0.28	0.12	**14**	0.78	0.15	0.07	**21a**	0.36	0.50	0.14
5	0.57	0.31	0.12	**15**	0.49	0.25	0.26	**21b**	0.40	0.46	0.13
6	0.80	0.11	0.08	**16**	0.36	0.41	0.23	**21c**	0.62	0.26	0.12
7	0.53	0.33	0.14	**17**	0.72	0.17	0.11	**21d**	0.49	0.44	0.07
8	0.71	0.20	0.09	**18**	0.63	0.17	0.20	**21e**	0.60	0.28	0.12
9	0.61	0.12	0.28	**19**	0.76	0.17	0.08	**21f**	0.39	0.44	0.17
10	0.63	0.26	0.11	**20a**	0.86	0.09	0.05				

Appendix B.4 – Mineralogical analyses

Sample	Gangue minerals	Primary sulphides	Sec. Minerals (Goe-rich)	Sec. Minerals (Hem-rich)	Other minerals	Goe-rich + Hem-rich
	%	%	%	%	%	%
1	56.0	1.4	29.8	12.8	0.0	42.6
2	54.5	1.5	12.3	31.7	0.0	43.9
3	81.6	1.0	14.2	2.8	0.5	17.0
4	55.2	4.5	10.7	29.5	0.0	40.3
5	46.0	0.9	12.8	40.3	0.0	53.1
6	53.2	6.5	29.6	10.8	0.0	40.3
7	30.7	21.5	10.2	37.1	0.5	47.3
8	40.4	16.1	39.2	4.4	0.0	43.6
9	25.1	14.9	40.0	20.0	0.0	60.0
10	54.7	0.7	26.8	17.8	0.0	44.6
11	40.9	10.9	38.6	9.6	0.0	48.2
12	39.4	9.7	44.1	6.8	0.0	50.9
13	35.0	13.4	39.5	12.0	0.0	51.6
14	57.9	3.7	29.4	9.0	0.0	38.4
15	34.2	11.8	36.0	18.0	0.0	54.1
16	78.8	2.8	16.5	1.8	0.0	18.4
17	65.0	0.8	23.9	10.3	0.0	34.2
18	26.1	4.6	57.7	11.5	0.0	69.3
19	83.6	1.3	13.6	0.3	1.2	13.8
20a	13.0	40.0	35.2	11.8	0.0	47.0
20b	11	45	40	2	2	42
20c	17	50	30	1	2	31
20d	10	58	30	0.0	2	30
21a	73.0	1.0	15.9	5.2	5.0	21.0
21b	88	1	9	0.0	2	9
21c	84	1	10	0.0	5	10
21d	83	1	13	0.0	4	13
21e	87	1	10	0.0	3	10
21f	81	1	15	0.0	4	15

Appendix B.5 – Chemical analyses

Sample	SiO_2	Al_2O_3	TiO_2	Fe_2O_3	MgO	CaO	Na_2O	K_2O	P_2O_5
	wt%	wt%	wt%	wt%	wt%	wt%	wt%	wt%	wt%
1	39.32	7.80	1.41	26.89	22.98	1.15	0.16	0.10	0.13
2	36.27	7.32	1.46	31.72	21.63	1.31	0.05	0.06	0.13
3	44.89	7.48	0.72	21.77	23.88	0.72	0.09	0.23	0.09
4	28.94	10.84	2.35	51.33	5.97	0.13	0.16	0.08	0.19
5	31.58	7.77	2.49	40.68	16.38	0.71	0.11	0.08	0.17
6	40.92	7.85	1.33	28.05	20.53	0.66	0.16	0.27	0.16
7	35.03	8.63	3.08	42.57	7.75	1.92	0.50	0.26	0.26
8	32.39	5.61	2.22	51.21	7.32	0.64	0.19	0.23	0.19
9	41.05	1.15	0.86	40.74	15.81	0.16	0.03	0.12	0.09
10	42.33	10.34	1.78	27.85	15.75	0.81	0.38	0.51	0.12
11	34.84	10.32	2.27	38.98	10.03	1.97	0.60	0.49	0.29
12	34.68	8.71	2.13	42.67	9.94	0.91	0.44	0.22	0.26
13	32.77	11.59	3.04	41.11	9.69	0.60	0.58	0.33	0.26
14	33.00	13.40	2.32	43.03	7.49	0.16	0.21	0.09	0.28
15	37.39	8.76	2.24	38.67	10.82	1.03	0.69	0.16	0.23
16	46.12	7.13	0.66	18.26	26.73	0.69	0.04	0.19	0.07
17	36.60	18.08	1.46	37.50	4.93	0.68	0.05	0.14	0.22
18	37.08	8.24	2.05	40.77	9.80	1.08	0.46	0.28	0.20
19	40.10	10.94	1.40	19.82	26.03	1.32	0.04	0.08	0.16
20a	n.a.	1.16	0.47	29.49	1.40	0.17	0.03	0.04	0.03
20b	n.a.	2.51	0.49	28.19	2.80	0.19	0.01	0.01	0.03
20c	n.a.	1.44	0.40	33.19	1.42	0.67	0.02	0.02	0.03
20d	n.a.	1.98	0.39	32.66	1.96	0.58	0.01	0.02	0.03
21a	n.a.	1.67	0.10	17.24	14.73	0.34	<.01	0.02	0.02
21b	n.a.	1.60	0.07	10.04	18.89	0.33	0.01	0.02	0.01
21c	n.a.	2.52	0.16	32.87	5.62	0.22	0.01	0.01	0.03
21d	n.a.	1.83	0.11	12.66	15.99	0.30	<.01	0.02	0.02
21e	n.a.	n.a.	n.a.	n.a.	n.a.	n.a.	n.a.	n.a.	n.a.
21f	n.a.	2.40	0.16	15.99	11.65	0.53	0.01	0.02	0.02

n.a. = not analysed

Sample	Cd	Co	Cr	Cu	Mn	Ni	V	Zn
	ppm	ppm	ppm	ppm	%	ppm	ppm	ppm
1	12	74	1117	1910	600	967	239	197
2	13	96	1259	3272	600	1214	223	196
3	9	170	2524	1240	1300	3579	180	192
4	23	98	713	163	100	142	365	311
5	21	85	971	160	300	860	316	318
6	11	70	1438	1700	500	1301	239	167
7	18	31	593	2414	100	216	357	33
8	18	56	846	2041	100	320	302	245
9	17	114	215	1546	100	96	112	89
10	12	139	1978	2474	1100	2287	290	133
11	16	104	477	1821	2100	294	404	508
12	15	40	931	3022	400	435	336	1126
13	17	35	756	3216	300	224	432	334
14	15	62	473	1258	100	175	403	282
15	12	46	549	4180	100	356	371	516
16	6	150	2005	902	1100	3207	126	88
17	16	408	541	1615	3500	252	541	317
18	3	59	1479	1887	400	453	343	130
19	6	94	498	989	1200	436	288	78
20a	0.6	78	253	>10000	131	93	200	74
20b	1.1	144	144	>10000	230	40	213	81
20c	1	175	120	>10000	164	34	164	141
20d	1.3	261	119	>10000	234	40	170	172
21a	1.7	66	972	5007	405	1063	121	161
21b	1	70	1304	3149	513	1480	83	139
21c	0.8	62	493	6965	266	409	178	117
21d	0.8	75	1083	4034	430	1184	105	141
21e	n.a.	n.a.	n.a.	n.a.	n.a.	n.a.	n.a.	n.a.
21f	1.4	79	825	4979	483	928	139	154

n.a. = not analysed

Appendix B.6 – AMD static tests

Sample	S	$S_{sulphate}$	$S_{sulphide}$	$S_{sulphate}$ / $S_{sulphide}$	S MPA	S-- MPA	ANC	S NAPP	S-- NAPP
	wt%	wt%	wt%	-	H_2SO_4 kg/t	H_2SO_4 kg/t	H_2SO_4 kg/t	H_2SO_4 kg/t	H_2SO_4 kg/t
1	0.04	n.a	n.c.	n.c.	1.22	n.c.	0.0	1.2	n.c.
2	0.00	n.a	n.c.	n.c.	0.31	n.c.	0.0	0.3	n.c.
3	0.00	n.a	n.c.	n.c.	0.31	n.c.	0.0	0.3	n.c.
4	0.66	n.a	n.c.	n.c.	20.2	n.c.	0.0	20.2	n.c.
5	0.02	n.a	n.c.	n.c.	0.61	n.c.	0.0	0.6	n.c.
6	0.73	n.a	n.c.	n.c.	22.34	n.c.	0.0	22.3	n.c.
7	2.50	n.a	n.c.	n.c.	76.5	n.c.	0.0	76.5	n.c.
8	2.22	n.a	n.c.	n.c.	67.93	n.c.	0.0	67.9	n.c.
9	2.11	n.a	n.c.	n.c.	64.57	n.c.	0.0	64.6	n.c.
10	0.00	n.a	n.c.	n.c.	0.31	n.c.	0.0	0.3	n.c.
11	1.34	n.a	n.c.	n.c.	41	n.c.	0.0	41.0	n.c.
12	0.98	n.a	n.c.	n.c.	29.99	n.c.	0.0	30.0	n.c.
13	1.07	n.a	n.c.	n.c.	32.74	n.c.	0.0	32.7	n.c.
14	0.50	n.a	n.c.	n.c.	15.3	n.c.	0.0	15.3	n.c.
15	0.99	n.a	n.c.	n.c.	30.29	n.c.	0.0	30.3	n.c.
16	0.13	n.a	n.c.	n.c.	3.98	n.c.	0.0	4.0	n.c.
17	0.00	n.a	n.c.	n.c.	0.31	n.c.	0.0	0.3	n.c.
18	0.74	n.a	n.c.	n.c.	22.64	n.c.	0.0	22.6	n.c.
19	0.22	n.a	n.c.	n.c.	6.73	n.c.	0.0	6.7	n.c.
20a	5.71	0.85	4.86	0.17	174.73	148.72	0.00	174.7	148.72
20b	8.20	1.72	6.48	0.27	250.92	198.29	41.8	209.1	156.49
20c	12.20	2.78	9.42	0.30	373.32	288.25	0.0	373.3	288.25
20d	16.52	2.43	14.09	0.17	505.51	431.15	37.0	468.5	394.15
21a	0.50	0.00	0.50	n.c.	15.30	n.c.	83.9	-68.6	n.c.
21b	0.14	0.00	0.14	n.c.	4.28	n.c.	51.6	-47.3	n.c.
21c	0.20	0.00	0.20	n.c.	6.12	n.c.	156.5	-150.4	n.c.
21d	0.47	0.00	0.47	n.c.	14.23	n.c.	42.0	-27.7	n.c.
21e	n.a.	0.00	-	n.c.	-	n.c.	n.c.	n.c.	n.c.
21f	0.29	0.00	0.29	n.c.	8.87	n.c.	21.3	-12.4	n.c.

n.a = not analysed; n.c. = not calculated

Appendix B.7 – Variogram parameters

Variable	Model	Scale	Length	Anisotropy
MgO	exponential	70	25	1
Fe_2O_3	exponential	100	20	1
S	exponential	1.5	20	1
Silicate	exponential	250	10	1
Oxide	exponential	400	90	1
Sulphide	exponential	80	10	1
Cr	spherical	400000	60	1
Ni	gaussian	1240000	40	1
MPA	exponential	2000	25	1
ANC	spherical	1	1	1

References

Abbate E., Bortolotti V., Galbiati B. & Principi G. (1980) *Carta geologica delle ofioliti del bargonasco e dell'Alta Val Graveglia* S.E.L.C.A. Firenze

Accornero M., Marini L., Ottonello G. & Vetuschi Zuccolini M. (2005) *The fate of major constituents and chromium and other trace elements when acid waters from the derelict Libiola mine (Italy) are mixed with stream waters* Appl. Geochem. v. 20, pp. 1368-1390

Agricola G. (1556) *De re metallica* Translated by Hoover H.C. & Hoover L.H. (1950) Dover Publications, New York, 638 pp.

Alfrey J. & Clark C. (1993) *The Landscape of Industry* Routledge ed.

ANPA –Agenzia Nazionale per la Protezione dell'Ambiente- & Environ Italy (2002) *ReasOnable Maximum Exposure - ROME 2.1:* http://www.apat.gov.it/site/it-IT/Modulistica_e_Software/Software_Rome_2.1/

APAT -Agenzia per la Protezione dell'Ambiente e per i Servizi Tecnici- (2006) *Censimento dei siti minerari abbandonati:* http://www.apat.gov.it/site/_Files/SitiMinerariItaliani1870_2006.pdf

APAT -Agenzia per la Protezione dell'Ambiente e per i Servizi Tecnici- & ISS –Istituto Superiore di Sanità- (2006b) *Protocollo Operativo per la determinazione dei valori di fondo di metalli/metalloidi nei suoli dei siti d'interesse nazionale* Internal report

ARPAT -Agenzia Regionale per la Protezione Ambientale della Toscana- (2004) *Indagine ambientale sulle aree ex minerarie dell'Isola d'Elba - Parte 1a: relazione* Internal Report

Azzali E., Marescotti P., Carbone C., Lucchetti G. & Servida D. (2008) **M***ineralogical and chemical variations in a sulphide waste-rock dump (Libiola mine, Liguria)* Congresso SIMP 2008, Sestri Levante

Barberi F., Dallan L., Franzini M., Giglia G., Innocenti F., Marinelli G., Raggi R., Squarci P., Taffi L. & Trevisan L. (1969) *Note illustrative della Carta Geologica d'Italia alla scala 1:100.000 - Foglio 126 (Isola d'Elba)* Servizio Geologico d'Italia, 32 pp.

Bencini A., Giardi M., Pranzini G. & Tacconi B.M. (1986) *Le risorse idriche dell'isola d'Elba* Università di Firenze, Dipartimento di Scienze della Terra & Provincia di Livorno, Tacchi editore, Pisa

Benvenuti M., Mascaro I., Corsini F., Costagliola P., Parrini P., Lattanzi, P. & Tanelli G. (1999) *Environmental problems related to sulfide mining in Tuscany* Chronique de la recherche minière v. 534, pp. 29-45

Benvenuti M., Bortolotti V., Conticelli S., Pandeli E. & Principi G. (2001) *Elba Island - Introduction* Ofioliti v. 26 (2a), pp. 321-330

Beresnev I.A., Hruby C.E. & Davis C.A. (2002) *The use of multi-electrode resistivity imaging in gravel prospecting* Journal of Applied Geophysics, v. 49 (4), pp. 245-254

Blott S. (2000) *Gradistat – Grain size analysis program* University of London

Blowes D.W., Ptacek C.J., Jambor J.L. & Weisener C.G. (2003) *The geochemistry of acid mine drainage* In: Lollar B.S. (Ed.), Environmental geochemistry, pp. 149-204. In Holland H.D. & Turekian K.K. (Eds.), Treatise on geochemistry vol. 9, Elsevier-Pergamon, Oxford

Bonatti E., Zerbi M., Kay R. & Rydell H. (1976) *Metalliferous deposits from the Apennine ophiolites:Mesozoic equivalents of modern deposits from oceanicspreading center* Goelogical Society of America Bulletin, v. 87, pp. 83-94

Bortolotti V., Castellarin A., Cita M.B., Dal Piaz G.V., D'argento B., Praturlon A., Ricchetti G. & Vanissi M. (1994) *Guida geologica regionale numero 6: Appennino Ligure-Emiliano*

Bortolotti V., Fazzuoli M., Pandeli E., Principi G., Babbini A. & Corti, S. (2001) *Geology of central and eastern Elba Island, Italy* Ofioliti v. 26 (2a), pp. 97-150

British Geological Survey (2002) *MINDEC* http://www.bgs.ac.uk/dfid-kar-geoscience/mindec/home.html

Carbone C. (2002). *Caratterizzazione delle fasi mineralogiche secondarie della miniera di Libiola correlate a processi di alterazione di solfuri:mineralogia e processi genetici.* Tesi di Laurea, Università di Genova

Carbone C., Di Benedetto F., Marescotti P., Martinelli A., Sangregorio C., Cipriani C., Lucchetti G., Romanelli M. (2005) *Genetic evolution of nanocrystalline Fe-oxide and oxyhydroxides assemblages from the Libiola Mine (Eastern Liguria, Italy): structural and microstructural investigation* European Journal of Mineralogy, v. 17, pp. 785-795

Carbone C. (2008) *Cristallochimica e minerogenesi di ossidi e ossi-idrossidi di ferro correlati a processi di AMD (Acid Mine Drainage) nell'area mineraria di Libiola (Sestri Levante, GE)* Tesi di dottorato, Università di Genova

Castrilli J. (2007) *Report on the legislative, regulatory, and policy framework respecting collaboration, liability, and funding measures in relation to orphaned/abandoned, contaminated, and operating mines in Canada*

Centre for Mined Land Rehabilitation (2008) *Abandoned, Derelict & Orphan Mines* http://www.cmlr.uq.edu.au/abandonedMines.htm

Comune di Rio Marina (2003) *Piano Strutturale* Internal Report

Cortecci G., Boschetti T., Dinelli E. & Cabella R. (2008) *Sulphur isotopes, trace elements and mineral stability diagrams of waters from the abandoned Fe-Cu mines of Libiola and Vigozzano* Water Air Soil Pollut, v.192, pp. 85-103

Cortesogno L., Galbiati B., Principi G. & Venturelli G. (1978) *Le brecce ofiolitiche della Liguria Orientale; nuovi dati e discussione sui modeli paleogeografici* Ofiliti, v. 3 (2/3), pp. 99- 160

Cortesogno L., Cassinis G., Dallagiovanna G., Gaggero L., Oggiano G., Ronchi A., Seno S., & Vanossi M. (1994) *The Variscan post-collisional volcanism in Late Carboniferous–Permian sequences of Ligurian Alps, Southern Alps and Sardinia (Italy): a synthesis* Lithos, v. 45, pp. 305-328

Craig J.R., Vaughan D.J. & Skinner B.J. (1996) *Resources of the Earth – Origin, Use, and the environmental impact* Prentice Hall

Dahlin T. (2001) *"The development of DC resistivity imaging techniques"* Comput. Geosci. v. 27, pp. 1019-1029

Dall'Aglio M. (2004) *Geochimica ambientale e salute, Principi e applicazioni* Aracne editrice, Roma

Decreto Legislativo n. 22 del 5 febbraio 1997 *Attuazione delle direttive 91/156/CEE sui rifiuti, 91/689/CEE sui rifiuti pericolosi e 94/62/CE sugli imballaggi e sui rifiuti di imballaggio* Gazzetta Ufficiale n. 38 del 15 febbraio 1997 - Supplemento Ordinario n. 33

Decreto Legislativo n. 42 del 22 gennaio 2004 *Codice dei beni culturali e del paesaggio, ai sensi dell'articolo 10 della legge 6 luglio 2002, n. 137* Gazzetta Ufficiale n. 45 del 24 febbraio 2004 - Supplemento Ordinario n. 28

Decreto Legislativo n. 152 del 3 aprile 2006 *Norme in material ambientale* Gazzetta Ufficiale Supplemento ordinario n. 96

Decreto Ministeriale n. 471 del 25 ottobre 1999 *Regolamento recante criteri, procedure e modalità per la messa in sicurezza, la bonifica e il ripristino ambientale dei siti inquinati ai sensi dell'art. 17 del D.Lgs. 22/97 e successive modificazioni e integrazioni* Gazzetta Ufficiale n. 293 del 15 dicembre 1999 - Supplemento ordinario 218/L

Deschamps Y., Dagallier G., Macaudière J., Marignac C., Moine B. & Saupé F. (1983 a) *Le gisement de pyrite-hématite de Valle Giove (Rio Marina, Ile d'Elbe, Italie) - Partie 1* Schweiz. Miner. Petrog. v. 63, pp. 149-165

Deschamps Y., Dagallier G., Macaudière J., Marignac C., Moine B. & Saupé F. (1983 b) *Le gisement de pyrite-hématite de Valle Giove (Rio Marina, Ile d'Elbe, Italie) - Partie 2* Schweiz. Miner. Petrog. v. 63, pp. 301-327

Deshaies M. (2002) *Les bassins houillers en Europe* In http://geoconfluences.ens-lsh.fr/doc/transv/paysage/PaysageScient3.htm

Dinelli E., Cortecci G., Lucchini F. & Fabbri M. (1999) *REE mobility associated to acid mine drainage: investigation in the Libiola area, northern Italy.* In: Ármannsson H. (Ed.) Geochemistry of the Earth's Surface: Proceedings of the 5th International Symposium, Reykjavik, 15-20 August 1999 by Iceland, pp. 173-176

Dinelli E., Lucchini F., Fabbri M. & Cortecci G. (2001) *Metal distribution and environmental problems related to sulphide oxidation in the Libiola copper mine area (Ligurian Apennines, Italy)* J. Geochem. Explor. v. 74, pp. 141-152

Dinelli E. & Tateo F. (2002) *Different types of fine-grained sediments associated with acid mine drainage in the Libiola Fe-Cu mine area (Ligurian Apennines, Italy)* Appl. Geochem. v. 17, pp1081-1092

D'Oriano V. (2007) *Planimetria di Rio Marina* Internal Report

Eden Project http://www.postmining.org/

Elba Island Mineralogical and Mining Park (1991) http://www.parcominelba.it/

Eurometeo (1995-2008) http://www.eurometeo.com/italian/climate/city_LIMJ/meteo_Genova-Sestri

European Mining Heritage Initiative (2006) http://www.enmr.org/FILES/Mintour.html

Evangelou V.P. (1998) *Pyrite chemistry: the key for abatement of acid mine drainage* In: Geller A., Klapper H. & Salomons W. (Eds.) *Acidic Mining Lakes: Acid Mine Drainage, Limnology and Reclamation* Springer - Berlin, pp. 197-222

Evans A.M. (1987) *An introduction to ore geology* 2nd ed.

Ferrario A. (1973) *I giacimenti cupriferi nelle pillow lavas della Liguria Orientale* S.I.M.P., pp. 485-495

Ferrario A. & Garuti G. (1980) *Copper deposits in the basal breccias and volcano-sedimentary sequences of the Eastern Ligurian ophiolites (Italy)* Miner. Deposita v. 15, pp. 291-303

Ficklin W.H., Plumlee G.S., Smith K.S. & McHugh J.B. (1992) *Geochemical classification of mine drainages and natural drainages in mineralised areas* In: Kharaka Y.K. & Maest A.S. (Eds.) Proceedings of water-rock interaction n. 7, Balema, Rotterdam, pp. 381–384

Garuti G. & Zaccarini F. (2005) *Minerals of Au, Ag, and U in volcanic rock-associated massive sulphide deposits of the northern Apennine ophiolite, Italy* Can. Mineral. v. 43, pp. 935-950

Gazea B., Adam K. & Kontopoulos A. (1996) *A review of passive systems for the treatment of acid mine drainage* Miner. Eng. v. 9 (1), pp. 23-42

Godio A. & Naldi M. (2003) *Two-dimensional electrical imaging for detection of hydrocarbon contaminants* Near Surface Geophysics, v. 1, pp. 131-137

GSI Environmental Inc. (2008) *RBCA Tool Kit for Chemical Releases, version 2.01* http://www.gsi-net.com/Software/RBCA_tk_v2.asp

Guérin R., Bégassat P., Benderitter1 Y., Jacques David J., Tabbagh A. & Thiry M. (2004) *Geophysical study of the industrial waste land in Mortagne-du-Nord (France) using electrical resistivity* Near Surface Geophysics, v. 2(3), pp. 137-143

Guilbert J.M. & Park C.F. Jr. (1986) *The geology of ore deposits* Freeman and Company, New York

Jambor J.L. & Owens D.R. (1993). *Mineralogy of tailings impoudement at the former Cu-Ni deposit of Nichel* Rim Mines Ltd. Eastern edge of the Sudbury Structure Ontario. Canmet

Division Repart MSL 93-4 (CF). Dept. Energy Mines Resource Canada

Jambor, J.L. & Blowes, D.W. (1994) *Short course on environmental geochemistry of sulfide-mine wastes* In: Mineralogical Association of Canada (Ed.) Short Course Handbook Volume v. 22, 438 pp.

Johnson D.B. & Hallberg K.B. (2005) *Acid mine drainage remediation options: a review* Sci. Total Environ. v. 338, pp. 3-14

Krige D.G. (1951) *"A statistical approach to some basic mine valuation problems on the Witwatersrand"* Journal of the Chemical, Metallurgical and Mining Society of South Africa v. 52, pp. 119–139

Kwong Y.T.J. (1993) *Prediction and prevention of acid rock drainage from a geological and mineralogical perspective* MEND Project 1.32.1, 47 pp.

ISPRA -Istituto Superiore per la Protezione e la Ricerca Ambientale- (2008) *Linee guida per la gestione e valorizzazione di siti e parchi geominerari* http://www.apat.gov.it/site/_contentfiles/00153200/153291_manuali_43_2008_geominerari.pdf

IWRI -Ian Wark Research Institute- & EGI -Environmental Geochemistry International- (2002) *ARD Test Handbook - AMIRA P387A Project: Prediction and kinetic control of Acid Mine Drainage* AMIRA International, Melbourne

Land Restoration Trust (2004) http://www.landrestorationtrust.co.uk/template.asp?l1=1

Landi S. (1972) *I rimboschimenti dell'Isola d'Elba* Firenze

Li M.G. Aube B.C. & St-Arnaud L.C. (1997) *Considerations in the use of shallow water covers for decommissioning reactive tailings* Proceedings of the Fourth International Conference on Acid Rock Drainage, May 30–June 6 1997, Vancouver, vol. 1, pp. 115– 30

Live Search (2007) http://maps.live.it/?mkt=it-it?

Loke M.H. & Barker R.D. (1995) *Least-squares deconvolution of apparent resistivity pseudosections* Geophysics v. 60, pp. 1682–1690

Loke M.H. & Barker R.D. (1996) *Practical techniques for 3D resistivity surveys and data inversion* Geophysical Prospecting v. 44, pp. 499-523

Loke M.H. (1999) *RES2DINV—rapid 2-D resistivity and IP inversion using the least-squares method* Software manual, 81 pp.

Mascaro I., Benvenuti M., Corsini F., Costagliola P., Lattanzi P., Parrini P. & Tanelli, G. (2001) *Mine wastes at the polymetallic deposit of Fenice Capanne (southern Tuscany, Italy) - Mineralogy, geochemistry and environmental impact* Environ. Geol. v. 41, pp. 417-429

Marescotti P. & Cabella R. (1996) *Significance of chemical variations in a chert sequence of the "Diaspri di Monte Alpe" formation (Val Graveglia, North Apennine, Italy)* Ofioliti, v. 21(2), pp. 139-144

Marescotti P. & Carbone C. (2003) *La miniera dismessa di Libiola (Sestri Levante, Liguria Orientale): studio mineralogico sui processi di alterazione di solfuri di Fe e Cu e valutazione del loro impatto ambientale* GEAM v. 109 (3), pp. 45-53

Marescotti P., Carbone C., De Capitani L., Grieco G., Lucchetti G. & Servida D. (2008) *Mineralogical and geochemical characterisation of open-air tailing and waste rock dumps from the Libiola Fe-Cu sulphide mine (Easter Liguria, Italy)* Environ. Geol., v. 53, pp. 1613-1626

Marescotti P., Azzali E., Servida D., Carbone C., Grieco G., De Capitani L. & Lucchetti G. (submitted) *Mineralogical and geochemical spatial analyses of a waste-rock dump at the Libiola Fe-Cu sulphide mine (Eastern Liguria, Italy)* Mineralogical Magazine

Marini L., Saldi G., Cipolli F., Ottonello G. & Vetuschi Zuccolini M. (2003) *Geochemistry of water discharges from the Libiola mine, Italy* Geochem. J. v. 37(2), pp. 199-216

Matheron G. (1963) *"Principles of geostatistics"* Econ. Geol. v. 58, pp. 1246–1266

MATT -Ministero dell'Ambiente e della Tutela del Territorio-, RAS -Regione Autonoma della Sardegna- & Comune di Domusnovas (2003) *Interventi di bonifica e rispristino ambientale dell'area mineraria dismessa di Barraxiutta – Piano della Caratterizzazione, Relazione tecnica descrittiva*

MATT -Ministero dell'Ambiente e della Tutela del Territorio-, RAS -Regione Autonoma della Sardegna- & Comune di Domusnovas (2004) *Piano della Caratterizzazione dell'area mineraria dismessa di Barraxiutta – Piano di Investigazione Iniziale*

MATT -Ministero dell'Ambiente e della Tutela del Territorio-, RAS -Regione Autonoma della Sardegna- & Comuni di Arbus e Guspini (2003) *Interventi di bonifica e rispristino ambientale dell'area mineraria dismessa di Montevecchio Ponente-Ingurtosu – Piano della Caratterizzazione, Relazione tecnica descrittiva*

MATT -Ministero dell'Ambiente e della Tutela del Territorio-, RAS -Regione Autonoma della Sardegna- & Comuni di Arbus e Guspini (2006) *Interventi di bonifica e rispristino ambientale dell'area mineraria dismessa di Montevecchio Ponente-Ingurtosu – Piano della Caratterizzazione, Piano di Investigazione Iniziale*

Mele M., Servida D., Grassi D. & Crolla N. (2007) *Application of Electrical Resistivity Ground Imaging (ERGI) to aid the Acid Mine Drainage (AMD) evaluation in the Rio Marina mining district (Elba Island)* Epitome v. 2, pp. 479–480

Mele M. & Servida D. (submitted) *Application of Electrical Resistivity Ground Imaging (ERGI) to geo-environmental modeling of Abandoned Mine Lands: the Rio Marina mining district (Elba Island, Italy),* Journal of environmental and engineering geophysics

Mehling P.E., Day S.J. & Sexsmith K.S. (1997) *Blending and layering waste rock to delay, mitigate or prevent acid generation: a case study review* In: Proceedings of the Fourth International Conference on Acid Rock Drainage, Vancouver, Canada, May 31 to June 6, Volume II, pp.951-969

MEND -Mine Environment Neutral Drainage- (2000) *MEND Manual – Volume 4: Prevention and control*

Mine Environment Neutral Drainage (1995) *MINEWALL 2.0 Literature review and conceptual models* MEND Project 1.15.2b

Morin K.A. & Hutt N.M. (2001) *Environmental geochemistry of minesite drainage: practical theory and case studies* MDGA Publishing - Vancouver, 333 pp.

Munro L.D., Clark M.W. & McConchie D. (2004) *A Bauxsol T-Based Permeable Reactive Barrier for the Treatment of Acid Rock Drainage* Mine Water and the Environment v. 23 (4) pp. 183-194

Murad E. & Rojík P. (2004) *Jarosite, schwertmannite, goethite, ferrihydrite and lepidocrocite: the legacy of coal and sulfide ore mining* Supersoil 2004: Australian New Zealand Soil Conference, Sydney

Mine Water and the Environment v. 23 (4) pp. 183-194

Naftz D. L., Morrison S. J., Fuller C. C. & Davis J. A. (2002) *Groundwater Remediation Using Permeable Reactive Barriers, Applications to Radionuclides, Trace Metals, and Nutrients* Academic Press, Amsterdam, 539 pp.

NAS -National Academy of Sciences- (1983) *Risk assessment in the federal government: managing the process* National Academy Press, Washington DC

NAS -National Academy of Sciences- (1994) *Alternatives for groundwater cleanup* National Academy Press, Washington DC

NOAMI –National Orphanded/Abandoned Mines Initiative http://www.abandoned-mines.org/home-e.htm

Nordstrom D.K. & Alpers C.N. (1999) *Geochemistry of acid mine waters* In: Plumlee G.S. & Logsdon M.J. (Eds.), The environmental geochemistry of mineral deposits. Reviews in Economic Geology v. 6a, pp. 133-160

Plumlee G.S., Smith K.S., Ficklin W.H., Briggs P.H. & McHugh J.B. (1993) *Empirical studies of diverse mine drainages in Colorado--implications for the prediction of mine-drainage chemistry* Proceedings of 1993 Mined Land Reclamation Symposium, Billings, Montana, v. 1, pp. 176-186

Plumlee G.S. & Nash J.T. (1995) *Geoenvironmental models of mineral deposits-fundamentals and applications* In: du Bray E.A. (Ed.) *Preliminary Compilation of Descriptive Geoenvironmental Mineral Deposit Models* USGS OFR-95–0831

Plumlee G.S. (1999). *The environmental geology of mineral deposits* In: Plumlee G.S. & Logsdon, M.J. (Eds.) The environmental geochemistry of mineral deposits Reviews in Economic Geology v. 6a, pp. 71-116

Plumlee G.S., Smith K.S., Montour M.R., Ficklin W.H. & Mosier E.L. (1999) *Geologic controls on the composition of natural waters and mine waters draining diverse mineral deposit types* In: Filipek L.H. & Plumlee G.S. (Eds.) The environmental geochemistry of mineral deposits. Reviews in Economic Geology, vol. 6b, pp. 373–432

Principi G.& Treves B. (1994) *Oceanisation processes and sedimentary evolution of the Northern Apennine ophiolite suite and discussion.* Mem. Soc. Geol. It., v. 48, pp. 117-136

Provincia di Milano & UNIMI -Università degli Studi di Milano- (2003) *Linee guida per la determinazione dei valori del fondo naturale nell'ambito della bonifica dei siti contaminate* Internal Report

Provincia di Milano & URS Italia (2006) *GIUDITTA 3.1 - Gestione Informatizzata DI Tollerabilità Ambientale* http://www.provincia.milano.it/ambiente/bonifiche/giuditta.shtml

Puls R.W. (1998) *Permeable reactive barrier research at the National Risk Management Research Laboratory* U.S. Environmental Protection Agency. Evaluation of Demonstrated Emerging technologies for the Treatment of Contaminated and Groundwater (Phase III): Special Session; Treatment Walls and

Permeable Reactive Barriers. North Atlantic Treaty Organisation/Committee on the Challenges of Modern Society

Regione Autonoma della Sardegna (2003) *Linee guida per la redazione di progetti e la realizzazione di interventi di bonifica e risanamento ambientale delle aree minerarie dismesse* In: Regione Autonoma della Sardegna Piano regionale di gestione dei rifiuti – Piano di bonifica siti inquinati, Allegato 3

RAS -Regione Autonoma della Sardegna- & Comune di Villaputzu (2003) *Piano della Caratterizzazione area Baccu Locci – Quirra – Relazione descrittiva*

RAS -Regione Autonoma della Sardegna- & Comune di Villaputzu (2004) *Piano della Caratterizzazione area Baccu Locci Quirra – Piano di investigazione iniziale*

Regione Liguria (1999) *Piano regionale di bonifica delle aree inquinate*

Regione Toscana (2002) *Studio complessivo esteso alle aree interessate da fenomeni di inquinamento in atto presso la miniera di Campiano in commune di Montieri – Rapporto di sintesi*

Robb L. (2005) *Introduction to ore-forming processes* Blackwell Publishing

Rose A.W., Hawkes H.E. & Webb J.S. (1979) *Geochemistry in mineral exploration* (2nd Ed.) Academic Press - New York, 657 pp.

Servida D., Grieco G. & De Capitani L. (2009) *Geochemical hazard evaluation of sulphide-rich iron mines: The Rio Marina district (Elba Island, Italy)* J. Geochem. Explor., v. 100, pp. 75-89

Smith K.S., Plumlee G.S. & Ficklin W.H. (1994) *Predicting water contamination from metal mines and mining waste* USGS OFR-94-264, 112 pp.

Smith K.S. & Huyck H.L.O. (1999) *An overview of the abundance, relative mobility, bioavailability and human toxicity of metals* In: Plumlee G.S. & Logsdon M.J. (Eds.), The environmental geochemistry of mineral deposits. Reviews in Economic Geology v. 6a, pp. 29-70

Sobek A.A., Schuller W.A., Freeman J.R. & Smith R.M. (1978) *"Field and laboratory methods applicable to overburdens and minesoils (EPA-600/2-78-054)"* U.S. Environmental Protection Agency, Cincinnati, pp. 47–50

Sobolewski A. (1997) *Wetlands for Treatment of Mine Drainage* http://www.enviromine.com/wetlands/Welcome.htm

Soregaroli B.A. & Lawrence R.W. (1997) *Waste rock characterization at Dublin Gulch: a case study.* Proceedings of the 4th international conference on acid rock drainage, Vancouver, pp. 631-645

Studio Chines (1999) *Progetto per il potenziamento delle risorse idriche per uso idropotabile nell'Isola d'Elba - Relazione tecnica* Internal report

Swanson D.A., Barbour S.L., Wilson G.W. (1997) *Dry-site versus wet-site cover design.* Proceedings of the Fourth International Conference on Acid Rock Drainage, May 30–June 6 1997, Vancouver, vol. 4, p. 1595–610

Tanelli G. & Lattanzi P. (1986) *Metallogeny and mineral exploration in Tuscany: state of the art* Mem. Soc. Geol. It. v. 31, pp. 299-304

Tanelli G., Benvenuti M., Costagliola P., Dini A., Lattanzi P., Maineri C., Mascaro I., Ruggieri G. (2001) *The iron mineral deposits of Elba Island: state of the art* Ofioliti v. 26 (2a), pp. 239-248

Thornthwaite C.W. (1948) *An approach toward a rational classification of climate* Geogr. Rev., v. 38, pp. 55–94

Trevisan L. (1950) *L'Elba Orientale e la sua tettonica di scivolamento per gravità* Mem. Inst. Geol. Min. Univ. Padova v. 16, pp. 5-39

TRIANET project (1999) http://nibis.ni.schule.de/~trianet/elba/elba04.htm

Trinder B. (1987) *The making of the industrial landscape***,** Alan Sutton ed.

Tuscan Archipelago National Park (1996) http://www.islepark.it/

USDA -Department of Agriculture- & SCS -Soil Conservation Service- (1972) *National Engineering Handbook***,** Hydrology Section 4, Chapters 4–10

US EPA -Environmental Protection Agency- (1989) *Risk assessment guidance for Superfund: Environmental evaluation manual* (EPA/540/1-69/001A, OSWER directive 9285.7-10) Environmental Protection Agency , Government Printing Office, Washington DC

US EPA -Environmental Protection Agency- (1994) *National oil and hazardous substances pollution Contingency Plan* Federal Register, v. 59, pp. 47384-47495

US EPA -Environmental Protection Agency- (1997) *National Hardrock Mining Framework* EPA 833-B-97-003, Washington DC

US EPA -Environmental Protection Agency- (1998) *Permeable Reactive Barrier Technologies for Contaminant Remediation*. EPA/600/R-98/125, Washington DC

US EPA -Environmental Protection Agency- (2000) *Abandoned mine site characterization and cleanup handbook* EPA 910-B-00-001, Seattle

US EPA -Environmental Protection Agency- (2002) *Guidance on choosing a sampling design for environmental data collection (QA/G-5S)* Office of environmental Information, Washington DC

US EPA -Environmental Protection Agency- (2002b) *Guidance for Comparing Background and Chemical Concentrations in Soil for CERCLA Sites* (EPA 540-R-01-003, OSWER 9285.7-41) Office of Emergency and Remedial Response, Washington DC

US EPA -Environmental Protection Agency- (2008) http://www.epa.gov/superfund/programs/aml

Vichery A. & Hobbs B. (2003) *Resistivity imaging to determine clay cover and permeable units at an ex-industrial site* Near Surface Geophysics, v. 1, pp. 21-30

Von der Heyden C. & New M. (2005) *Differentiating dilution and retention processes in mine effluent remediation within a natural wetland on the Zambian Copperbelt* Appl. Geoch. v. 20 (7) pp. 1241-1257

Vranesh G. (1979) *Mine drainage – the common enemy* In: Argal G.O. Jr. & Brawner C.O. (Eds.) Proceedings of 1st International Mine Drainage Symposium, Miller Freeman Publications, pp. 54-97

Watts R.J. (1998) *Hazardous wastes: sources, pathways, receptors* Wiley, New York

Watts R.J. & Teel A.L. (2003) *Risk, toxicity, exposure, assessment, policy, and regulation* In: Lollar B.S. (Ed.), Environmental geochemistry, pp. 1-16. In Holland H.D. & Turekian K.K. (Eds.), Treatise on geochemistry vol. 9, Elsevier-Pergamon, Oxford

Webster R. & Oliver M.A. (2001) *Geostatistics for environmental scientists* John Wiley &Sons Ltd, Chichester

Zuffardi P. (1990) *The iron deposits of the Elba Island (Italy): remarks for a metallogenic discussion* Memorie Lincee Scienze Fisiche e Naturali serie IX, 1 (4) 97-128

Acknowledgements

Vorrei ringraziare tutte le persone che hanno reso possibile lo svolgimento di questo dottorato di ricerca e quelle che in questi tre anni hanno incrociato la loro strada con la mia, percorrendola insieme per periodi più o meno lunghi, arricchendomi professionalmente e umanamente.

Un GRAZIE in particolare a:

Luisa e Giovanni, per tutto quello che hanno fatto, perché senza di loro questo lavoro non sarebbe nemmeno cominciato,

Maurino, perché siamo i campioni del mondo (N.B. sai cosa faremo nel futuro!),

Francesco, a problem-solving man,

Marco, Giovanni e lo staff del Parco Minerario dell'Isola d'Elba, per l'immensa disponibilità e la sincera amicizia,

Pietro, Cristina ed Eva del DIP.TE.RIS di Genova, per la proficua collaborazione nello sviluppo del lavoro di Libiola,

Angelo, Mara, Alessio, Edoardo e Matteo, per il supporto con le loro tesi di laurea allo sviluppo del lavoro di Rio Marina,

Riccardo, Mauro, Fabrizio, Marco e Glauco, per le consulenze scientifiche;

Elena e Franco, per il supporto tecnico in laboratorio;

il Dott. Pilurzu di PROGEMISA, per gli utili scambi di opinioni,

i.Geo s.r.l., per la strumentazione geofisica messa a disposizione,

Petroltecnica s.p.a., per il fondamentale anno di esperienza,

il Prof. Carmignani ed Enrico del CGT di Siena, per l'esempio di professionalità accademica,

tutti i dottorandi del XXI ciclo di Scienze della Terra, per aver vissuto insieme questa esperienza,

Elena, l'altra metà della mia vita…

…ABRA-CADABRA!!!

(The Prestige)